Bone

16

Henryk A. Domanski, Xiaohua Qian,
and Donald E. Stanley

Introduction

Skeletal FNAC

Methods for percutaneous sampling such as core needle biopsy (CNB) and fine needle aspiration (FNA) have, in recent years, emerged as important diagnostic substitutes for open biopsy of bone neoplasms. FNAC has been used for many years in the diagnosis of skeletal lesions. As early as 1931, Coley and Ellis [1] applied this sampling method to bone neoplasms. Since then, several large series of FNA examinations of bone lesions have been published [2–12]. FNAC may be relatively easily applied to a selected group of neoplasms such as metastatic depositions and recurrences of previously treated malignant bone tumors. FNAC may be also used as the first-line approach or as a complementary tool to core needle CNB in the diagnosis of primary bone neoplasms. The combination of FNAC and CNB techniques appears to increase overall diagnostic accuracy in the evaluation of bone neoplasms [13, 14].

Primary bone tumors are relatively uncommon, especially sarcomas, which account for only 0.2% of all neoplasms. Osteosarcoma is the most common primary bone sarcoma followed by chondrosarcoma, Ewing sarcoma, and chordoma. The most common benign bone neoplasms are osteochondroma, giant cell tumor, chondroma, osteoid osteoma, and metaphyseal fibrous defect. The incidence rates of specific bone tumors are age-related. The majority of benign bone tumors, osteosarcoma and Ewing sarcoma, arise in children and young adults, while chondrosarcoma and chordoma occur most frequently after the age of 50.

Radiographic examinations yield rich diagnostic information and comprise indispensable modality in the evaluation of bone lesions. Various imaging modalities such as plain radiography, ultrasonography, magnetic resonance imaging (MRI), computed tomography (CT), scintigraphy, and positron emission tomography (PET) all play important roles in the evaluation of bone lesions [15]. In many cases of benign bone lesions, radiography may be diagnostic, obviating the need of any biopsy. The most important task for the radiologist, however, is to evaluate the extent of the tumor, not the histologic diagnosis. In the differential diagnosis of majority of benign and malignant bone neoplasms, radiography may exclude or establish malignancy and limits the diagnostic options to one diagnosis or few differential diagnoses. Morphologic examinations, however, are considered to be a necessary part of the diagnostic work-up of malignant and many benign bone neoplasms since therapeutic regimens differ significantly for both malignant and benign/locally aggressive neoplasms. The microscopic diagnosis should confirm the radiological findings, and in cases of discordance between radiological imaging and cytological/histological diagnosis, the findings must be re-evaluated. In this aspect the cooperation between radiologist and pathologist/cytopathologist is mandatory. The importance of the radiologic–cytologic correlation approach to the diagnosis has been clearly demonstrated by Söderlund et al. [16]. In another study by this author, comparison of radiology and cytology showed diagnostic agreement in 256 cases (69%) and non-agreement in 101 (28%). The diagnostic error rate was 1% among the 256 compliant cases, compared to 17% among the 101 noncompliant cases [17]. Although not all patients with a skeletal lesion need to be referred to large medical centers for diagnosis and treatment, it is recommended that

H. A. Domanski (✉)
Department of Pathology, Skåne University Hospital,
Lund, Sweden
e-mail: henryk.domanski@med.lu.se

X. Qian
Department of Pathology, Brigham & Women's Hospital, Harvard Medical School, Boston, MA, USA
e-mail: xqian@bwh.harvard.edu

D. E. Stanley
Department of Pathology, Maine Medical Center,
Portland, ME, USA
e-mail: stanld@mmc.org

H. A. Domanski (ed.), *Atlas of Fine Needle Aspiration Cytology*, https://doi.org/10.1007/978-3-319-76980-6_16

patients with a suspected primary skeletal neoplasm should be referred to specialized orthopedic–oncology centers with expertise in musculoskeletal oncology.

Reporting the Diagnosis

A standardized reporting of bone FNA has been suggested by Åkerman et al. [18]:

- Sarcoma (histologic type of sarcoma or sarcoma not otherwise specified [NOS])
- Benign tumor (histologic type or benign tumor NOS)
- Metastasis (suggestion of primary or descriptive diagnosis)
- Lymphohematologic malignancy (exact subtype defined or general classification as malignant lymphoma, non-Hodgkin lymphoma)
- Nonneoplastic lesion (infectious, reactive)
- Nondiagnostic (including insufficient)

Diagnostic Accuracy

Reported diagnostic accuracy of FNA has varied depending on the era of the study, whether or not using radiology–cytology correlation and reporting terminology used at different centers. Earlier studies have reported lower diagnostic accuracy than later ones, with accuracies up to 98%. Diagnostic accuracy is higher at sarcoma centers specializing in musculoskeletal oncology with access to a multidisciplinary approach. The results of 8 large series comprising a total of 2152 total patients are summarized in Table 16.1 [7, 9, 17, 20–23]. In these series, the diagnostic accuracy regarding benign versus malignant was between 83% and 98%, and the rate of insufficient material for diagnosis was variable, ranging from 3% to 31% in seven studies.

Table 16.1 Fine needle aspiration cytology of bone tumors/lesions: diagnostic accuracy summarized from 8 series comprising 2152 patients

Authors	Publication year	Cases, *n*	Insufficient yield, %	Diagnostic accuracy, %
Kreicbergs et al. [9]	1996	300	8	95
Bommer et al. [7]	1997	450	14	98
Åkerman et al. [19]	1998	333	6	98
Jorda et al. [20]	2000	314	31	95
Agarwal et al. [21]	2000	226	–	83
Wedin et al. [22]	2000	110	8	93
Kilpatrick et al. [23]	2001	49	8	93
Söderlund et al. [17]	2004	370	3	95 (99 with radiologic correlation)

Advances and Limitations of FNAC in the Diagnosis of Bone Neoplasm

There are several advantages to skeletal FNAC. The procedure is less traumatic than either CNB or open biopsy, so it can be used safely in difficult sites such as vertebrae or pelvic bone. FNAC is an outpatient procedure which requires fewer resources than other biopsy techniques. The procedure is well tolerated by most patients with local anesthesia and has negligible risks for serious complications. FNAC allows rapid on-site evaluation (ROSE) with immediate triage decisions and coordination of further investigations, as well as planning of anticipated therapy (see Chaps. 1 and 2). Compared to open biopsy, FNAC has also some limitations. The main disadvantage of FNAC is a lack of well-trained expertise in the cytologic evaluation of bone lesions. In addition FNA samples are small, and it can be occasionally difficult to obtain sufficient material for both morphological examination and all necessary ancillary studies. However, ancillary techniques such as immunocytochemistry and molecular–genetic techniques may be successfully applied on very small cytological samples.

Important limitations of FNAC of bone tumors are:

1. Poor or technically suboptimal material; extensive necrosis and hemorrhage are limiting factors.
2. Inability to aspirate sufficient material for evaluation. Intervention is limited by intramedullary lesions when cortex is intact, and the lesion is sclerotic with significant ossification and calcification. The radiologic features of a bone lesion often indicate whether an aspiration is feasible.
3. Sampling error. When tumors with a heterogeneous architecture are needled, the aspirated material may not correspond to the diagnostic tissue. An example of this pitfall is the aspiration of giant cell-rich osteosarcoma when the smears are dominated by benign osteoclast-like cells, giving the false impression of giant cell tumor.
4. Misinterpretation of the material. Lack of experience in cytological diagnosis of bone lesions. Well-known difficulties in FNA diagnosis of bone neoplasm include distinguishing well-differentiated chondrosarcoma from benign cartilaginous tumors such as enchondroma and reactive osteoblastic proliferation from osteoblastic neoplasm. Clinical and radiologic correlation is required.

Technical Considerations

Sampling Technique

Because of destructive growth and frequent soft tissue extension, primary malignant bone neoplasms are easily accessible by FNA [24]. Destroyed or "moth-eaten" cortical bone can be easily penetrated by thin needles as well. Percutaneous puncture of palpable lesions can be performed in outpatient clinics with or without local anesthesia and with or without radiologic guidance. FNA of non-palpable bone lesions should be guided by radiologic findings. In cases of obvious bone destruction, the needling can be performed under fluoroscopic guidance. CT-guided aspiration biopsy should be the method of choice for deep lesions.

One advantage of using CT is that the needles may be directed to various parts of a heterogeneous mass for a more representative sampling. In open MRI systems, aspiration biopsy can be performed using special non-ferromagnetic needles. The equipment used for FNA of bone lesions is the same as for needling other sites. A syringe holder permitting aspiration with one hand is essential. In most cases, 22-gauge (0.7 mm) needles are sufficient. Needles with a stylet are recommended for deep-seated tumors/lesions. The stylet strengthens the needle and prevents the contamination by the cells aspirated through the needle tract in the surrounding tissues.

For intramedullary lesions when the cortex is intact, trocar with a drill in most cases is necessary. Biopsy instruments available for penetrating cortical bone include a coaxial biopsy system with an eccentric drill [25].

In patients with clinically suspected malignancy, tattoo of needle insertion point is recommended as in FNA of soft tissue sarcomas, so that the needle track can be removed at surgery.

Preparation of Specimen and Ancillary Techniques

Regarding preparing FNA specimens for microscopic examination and for ancillary techniques, the same principles apply for bone aspirates as for other types of FNA specimens (see Chap. 1).

Immunocytochemistry and molecular–genetic analyses are the most valuable ancillary techniques to facilitate the specific diagnosis in FNA of bone neoplasms. These techniques are essential in the cytologic evaluation of small round cell neoplasms [26–29]. Immunocytochemical studies are indispensable to suggest site of origin in the work-up of bone metastasis. Useful antibodies in the diagnosis of primary and metastatic bone neoplasm are listed in Tables 16.2 and 16.4.

Electron microscopic examinations are most useful in the diagnosis of Langerhans cell histiocytosis (Birbeck granule) and selected cases of osteosarcoma (osteoid) [30].

Table 16.2 Useful antibodies in the diagnosis of primary bone neoplasm

Tumor/lesion	Antibody	Comments
Chondroblastoma	H3K36M,S-100 protein, SOX-9	H3K36M is mutation-specific
Chondrosarcoma	S-100 protein	Strong staining in low-grade malignant tumors
		Weak staining in high-grade malignant tumors
Giant cell tumor of the bone	H3G34W	H3G34W is mutation-specific
Mesenchymal chondrosarcoma	CD99, S-100 protein	CD99: rather cytoplasmic than a membranous pattern
Clear cell chondrosarcoma	S-100 protein, collagen II	
Chordoma	S-100 protein, cytokeratin, epithelial membrane antigen (EMA), Brachyury	Double staining of S-100 protein and epithelial markers; Brachyury: nuclear staining
Ewing sarcoma	CD99, FLI-1, NKX2.2	CD99, membrane staining; FLI-1 and NKX2.2, nuclear staining
Langerhans cell histiocytosis	S-100 protein, CD1a, langerin, CyclinD1	Langerin and CD1a more specific than S-100 protein
Osteosarcoma	Osteocalcin, osteonectin, SATB2	
Osteofibrous dysplasia	Cytokeratin	Scattered single spindle cells
Adamantinoma	Cytokeratin, EMA, p63, D2–40	Fibrous area staining for vimentin only and coexpression of vimentin and other markers in epithelial cells
Angiosarcoma	CD31, CD34, Fli-1, ERG	CD34 variable; ERG: nuclear staining
Epithelioid hemangioendothelioma	CD31, CD34, ERG, cytokeratin, CAMTA1	CD34 and cytokeratin variable CAMTA-1 reflects *WWTR1-CAMTA1* gene fusion
Diffuse large B-cell lymphoma	CD20, CD3, BCL-6, PAX 5	
Precursor lymphoma	CD3, CD79A, CD10, TdT	
Anaplastic large cell lymphoma	CD30, EMA, Alk-1; CD2, CD3, CD4	
Plasmacytoma/myeloma	CD138, kappa/lambda, EMA, CD56	EMA positivity in approximately 40% of cases

Cytochemical Examinations

Alkaline phosphatase (ALP) staining is useful in the demonstration of osteoblastic differentiation of tumor cells in aspirates from osteosarcoma as tumor cells from all subtypes of osteosarcoma contain abundant cytoplasmic ALP. Strong ALP positivity confirms the osteosarcoma diagnosis and helps to distinguish it from metastatic carcinoma, malignant melanoma, or anaplastic large cell lymphoma of the bone. ALP staining in the cytologic evaluation of osteosarcoma has been underutilized in previous reports of FNA diagnosis of osteosarcoma. In a series reported from Lund of 59 patients with primary osteosarcoma examined by FNA, strong cytoplasmic ALP positivity could be demonstrated in all 30 cases in which this method was applied on FNA smears [31].

Complications of FNA of the Bone

Complications reported are pneumothorax following needling of tumors in the ribs and neurologic sequel to needling of lesions in the vertebrae [32].

Normal Elements

Osteoblasts

Osteoblasts are most often seen as single cells, occasionally as small cell clusters or rows. They are uniform cells of rounded or triangular shape, with abundant cytoplasm, which often contains a clear "hof" area adjacent to the nucleus. The round nuclei with a central nucleolus are situated very close to the cytoplasmic membrane giving impression of almost protruding through it (see Fig. 16.1).

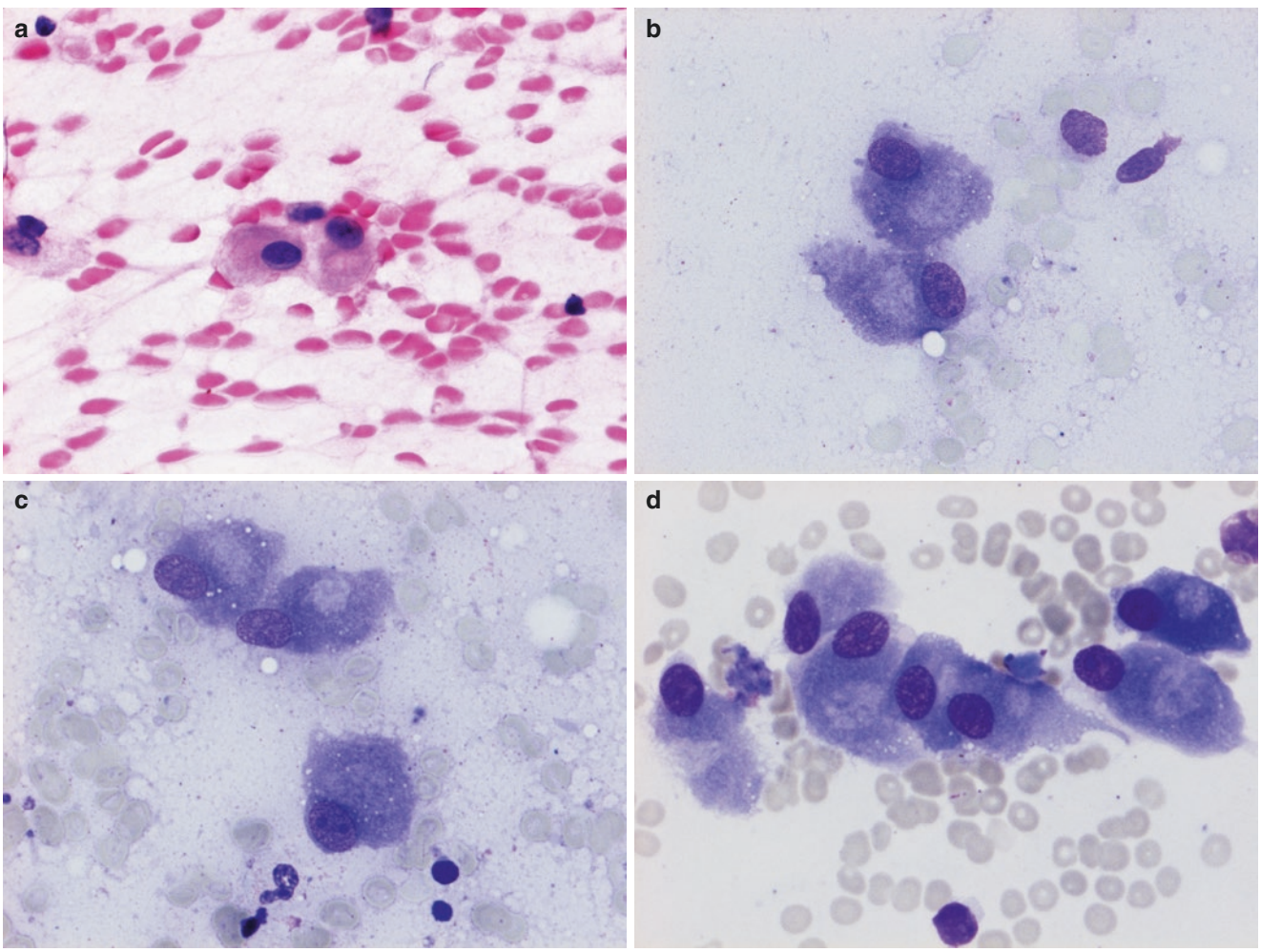

Fig. 16.1 Osteoblasts. (**a**–**d**) Triangular or rounded to oval cells with eccentric nuclei and abundant cytoplasm. Perinuclear clear "hof" visible in most cells (H&E and MGG)

Osteoclasts

Osteoclasts appear as scattered single large cells with abundant cytoplasm and multiple, uniform, round to oval nuclei. In May-Grünwald-Giemsa (MGG)-stained smears, a fine red cytoplasmic granulation is seen (see Fig. 16.2).

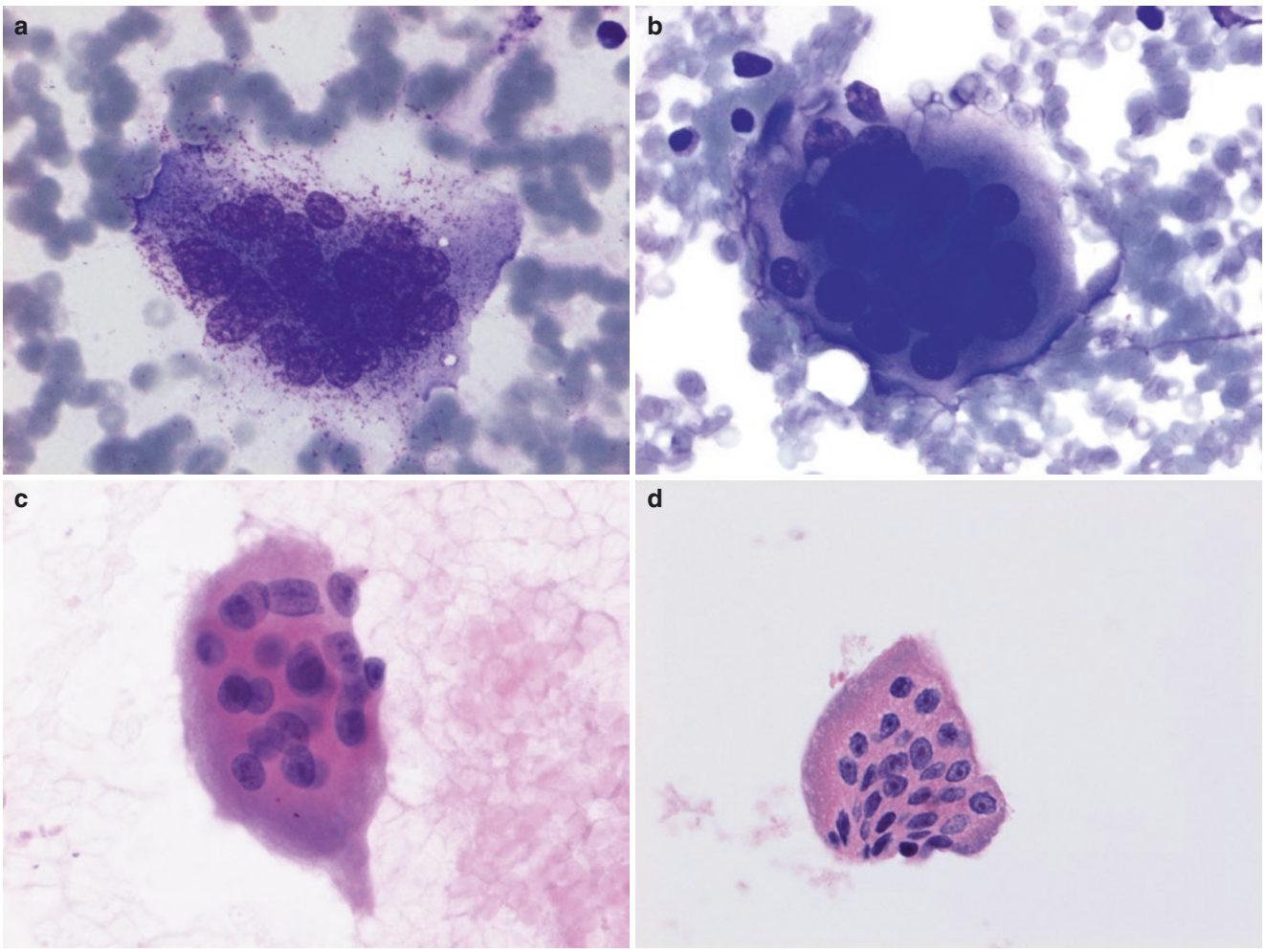

Fig. 16.2 Osteoclasts. (**a**–**d**) Large multinucleated cells with abundant cytoplasm and 12–20 uniform, round to oval nuclei. (**a**) Fine red granulation is often visible in MGG-stained smears (**b** Diff-Quik; **c** H&E; **d** cell block, Cellient; Hologic; Bedford, MA, USA)

Cartilage and Chondrocytes

Fragments of benign cartilage may sometimes be found in FNA smears especially from lesions near joints and osteochondral junctions. These are composed of a hyaline matrix, which is reddish blue to violet with MGG (see Fig. 16.3) or pink with hematoxylin and eosin (H&E) stain. In Papanicolaou-stained preparations, the matrix has a pale grayish red amphophilic fibrillary appearance. Normal chondrocytes present infrequently as a single cell but may be occasionally observed in lacunae in cartilaginous fragments.

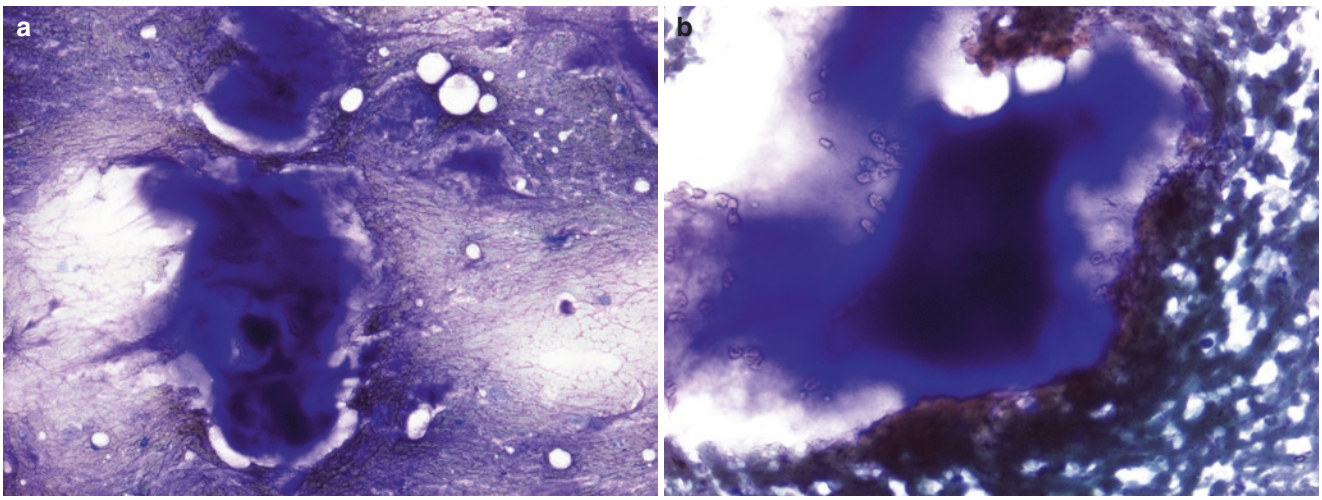

Fig. 16.3 Cartilage and chondrocytes. (**a**, **b**) The cartilage stains red blue to violet in MGG-stained smears. Chondrocytes are rare findings in normal cartilage (MGG)

Bone Marrow Cells

Bone marrow elements may be seen in aspirates from the ribs, vertebrae, and sacrum. They usually appear as a mixture of maturing erythropoietic, myelopoietic cells and megakaryocytes. It is important not to misinterpret immature hematopoietic cells and megakaryocytes as malignant cells (see Fig. 16.4).

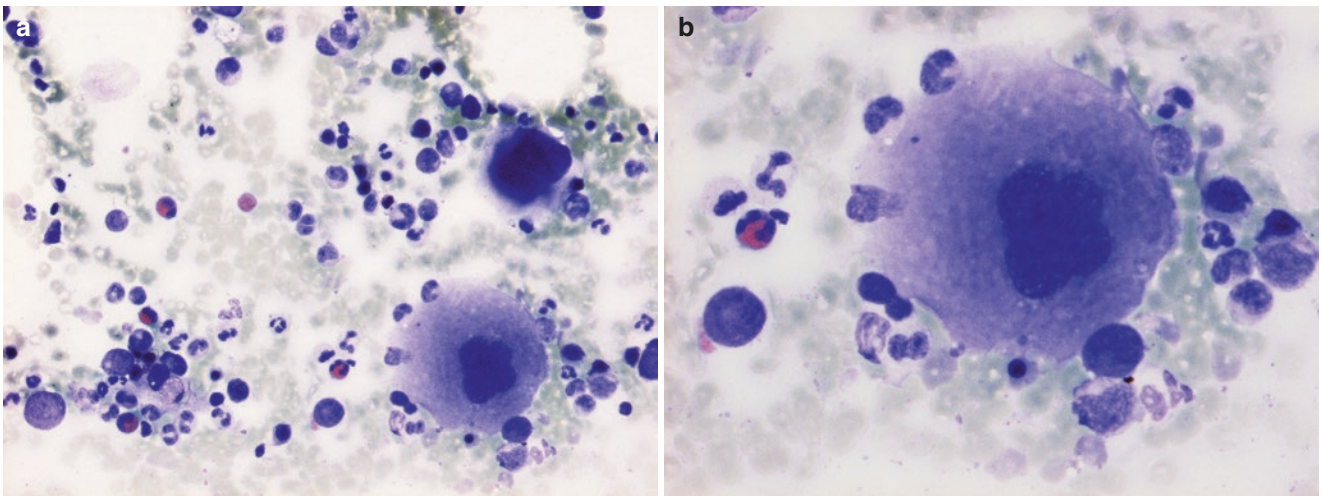

Fig. 16.4 Bone marrow cells. (**a**, **b**) Erythropoietic, myelopoietic cells and megakaryocytes appear occasionally in FNA smears from skeletal lesions. Megakaryocytes must not be misinterpreted as tumor cells (MGG)

Mesothelial Cells

Occasionally, aspirates from vertebral lesions include small flat sheets of mesothelial cells. It is important to distinguish reactive mesothelial cells from carcinoma cells in cases where a FNA is performed for suspected vertebral metastases.

Inflammatory and Nonneoplastic Entities

Osteomyelitis

Most cases of osteomyelitis are of bacterial origin, and *Staphylococcus* is a common pathogen. Anaerobic osteomyelitis is less common. In most cases, infection originates in another site and spreads directly from posttraumatic or operative infections. Acute hematogenous osteomyelitis occurs most often in patients younger than 15 years old but may occur in any age. The long bones are commonly affected.

Cytologic features (*see* Fig. 16.5):
- Abundant smears containing neutrophils
- Necrotic debris
- Histiocytes

Differential diagnosis:
- Langerhans cell histiocytosis

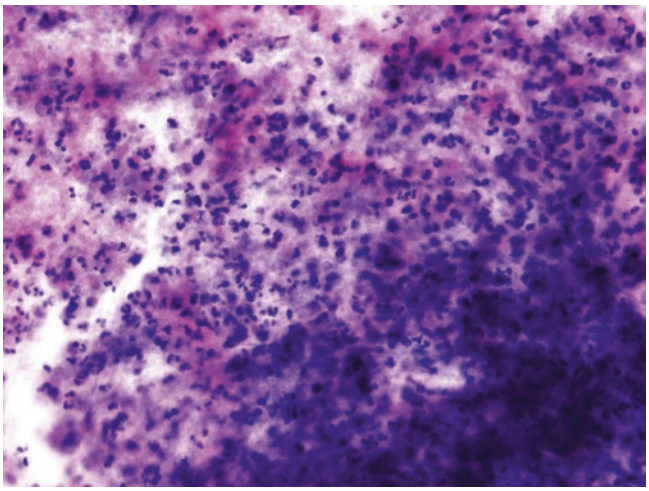

Fig. 16.5 Acute osteomyelitis. Abundant neutrophils and necrotic debris (H&E)

Granulomatous Osteomyelitis (See Fig. 16.6)

Tuberculous osteomyelitis is due to hematogenous spread from the lungs [4]. The most common sites are the vertebra followed by pelvic bones and the knees.

Cytologic features:

- Moderate to abundant smears composed of neutrophils and necrotic debris
- Epithelioid cell granulomas
- Occasional giant cells of Langerhans type

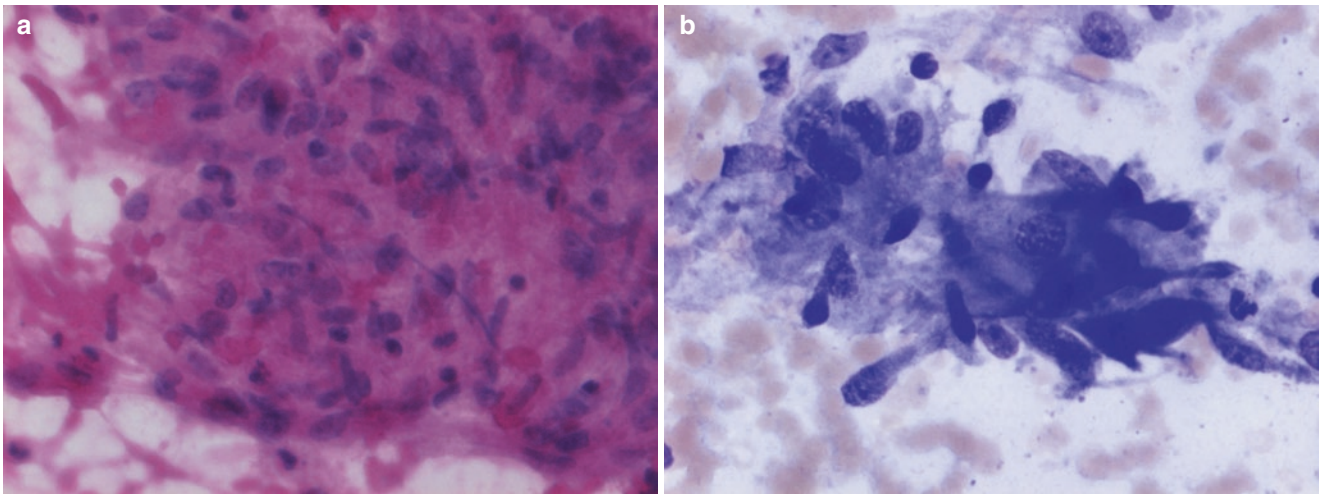

Fig. 16.6 Granulomatous osteomyelitis, tuberculosis. (**a**, **b**) Microscopic feature of granuloma includes clusters of moderately cohesive epithelioid cells with pale elongated nuclei and poorly demarcated cytoplasm (H&E and MGG)

Fracture Callus

Reactive osteoblastic proliferation with osteoid formation, such as seen in fracture callus, may be misdiagnosed as malignant bone neoplasm, commonly osteosarcoma (OS). Thus, fracture callus, a benign lesion, constitutes one of the most important differential diagnoses for OS. Similarly to OS, reactive osteoblasts in callus may display considerable pleomorphism with anisokaryosis and hyperchromatic nuclei with prominent nucleoli (see Fig. 16.7). Their chromatin pattern is quite regular, and the cytoplasmic "hof" is often visible in some cells. Clinical and radiologic correlation is essential to distinguish fracture callus from OS.

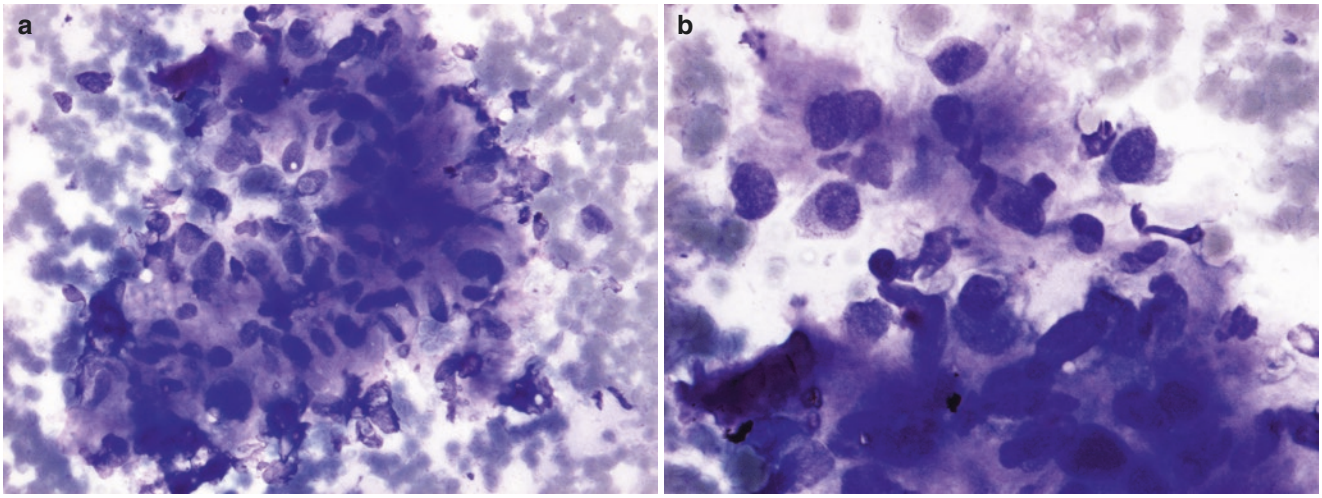

Fig. 16.7 Fracture callus. (**a**, **b**) Clusters of reactive osteoblasts with anisokaryosis and hyperchromatic nuclei embedded in osteoid-like matrix (MGG)

Osteogenic Neoplasm

Osteoid Osteoma and Osteoblastoma

Osteoid osteoma and osteoblastoma are benign osteoblastic tumors with some overlapping radiographic and histologic features. Because of the reactive, sclerotic bone surrounding the nidus, osteoid osteomas are practically never examined by FNAC. In addition, their distinctive clinical and radiographic features allow a correct diagnosis without biopsy in most cases. Osteoblastoma is a rare, intraosseous, benign neoplasm arising mostly often in the first three decades of life. Predilection sites are the spine and sacrum (up to 50% of cases), followed by the proximal and distal femur, proximal tibia, and other bones. Few FNAC cases of osteoblastoma have been reported to date [30, 33–35]. The diagnostic cells in FNA smears are osteoblasts, with eccentric round nuclei and cytoplasm containing often clear "hof." Cell and nuclear size may vary slightly, and binucleated cells may be found. A blue to red or pink matrix can be seen occasionally in cellular clusters on MGG staining (see Fig. 16.8). Cytologic criteria for the so-called aggressive (epithelioid) osteoblastoma have not been defined. FNA of primary bone tumors that exhibit large, atypical osteoblasts with prominent nucleoli should be reported as inconclusive in regard to benign osteoblastoma or osteosarcoma, irrespective of the radiologic features. Surgical biopsy is necessary to establish a correct diagnosis.

Cytologic features:
- Mono- and binucleated osteoblasts, dispersed or in small clusters
- Osteoclasts
- Occasionally small clusters of spindle cells
- Scant osteoid matrix

Differential diagnosis:
- Osteosarcoma

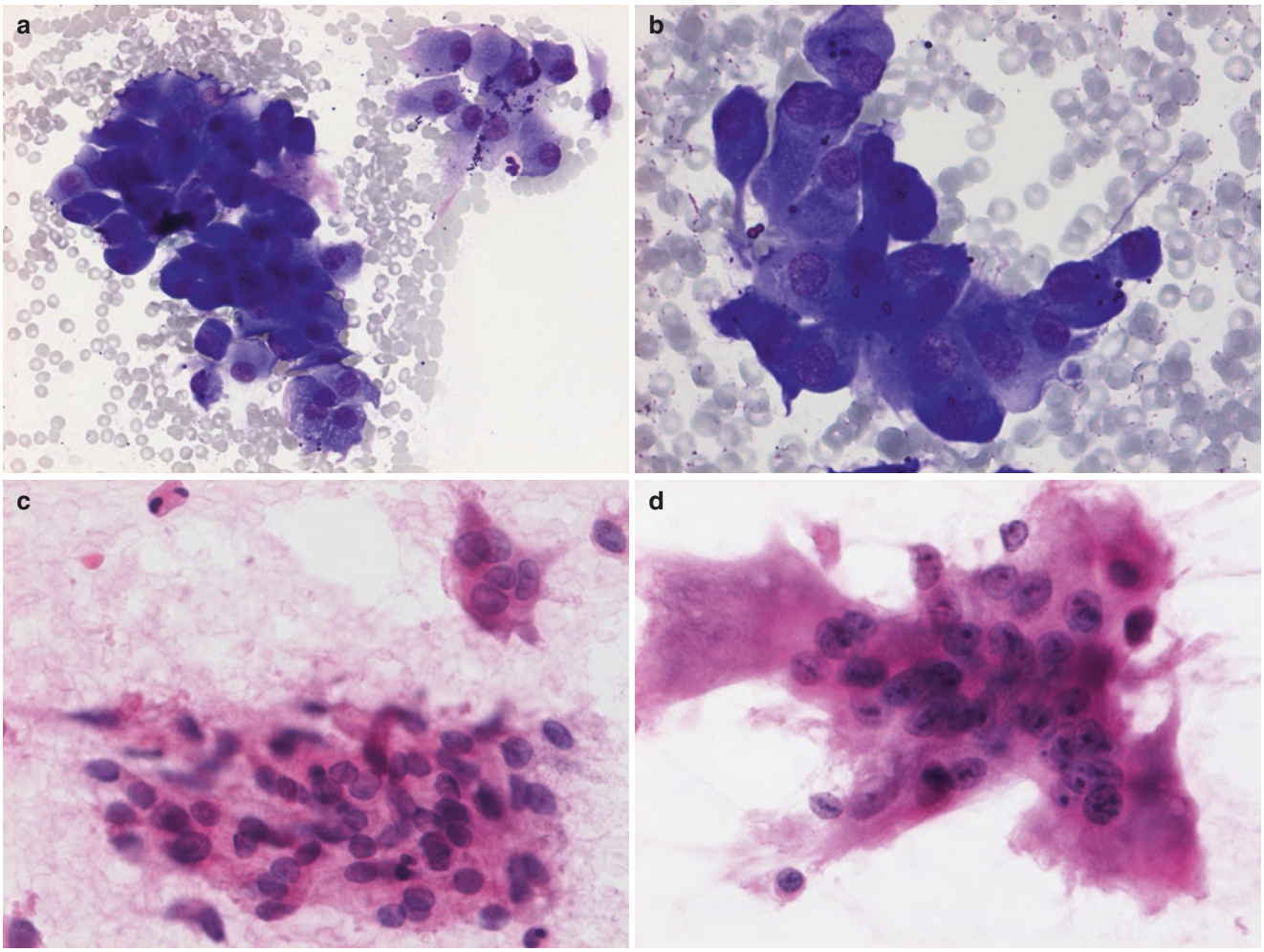

Fig. 16.8 Osteoblastoma. (**a**, **b**) Sheets of slightly pleomorphic osteoblasts (MGG). (**c**) A loosely cohesive cluster of bland oval and spindle cells and multinucleated giant cell. (**d**) Osteoclast-like giant cells mixed with some bland-looking single cells (H&E)

Osteosarcoma

Osteosarcoma (OS) is a primary bone tumor composed of cells, which at least focally produce osteoid. OS is the most frequent primary malignant bone tumor, with an incidence of 2.5 per million populations per year. Eighty to 90% of cases of OS are of the conventional highly malignant type, and the majority of them occur around the knee followed by the humerus and pelvic bones. Approximately 7–10% arise in the craniofacial bones (maxilla and mandible). OS is rare in the spine and in the small bones of hands and feet. The most common presentations are bone mass, often with a soft tissue involvement and pain. Children and young adults are the most affected age group, and a second incidence peak is around age 60. OS also occurs as a form of radiation-associated sarcoma in the bone.

Osteosarcoma shows a broad variation in site and morphologic appearance in both histologic sections and FNA smears [30, 31, 36–45]. The conventional intramedullary OS is a rapidly growing high-grade neoplasm, permeating cortical bone and extending to the surrounding soft tissue. Less common types of OS are periosteal, parosteal, or juxtacortical OS, central low-grade OS, and high-grade surface OS. With regard to microscopic features, most common histologic types are high-grade osteoblastic (see Fig. 16.9) and chondroblastic (see Fig. 16.10) OS, followed by fibroblastic, telangiectatic, and small cell OS.

Cytologic diagnosis of malignant neoplasm is usually facilitated by FNA smears of high-grade conventional OS. The clue to the diagnosis in routinely stained smears is the presence of malignant pleomorphic tumor cells combined with the intercellular osteoid and occasionally osteoblast-like tumor cells (see Fig. 16.11).

To find osteoid and prove osteoblastic differentiation of tumor cells may be difficult since osteoid occurs often focally and is difficult to visualize in smears. Differentiating osteoid from collagenous matrix can be difficult as well.

Osteoid is best appreciated in MGG-stained smears. Strong intracytoplasmic alkaline phosphatase (ALP) staining in tumor cells confirms their osteoblastic differentiation (see Figs. 16.11 and 16.13). ALP staining helps also to distinguishing chondroblastic osteosarcoma from high-grade malignant (grade 3) chondrosarcoma (see Fig. 16.11). Electron microscopic examination is another well-established method to define osteoid in fine needle aspirates.

The architecture of the tumor tissue, calcifications, and osteoid is better appreciated in cell block sections, especially when both malignant cells and strands of osteoid or fragments of cartilage are present in the cell block sections (see Fig. 16.12). Sclerotic intraosseous OS and tumors without cortical bone destruction are difficult to sample by FNA and give often poor yield [31].

Cytologic features of high-grade osteosarcoma:

Osteoblastic subtype
- Variable cellularity, often hypercellular smears
- Admixture of single cells and cell clusters
- Moderately to highly pleomorphic round to ovoid and polygonal tumor cells
- Osteoblast-like tumor cells with eccentric nuclei and a cytoplasmic "hof"
- Clusters of epithelioid tumor cells with distinct cytoplasmic borders and round nuclei with prominent nucleoli
- Multinucleated tumor giant cells
- Strands of osteoid matrix (red gray or purple stained in MGG, pale pink in H&E)
- Mitoses, often atypical
- Benign osteoclast-like giant cells
- Occasional necrosis and calcifications

Chondroblastic subtype [39, 45, 46]
- Myxoid background matrix (red; red violet in MGG)
- Fragments of hyaline cartilage
- Cartilage with atypical chondrocytes in lacunae
- Atypical mono- or binucleated chondroblasts
- Admixture of similar cell population as in osteoblastic osteosarcoma in variable proportions

Differential diagnosis and problems in diagnosis:
- Reactive osteoblastic proliferations as in fracture callus
- Myositis ossificans
- Osteoblastoma
- Giant cell tumor
- Aneurysmal bone cyst
- High-grade chondrosarcoma
- Undifferentiated pleomorphic sarcoma (so-called malignant fibrous histiocytoma [MFH]) and pleomorphic leiomyosarcoma primary in the skeleton
- Primary anaplastic large cell lymphoma in the bone
- Metastatic carcinoma
- Metastatic melanoma

Reactive osteoblastic proliferations such as fracture callus and myositis ossificans are the most important benign lesions that mimic OS. Scattered malignant cells may be overlooked in hypocellular smears from telangiectatic OS. Such FNA samples show a prominent bloody background, osteoclast-like benign giant cells predominating the smears, and only scattered malignant cells; therefore, this pattern may be misdiagnosed as an aneurysmal bone cyst. The multinucleated benign giant cells present in giant cell-rich osteosarcoma may be as numerous as in smears from giant cell tumors. It is important to look for obvious malignant cells and atypical mitoses (see Fig. 16.13). The tumor cells of OS may be clustered and exhibit epithelioid features that can be misdiagnosed as metastatic carcinoma. In addition, metastatic renal cell carcinoma may produce an extracellular matrix, which

can be easily confused with osteoid. Smears from anaplastic large cell lymphoma arising in bone contain large round cells with abundant cytoplasm, eccentric nuclei, and prominent nucleoli resembling osteoblast-like tumor cells in OS. Antibodies to cytokeratins, S-100-protein, HMB45, Melanin A, epithelial membrane antigen (EMA), anaplastic lymphoma kinase (ALK), CD45, and CD30 are suitable markers in the differential diagnosis.

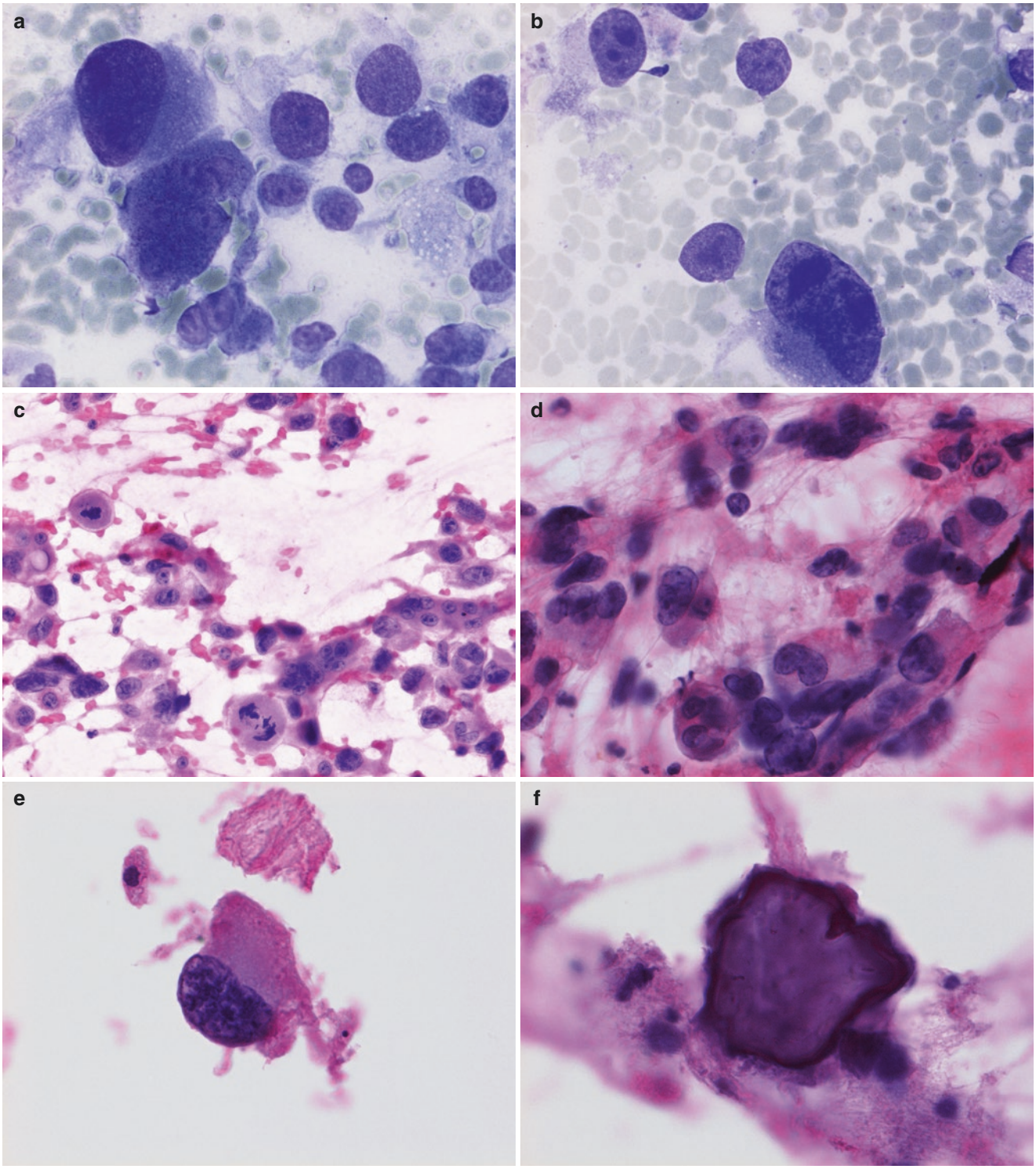

Fig. 16.9 Osteoblastic osteosarcoma. (**a**, **b**) Large, atypical tumor cells with round to oval, irregular nuclei, a moderate amount of cytoplasm, and large macronucleoli (MGG). (**c**, **d**) Poorly cohesive clusters of pleomorphic cells, some with atypical mitoses and admixture of osteoclasts (H&E). (**e**) Pleomorphic tumor cell resembling osteoblast and a small fragment of the bone. (**f**) Calcification seen in liquid-based preparations (H&E; ThinPrep)

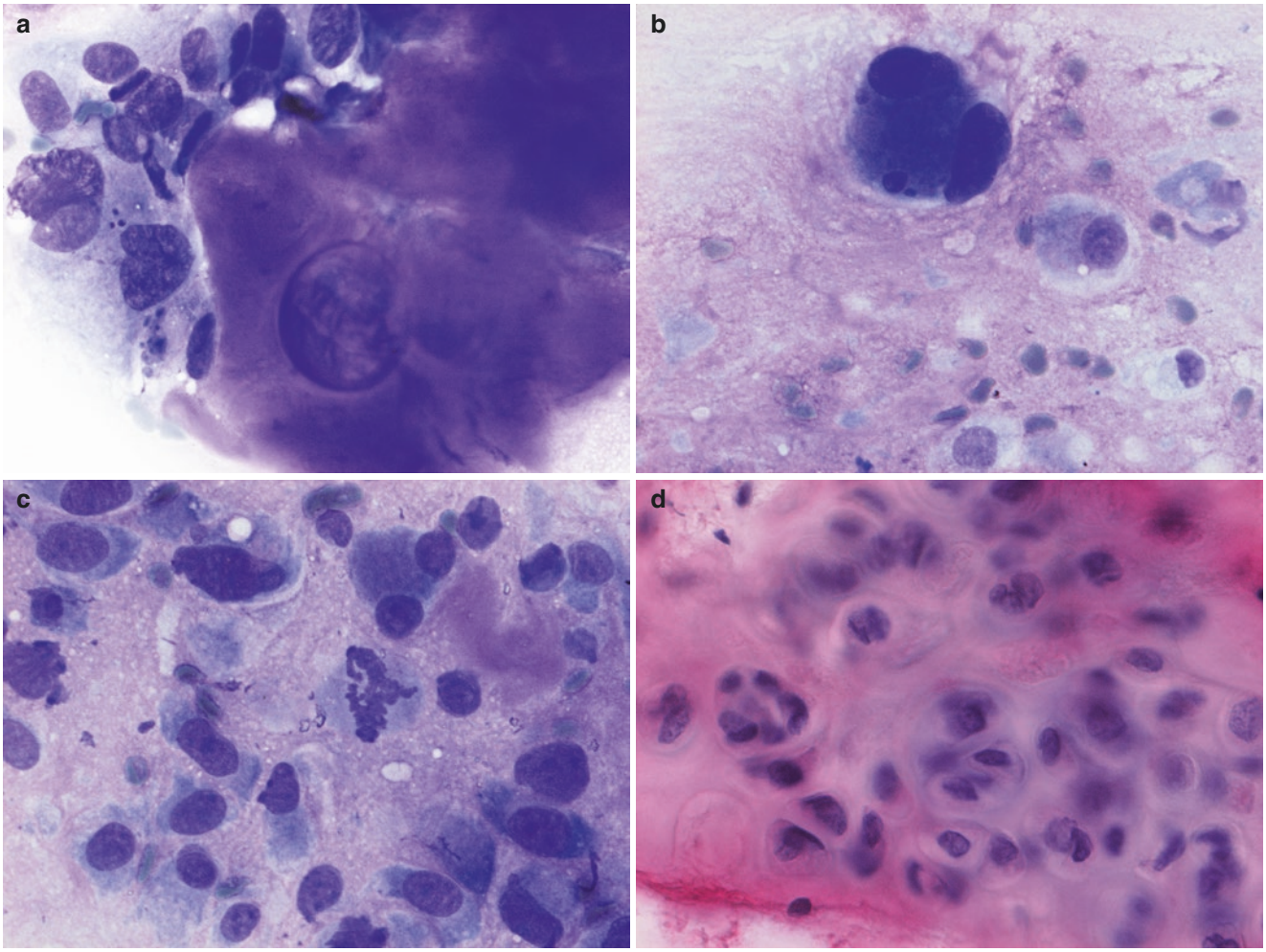

Fig. 16.10 Chondroblastic osteosarcoma. Large, atypical tumor cells (**a**) adjacent to the cartilaginous matrix or dispersed in the myxoid and chondroid background matrix (**b**, **c**), which is more abundant than osteoid matrix. Note tumor cells resembling osteoblasts and mitoses (MGG). (**d**) Malignant cartilage with atypical chondroblasts embedded in a chondroid matrix (H&E)

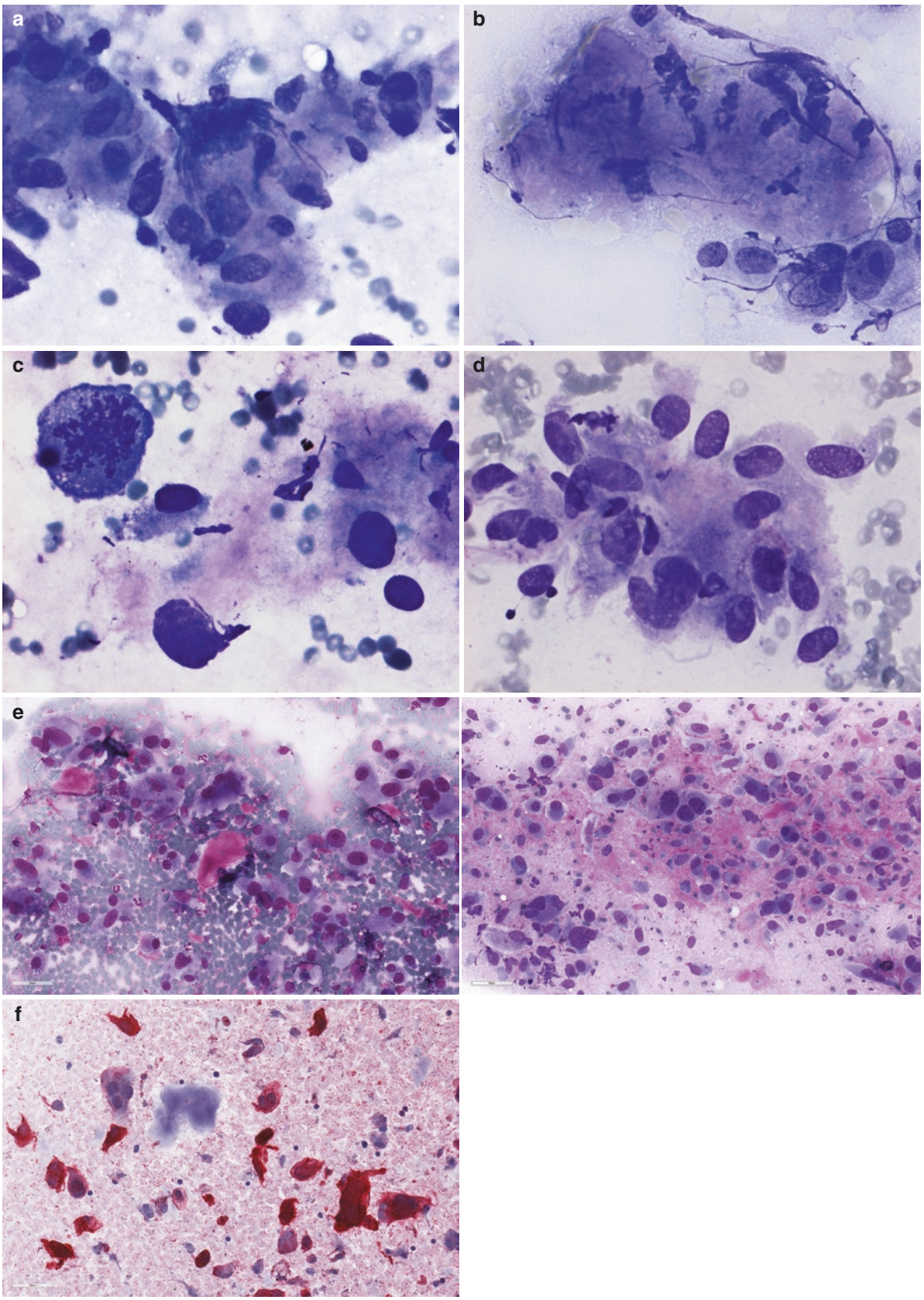

Fig. 16.11 High-grade osteosarcoma. (**a**–**d**) Clusters and dispersed pleomorphic cells with intercellular strands of pinkish-violet matrix consistent with osteoid matrix (MGG). (**e**) In smears from chondroblastic osteosarcoma, it can be difficult to distinguish chondroid matrix from osteoid (MGG). (**f**) Alkaline phosphatase staining stains red cytoplasm of cells with osteoblastic differentiation, whereas cartilage is unstained

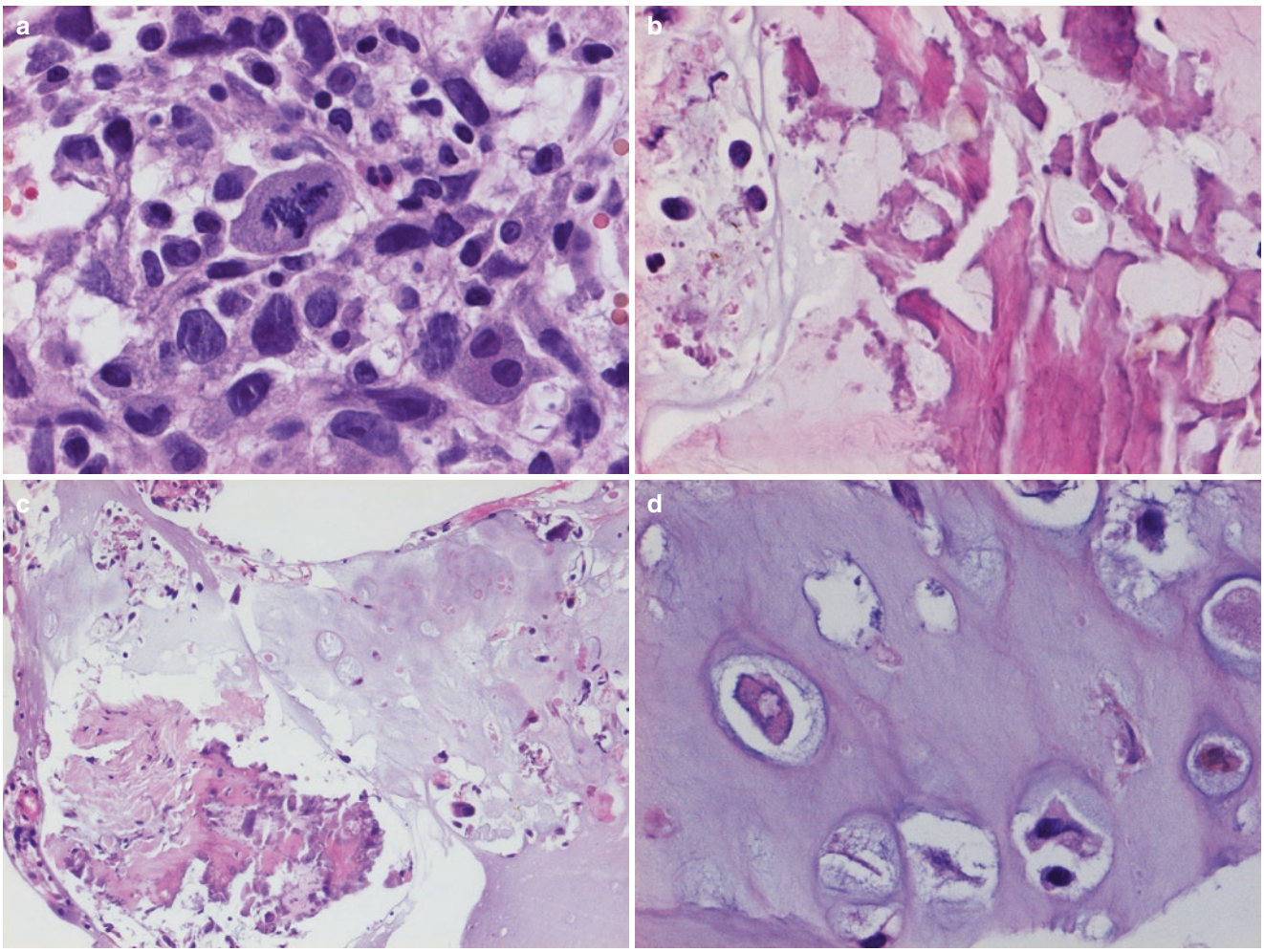

Fig. 16.12 High-grade osteosarcoma. Cell block sections appreciate diagnostic features of osteosarcoma. (**a**) High-grade sarcoma with pleomorphic malignant cells and mitoses. (**b**) Clearly visible strands of osteoid. (**c**, **d**) Clear chondroblastic differentiation in high-grade chondroblastic osteosarcoma (H&E)

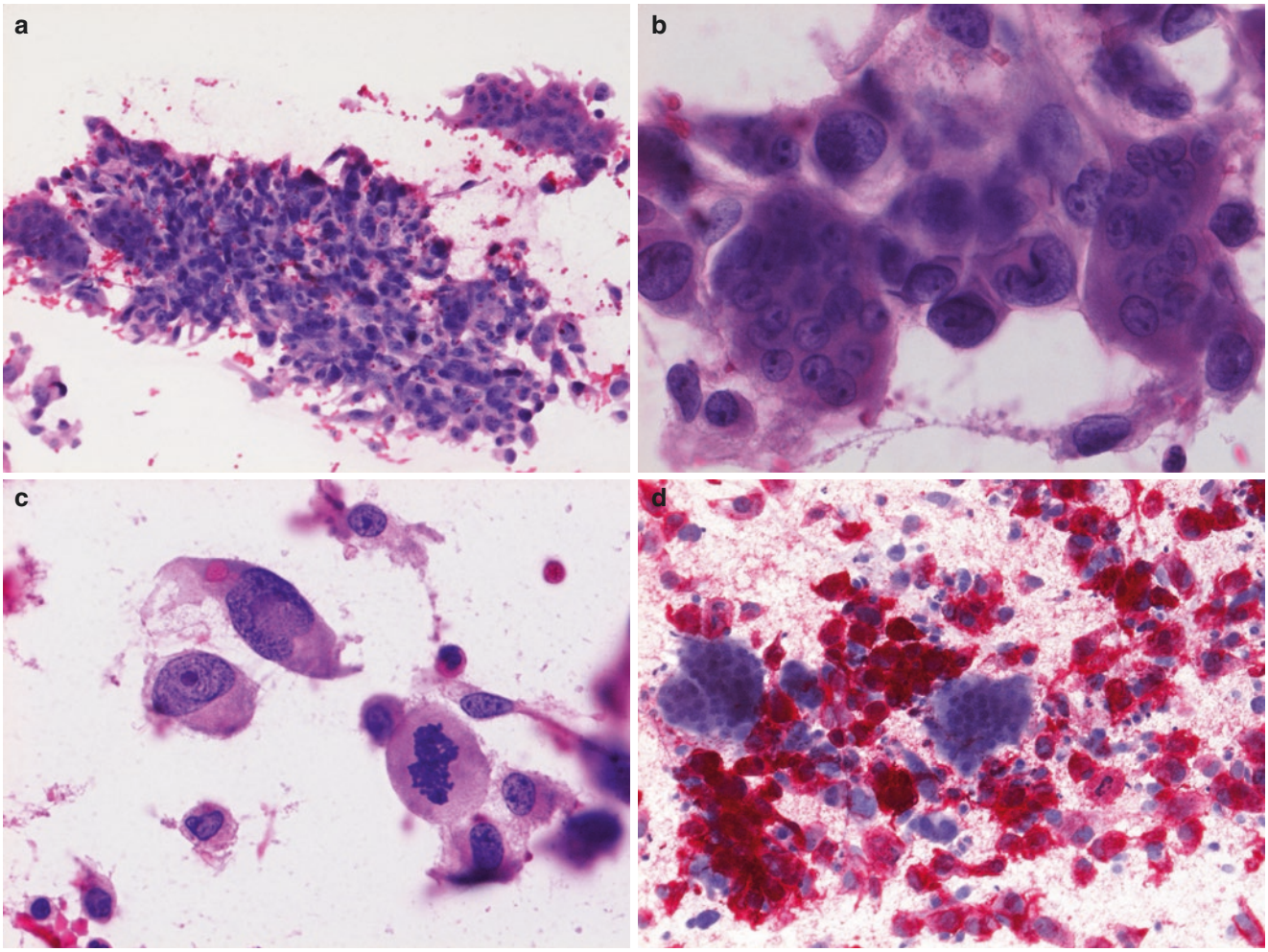

Fig. 16.13 Giant cell-rich osteosarcoma. (**a**–**c**) Smears resembling giant cell tumor but clearly pleomorphic tumor cells consist with highly malignant neoplasm (H&E). (**d**) Positive alkaline phosphatase staining in tumor cells but negative staining in the osteoclast-like giant cells (alkaline phosphatase stain)

Fibroblastic Osteosarcoma

Experience of the fibroblastic type is limited to single case reports. FNA smears contain predominantly slight to moderate pleomorphic spindle-shaped cells with fusiform nuclei and coarse chromatin. Osteoid is difficult to find (see Fig. 16.14).

Small Cell Osteosarcoma

The cytology of rare small cell osteosarcoma has been only briefly described [44, 47].

The main cytologic feature was a mixture of cohesive fragments and dispersed small- to medium-sized (three to four times of small mature lymphocytes). Slightly pleomorphic cells with round- or spindle-shaped nuclei, finely granular chromatin, and a high nuclear/cytoplasmic ratio. Identification of osteoid matrix is the key to the diagnosis but can be difficult (see Fig. 16.14).

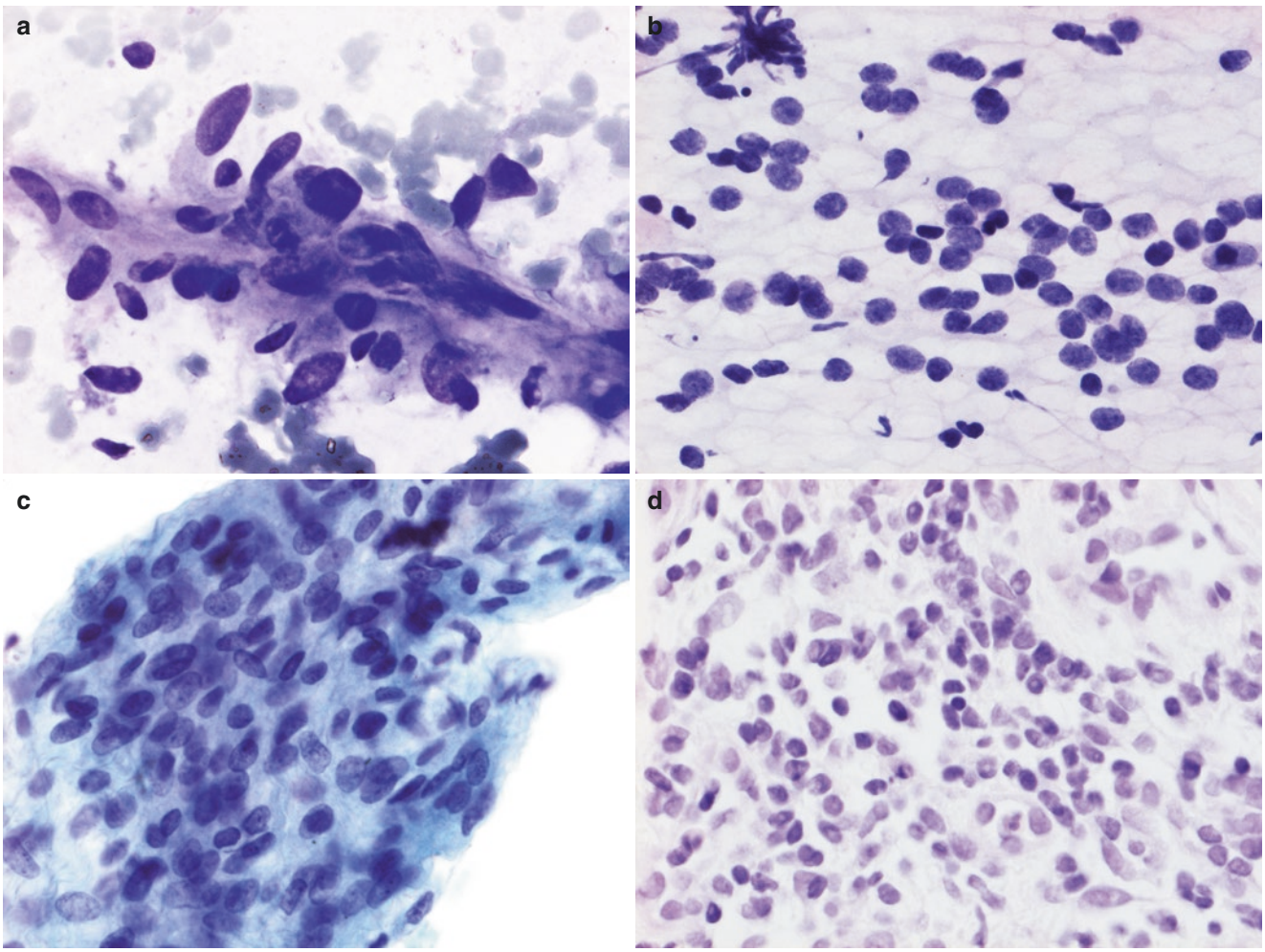

Fig. 16.14 (**a**) Fibroblastic osteosarcoma. Clusters of moderately atypical spindle cells embedded in osteoid-like matrix (MGG). Small cell osteosarcoma. (**b**, **c**) FNA smears (H&E and Pap stain). (**d**) Cell block. Small- to medium-sized tumor cells with rounded nuclei and scanty cytoplasm resembling Ewing sarcoma (H&E)

Parosteal Osteosarcoma

FNA diagnosis of parosteal osteosarcoma, a rare type of low-grade osteosarcoma arising on the surface of the bone, is difficult if not impossible [31–48]. The yield was very poor, consisting of scattered mildly atypical spindle cells and small fragments of cartilage. Parosteal osteosarcomas are less suitable for FNA than other types of osteosarcoma. Core needle biopsy with correlation of characteristic radiologic findings is the key to a successful preoperative diagnosis (see Fig. 16.15).

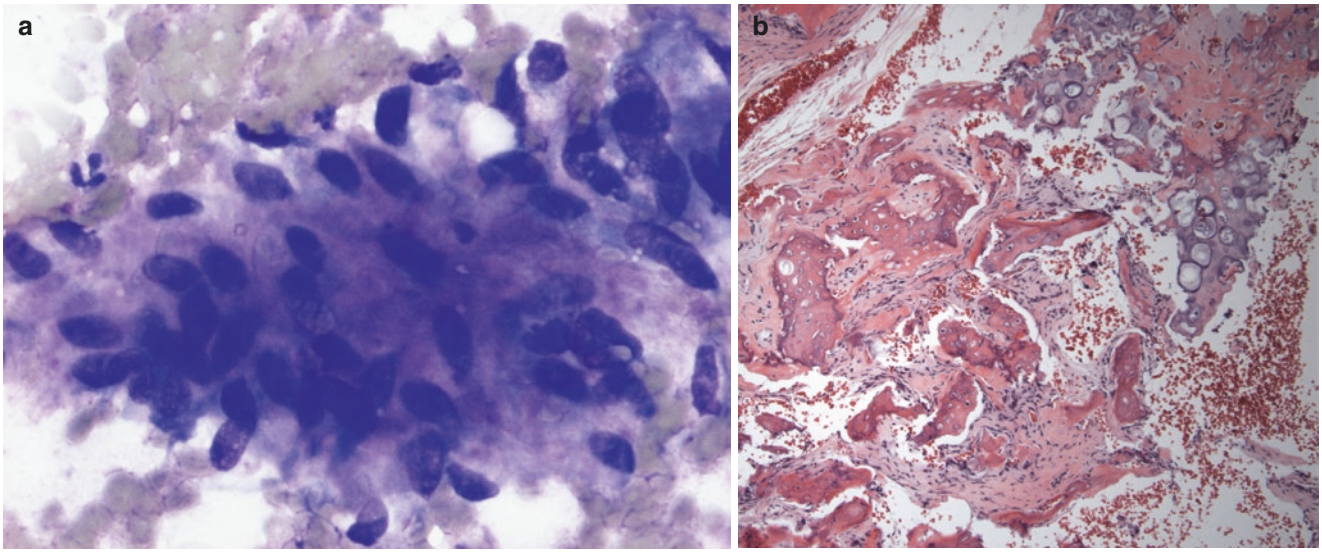

Fig. 16.15 (**a**) Parosteal osteosarcoma. Clusters of slightly atypical spindle cells embedded in osteoid-like matrix (MGG). (**b**) Histologic section showing trabeculae of neoplastic woven bone surrounded by atypical spindle cells and strands of cartilage (H&E)

Chondroblastic Tumors

Osteochondroma

Osteochondroma is the most common benign neoplasm of the bone, accounting for 10% of all bone neoplasms. FNA smears from osteochondroma contain usually fragments of cartilage sampled from the cartilaginous cap (see Fig. 16.16). Typical osteochondroma is rarely sampled by FNAC as its radiologic appearances are diagnostic. Occasionally malignant transformation (chondrosarcoma) of osteochondroma occurs, and FNAC may be requested to help establish the diagnosis. The presence of significant cellular and nuclear pleomorphism and myxoid matrix may suggest malignant transformation; however, the morphology of malignant transformation is often quite subtle. Therefore, correlation with radiology is essential, and surgical biopsy remains necessary to confirm the diagnosis.

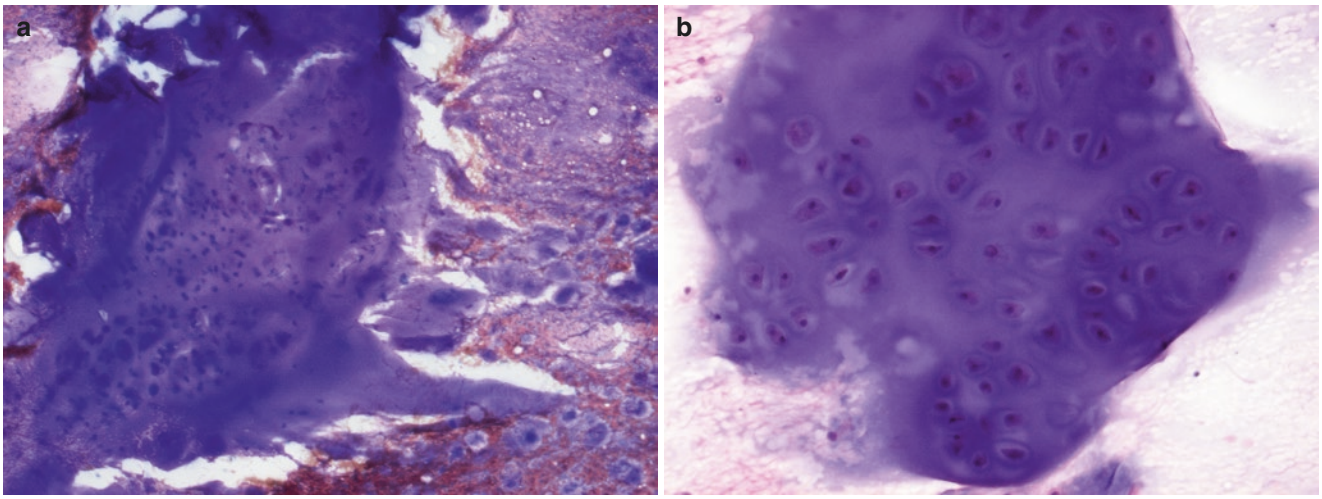

Fig. 16.16 Osteochondroma. (**a**, **b**) FNA smears contain large fragments of cartilage with uniformed chondrocytes in lacunae (MGG and H&E)

Chondroma

Chondromas may present as single or multiple lesions and are composed of mature hyaline cartilage interspersed with areas of degenerative cartilage. Chondromas are the most common tumors in the small bones of the hands and feet.

Cytologic features:
- Cartilaginous fragments containing cells in lacunar spaces
- Cells with small regular nuclei
- Mild cytologic pleomorphism

Diagnostic specimens from chondromas are sampled easily. Characteristically, smears contain numerous fragments of cartilage; dispersed cells are uncommon. Cartilage fragments stain strongly violet or blue violet with MGG and faintly pink with H&E. Small round and uniform cells with regular nuclei are seen in lacunae within cartilage fragments (see Fig. 16.17). Binucleated cells are not found, but the cartilage may focally exhibit high cellularity and cytologic pleomorphism, especially in chondromas of small peripheral bones. Focal nuclear atypia and pleomorphism should not be mistaken for signs of malignancy.

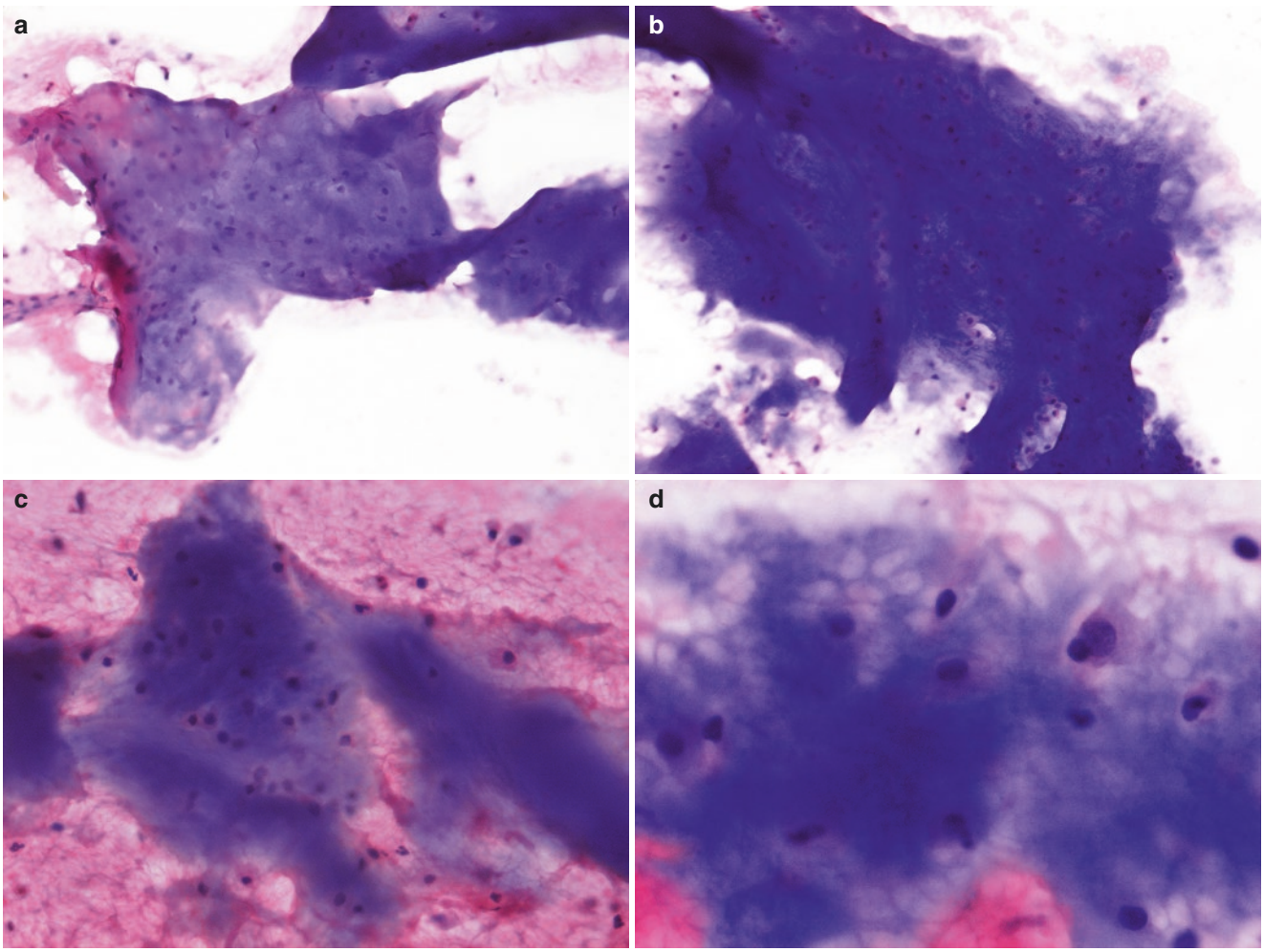

Fig. 16.17 Chondroma. (**a**, **b**) Fragments of cartilage with areas of random scattered uniform chondrocytes, some in lacunar spaces. (**c**, **d**) Some chondrocytes showing slight atypia (H&E)

Chondroblastoma

Chondroblastomas occur in children and adolescents with an immature skeleton, especially in the second decade of life, with slight prevalence in males. The most common site is the epiphysis of long bones, but small tubular and flat bones can also be affected. The tumor is composed of immature chondroblasts and osteoclast-like giant cells, with focal calcifications and occasional areas resembling an aneurysmal bone cyst. Chondroblastomas are often painful.

Cytologic features:

- Mononuclear chondroblasts characterized by well-defined cytoplasm and round nuclei
- Multinucleated osteoclast-like cells
- Fragments of chondroid matrix

The FNA smears are usually diagnostic, with a mixed pattern of fragments of chondroid matrix, mononuclear chondroblasts, and multinucleated osteoclasts [49–51]. The most characteristic finding is the presence of distinctive chondroblasts, which have monomorphic or slightly pleomorphic round to oval nuclei placed centrally or slightly eccentrically and well-demarcated cytoplasm. Nuclei may vary in size and binucleated cells may be present. Mitoses are uncommon. Acellular fragments of cartilage are often seen in the smears, staining red to reddish blue with MGG and faintly eosinophilic in H&E preparations (see Fig. 16.18).

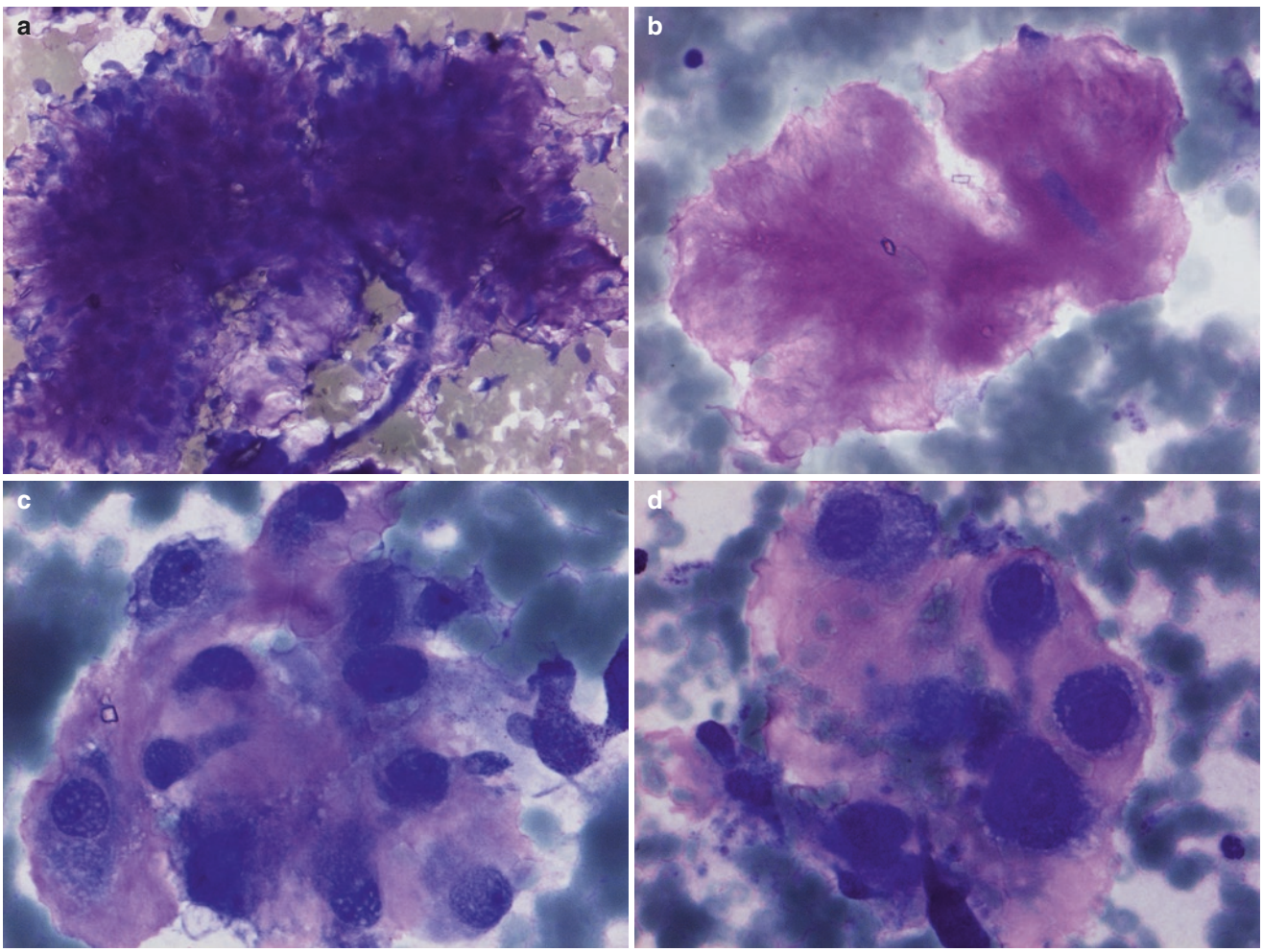

Fig. 16.18 Chondroblastoma. (**a**) In scanning power cohesive cluster of uniform round to oval cells embedded in the chondroid matrix. (**b**) Acellular fragment of a cartilaginous matrix. (**c**, **d**) Mononuclear rounded cells with rather abundant well-defined cytoplasm embedded in the chondroid matrix (MGG)

Chondromyxoid Fibroma

Chondromyxoid fibroma is a rare, benign cartilaginous tumor of young adults in second and third decades of life. Chondromyxoid fibroma arises usually in the metaphyseal region of long tubular bones, especially the tibia. FNA smears contain fusiform stellate or spindle cells and chondroblast-like cells embedded in fragments of cartilaginous–myxoid tissue. Spindle cells vary in size, but both chondroblast-like cells and spindle cells may show moderate pleomorphism with plump nuclei and small but prominent nucleoli (see Fig. 16.19).

Cytologic features:

- Myxoid background matrix
- Cartilaginous fragments (with chondroblast-like cells in lacunae)
- Dispersed or clustered stellate or spindle-shaped myofibroblastic cells
- Osteoclastic giant cells

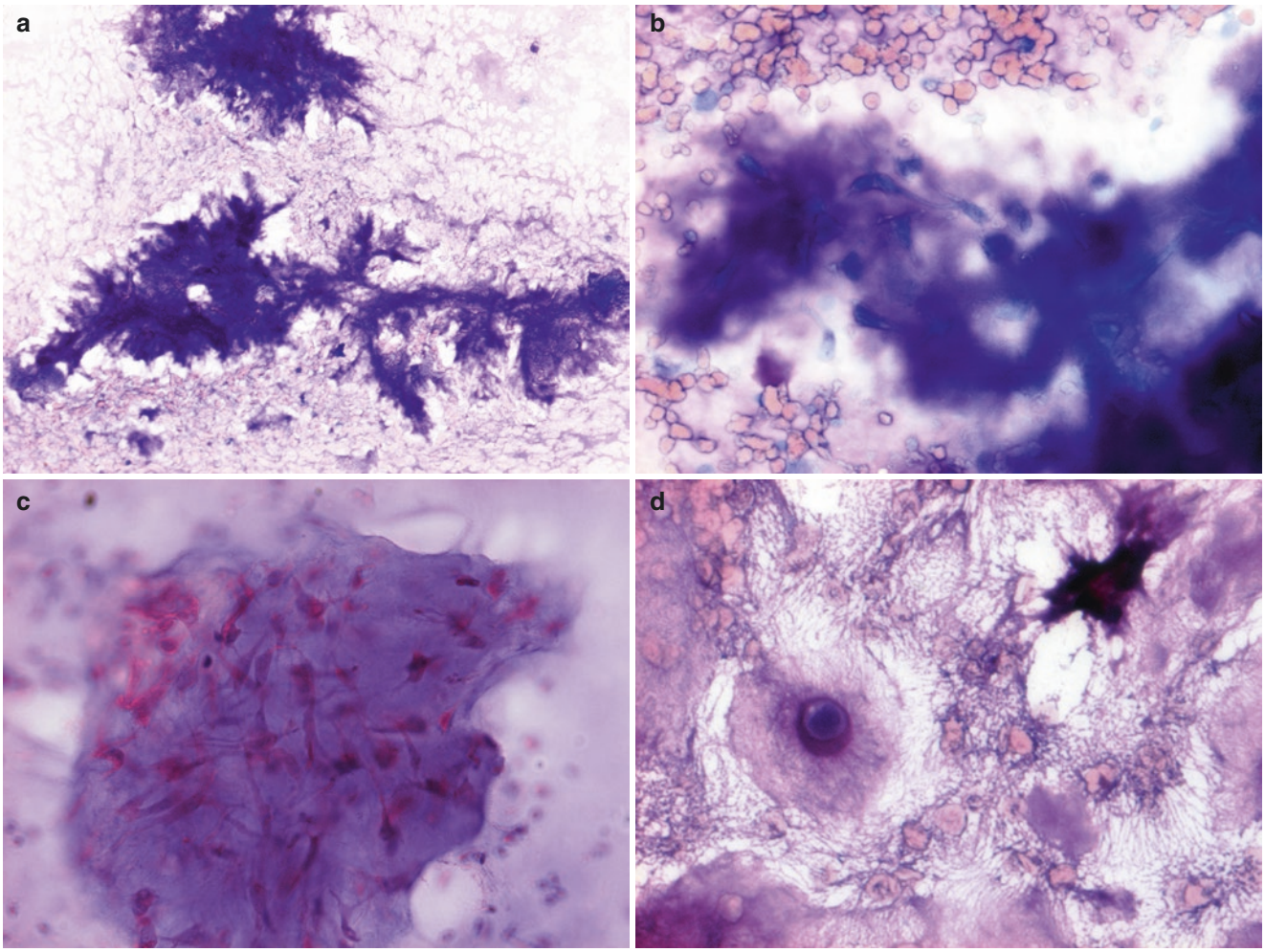

Fig. 16.19 Chondromyxoid fibroma. (**a**) FNA smears with fragments of cartilaginous–myxoid tissue (MGG). (**b**, **c**) Fusiform, stellate, or spindle cells embedded in cartilaginous tissue fragments in high-power view (MGG; H&E). (**d**) Chondroblast- or chondrocyte-like cells occur in the myxoid background (H&E)

Chondrosarcoma

This group of tumors occur in adults, predominantly in the fourth to seventh decades of life. Tumor predilection sites are the large bones of axial skeleton with majority of chondrosarcomas occurring in the femur, humerus, pelvic bones, and ribs. Uncommon sites are acral and extraskeletal regions. Results from several studies confirm that grading of chondrosarcomas is important in predicting prognosis. It is important to separate grade 1 from grade 2 or higher chondrosarcoma as most low-grade chondrosarcomas often have a clinical course and prognosis comparable with benign chondroma [52].

Most chondrosarcomas are convenient targets for FNA and often yield richly with fragments or "microbiopsies" of tumor tissue in smears. The cytology of chondrosarcoma has been described in three rather large series [52–54]. The cytologic features are closely related to the grade of malignancy [9, 54, 55].

Low-grade chondrosarcomas yield tumor cells in fragments of variable size, and dispersed cell pattern is an infrequent finding. Variable cellularity occurs in the fragments of cartilaginous tissue, with some cells lying in lacunar spaces. Individual tumor cells display a slight to moderate atypia, but some of them are binucleated (see Fig. 16.20).

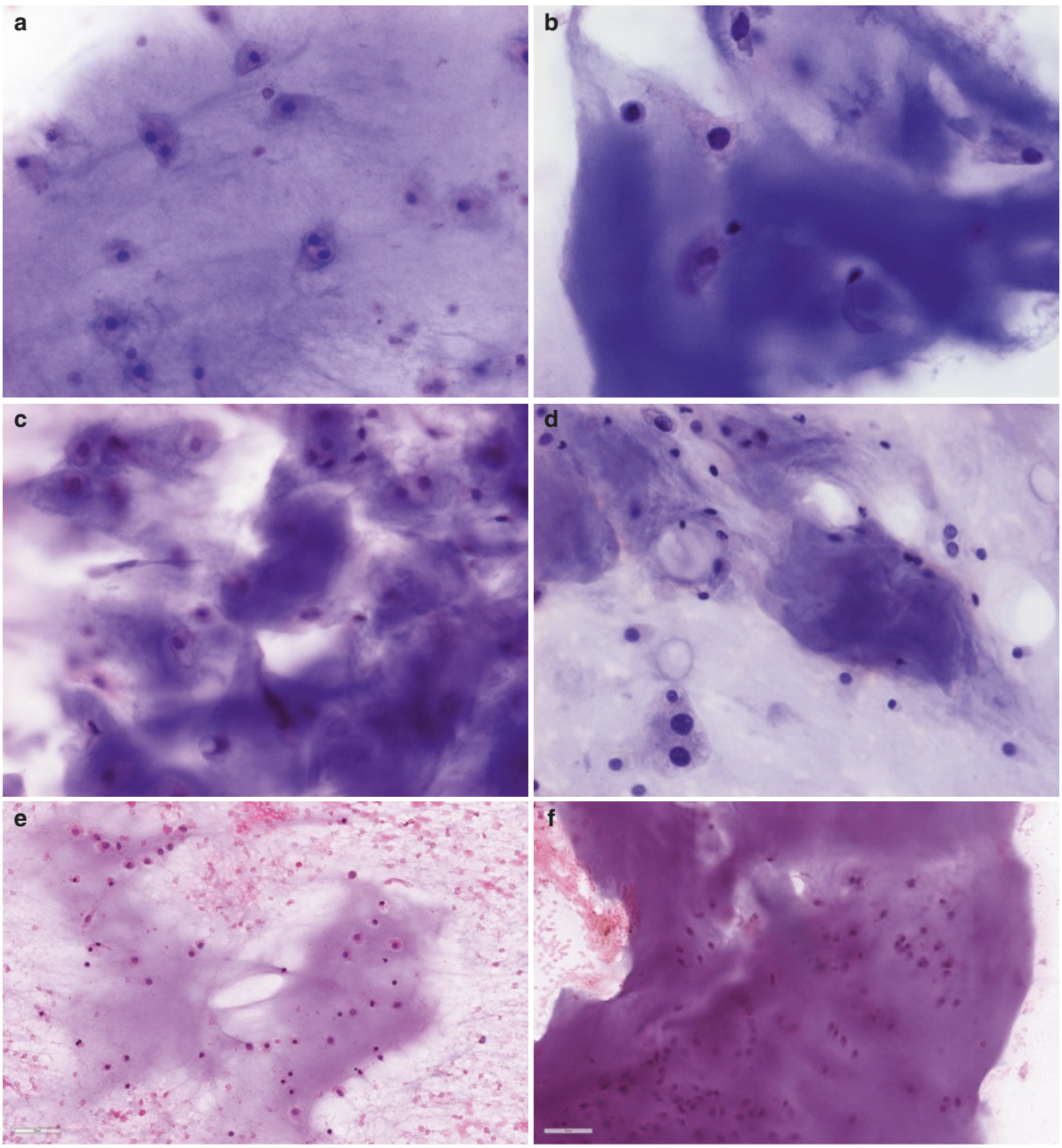

Fig. 16.20 Chondrosarcoma, G1. (**a**–**f**) Cartilaginous fragments containing randomly distributed uniform or slightly atypical cells, many of them in lacunar spaces. Note binucleated chondrocytes (H&E)

Smears from high-grade (grades 2 and 3) chondrosarcoma are generally hypercellular with cellular tissue fragments and often prominent myxoid background matrix. As a rule of thumb, the number of fragments is lower than in low-grade neoplasms, and dispersed tumor cells are much more common (see Figs. 16.21 and 16.22). The cellular and nuclear pleomorphism is marked, and occasional mitoses may be seen in smears, especially in grade 3 tumors (see Fig. 16.23).

Dedifferentiated chondrosarcoma progresses in approximately 10–15% of chondrosarcomas and has a very aggressive clinical course. The most common sites of involvement include the distal femur, pelvis, and humerus. The transition from a

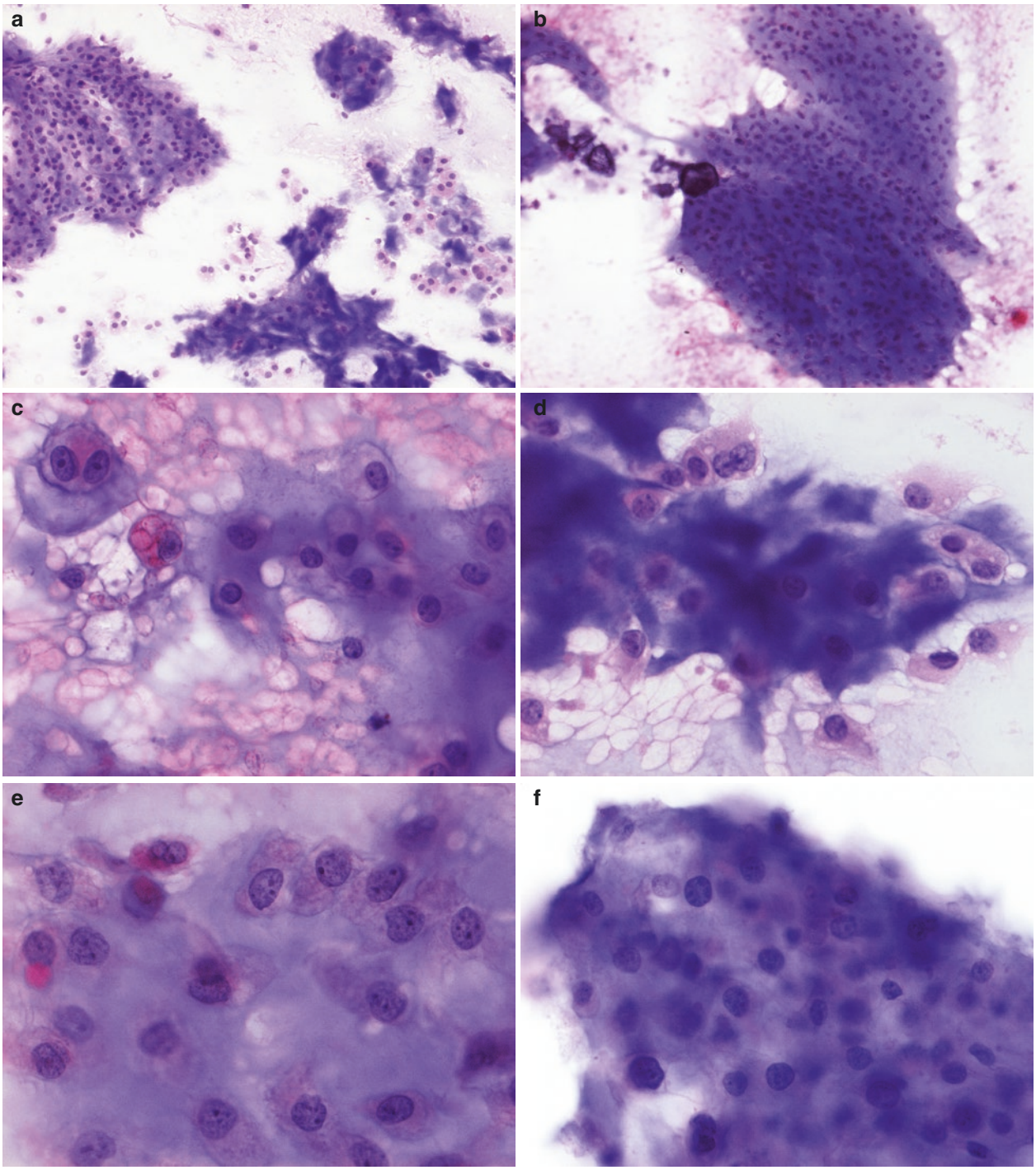

Fig. 16.21 Chondrosarcoma, G2. (**a**–**f**) These aspirates from different tumors show the difficulty of chondrosarcoma grading and making the distinction between G1 and G2 chondrosarcomas in FNA smears. Fragments of hyaline cartilage with variable cellularity. Occasional calcifications. Cellular areas indicate G2 tumor. Rather uniform tumor cells with slight to moderate nuclear atypia and occasional small nucleoli (H&E)

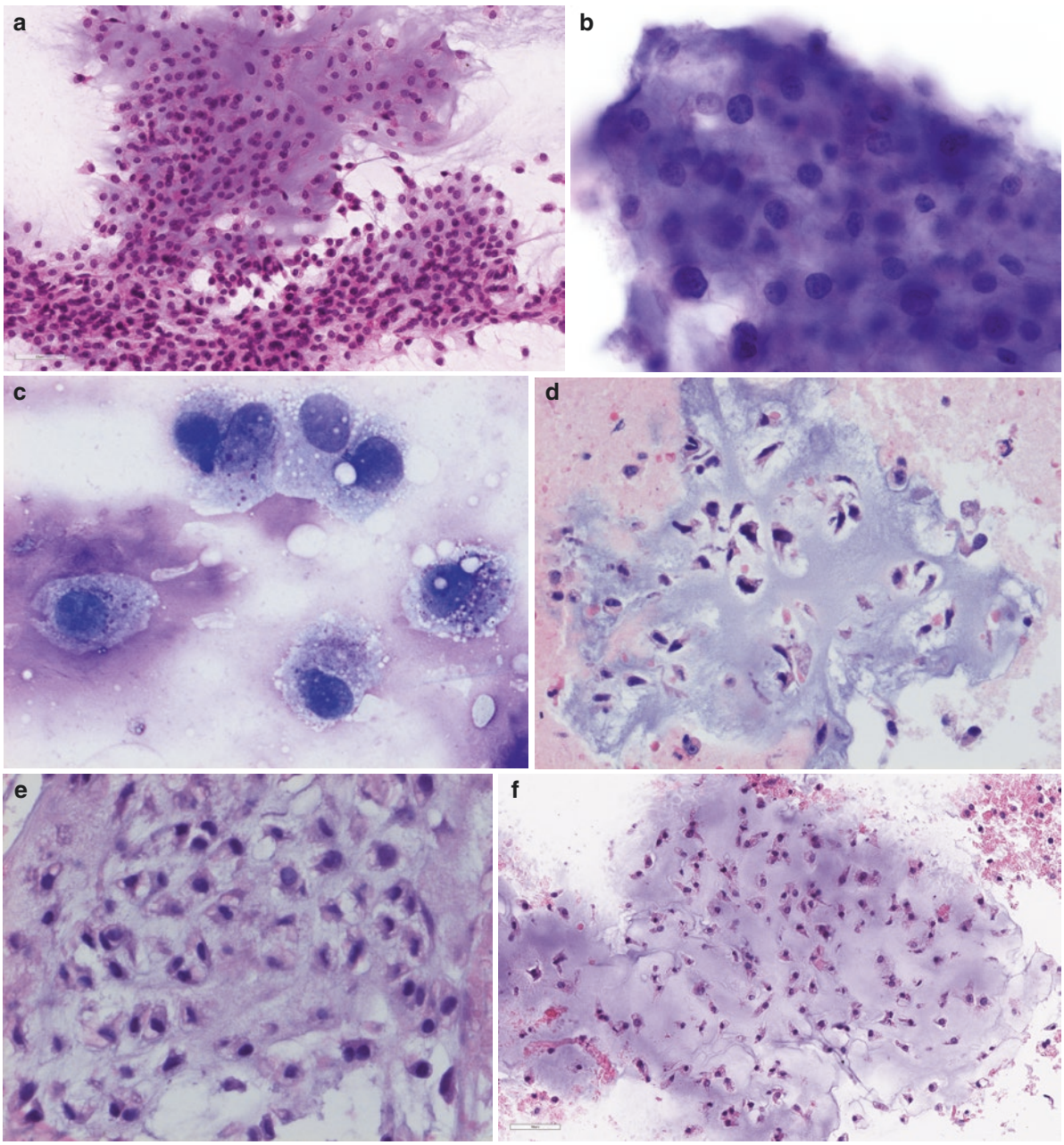

Fig. 16.22 Chondrosarcoma, G2. (**a**, **b**) Fragment of cartilage with cellular area (H&E, MGG). (**c**) Moderately atypical chondrocytes with abundant cytoplasm (MGG). (**d**–**f**) Cell blocks with moderately cellular cartilaginous tissue, moderately atypical chondrocytes, and myxoid areas indicative of G2 chondrosarcoma (H&E)

low-grade chondrosarcoma component to a high-grade noncartilaginous pleomorphic sarcoma area is usually abrupt, and the proportions of two components are very variable. Sampling only one of the components is a common pitfall in the FNAC diagnosis of this bimorphic sarcoma (see Fig. 16.23).

Cytologic features:

- Fragments of hyaline cartilage
- Myxoid background matrix
- Variable cellularity within the cartilaginous fragments
- Mononuclear and binucleated tumor cells often in lacunae
- Large round individual cells with well-defined cytoplasm and irregular, lobulated nuclei
- Number of dispersed cells and degree of pleomorphism increase in higher-grade tumor
- Presence of noncartilaginous pleomorphic sarcoma suggesting dedifferentiation

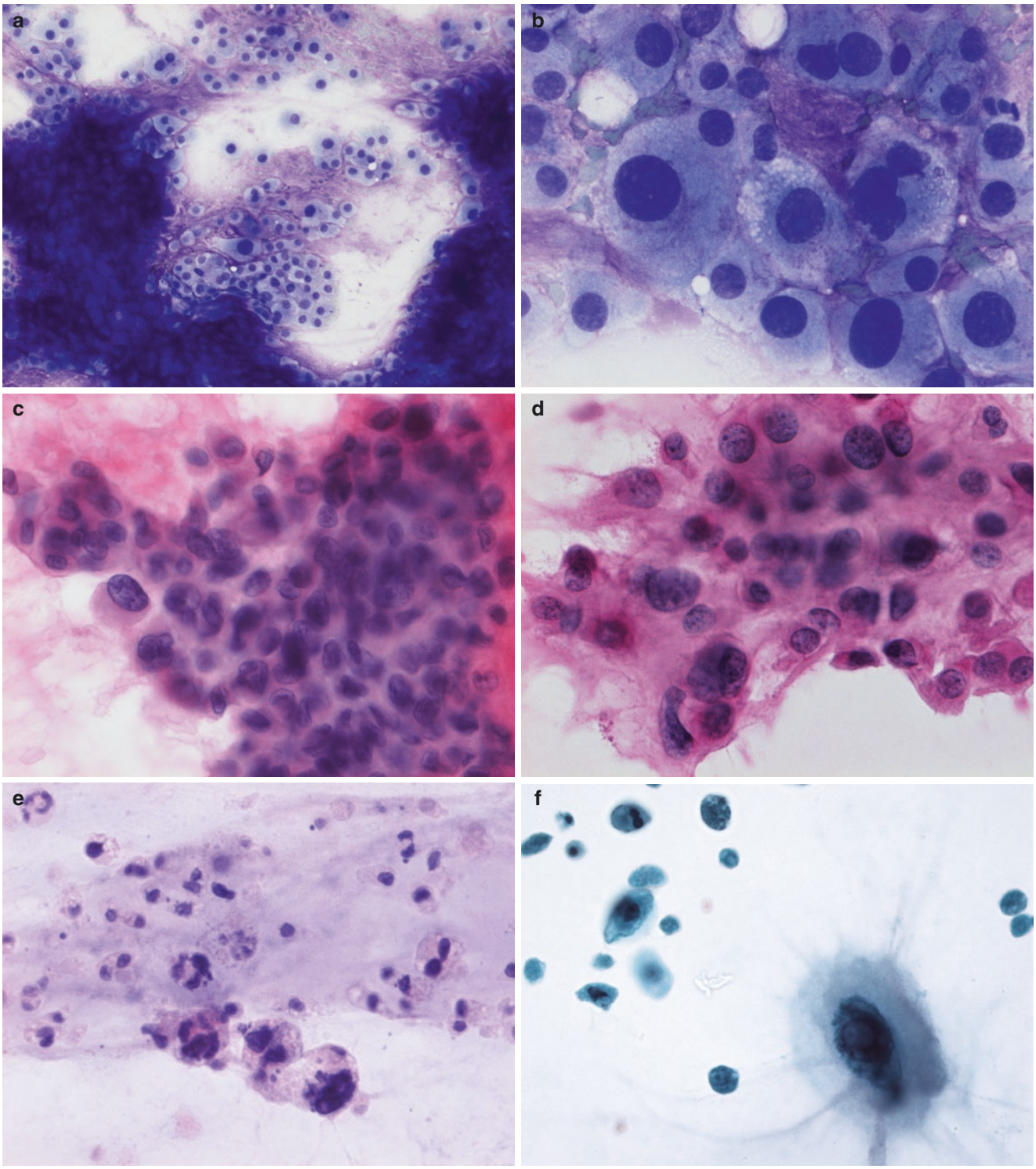

Fig. 16.23 High-grade chondrosarcoma (grade 3). (**a**, **b**) Compared to low-grade chondrosarcoma, there is increased cellularity and marked cellular and nuclear atypia (MGG). (**c**–**e**) Tumor fragments are highly cellular with moderate to marked nuclear pleomorphism, myxoid background matrix, and necrosis, obscuring the nuclear details (H&E). (**f**) Dedifferentiated chondrosarcoma: sampling only one of the components is a common pitfall in the FNAC diagnosis of this bimorphic sarcoma (Pap stain)

Clear Cell Chondrosarcoma

Clear cell chondrosarcoma is a rare variant of low-grade chondrosarcoma, arising in the epiphyses of long bones. The FNA smears are cellular and dominated by large epithelioid tumor cells with abundant finely vacuolated cytoplasm, a central nucleus, and prominent nucleoli (see Fig. 16.24). Fragments of cartilage and occasional osteoclast-like cells are also present. The main differential diagnoses include chondroblastoma and metastatic carcinoma, especially clear cell renal cell carcinoma [56, 57].

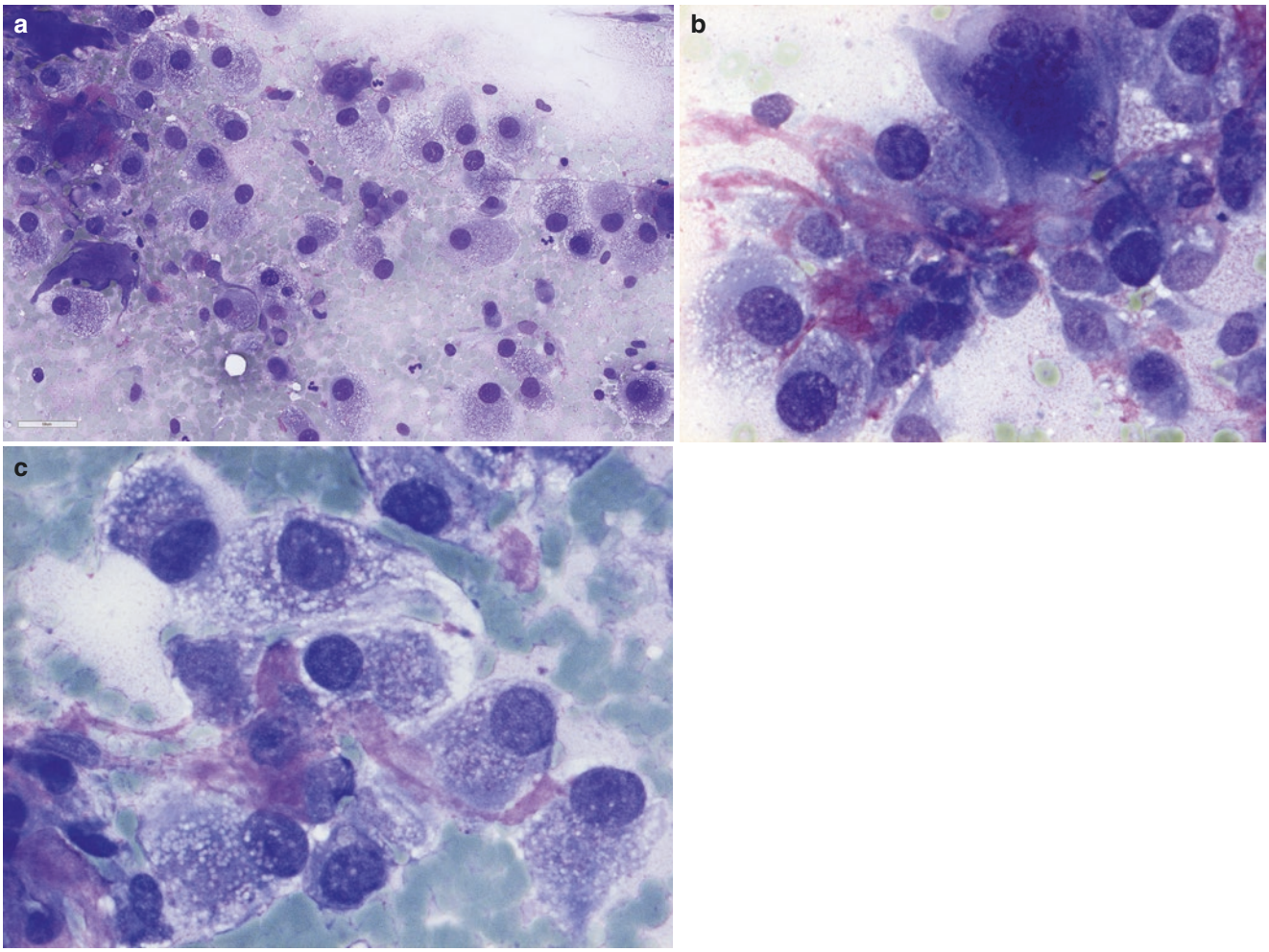

Fig. 16.24 Clear cell chondrosarcoma. (**a**–**c**) Large epithelioid cells with abundant finely vacuolated cytoplasm, a central or paracentral nucleus, fragments of cartilage, and occasional osteoclast-like giant cells (MGG)

Mesenchymal Chondrosarcoma

Mesenchymal chondrosarcoma is a rare high-grade bimorphic malignant tumor composed of islands of low-grade hyaline cartilage and malignant small round cells. The cytologic features of mesenchymal chondrosarcoma in FNA smears have been reported in a few case reports [58–60]. Small, round monomorphic (Ewing sarcoma-like) tumor cells in cohesive clusters, some embedded in a fibrillar matrix, have been described (see Fig. 16.25). Fragments of cartilaginous matrix may be observed as well as osteoclast-like giant cells. The main differential diagnoses include Ewing sarcoma, small cell osteosarcoma, and lymphoblastic lymphoma.

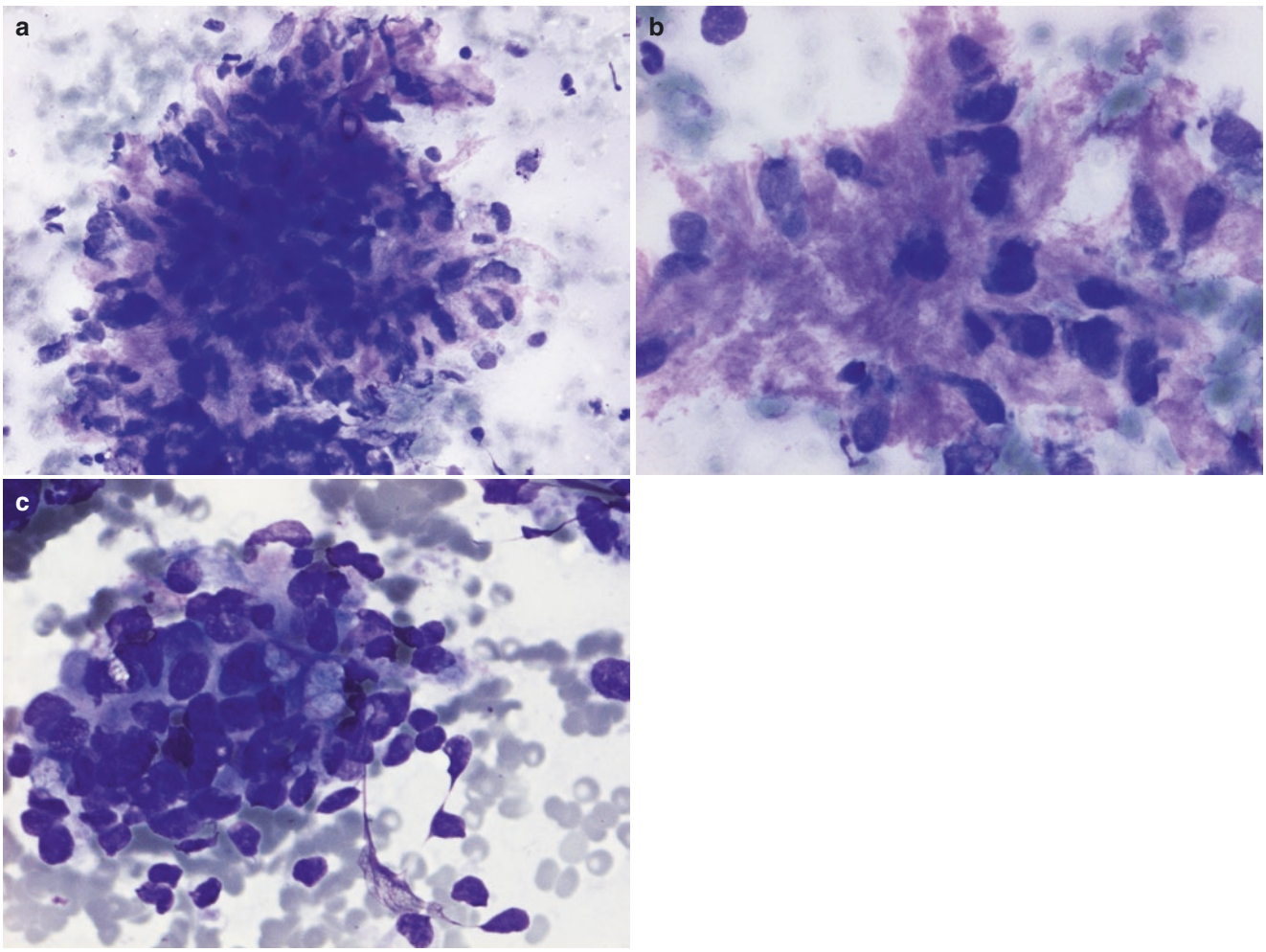

Fig. 16.25 Mesenchymal chondrosarcoma. (**a**–**c**) Clusters of small, round to oval tumor cells with sparse cytoplasm and irregular nuclei. Cells embedded in a blue-violet collagenous matrix (MGG)

Giant Cell-Rich Lesions

Giant Cell Tumor

Giant cell tumor (GCT) is a locally aggressive neoplasm comprising approximately 5% of primary bone tumors. This neoplasm displays a tendency to local recurrences and approximately 2% of GCT develops pulmonary metastasis, the so-called benign metastasizing GCT. Most patients are between 20 and 40 years of age, and GCT is very rare in patients younger than 15 years old. GCT commonly arises in the distal part of the femur, in the proximal part of the tibia, and in the distal part of the radius followed by proximal humerus and pelvic bones. The typical histologic pattern, characterized by numerous large osteoclast-like giant cells admixed with mononuclear macrophage-like cells, is often modified by hemorrhage, necrosis, or reactive fibrous tissue. Aneurysmal bone cyst-like areas may be present. The cytologic features of conventional GCT have been described in some series and case reports [61–65]. FNA smears of GCT are characterized by the mixture of cohesive or loose clusters of mononuclear cells and osteoclast-like giant cells as well as clusters of mononuclear cells bordered by giant cells at the periphery [61–65].

Cytologic features:
- Hypercellular yield with both cohesive cell clusters and single cells.
- Double-cell population: mononuclear spindle or round to ovoid cells and multinucleated osteoclast-like giant cells.
- Mononuclear cells contain nuclei with open chromatin and prominent nucleoli.
- The size of mononuclear cell nuclei is comparable to that in the osteoclast-like giant cells.
- Classical pattern of smears includes giant cells attached to the periphery of clusters of mononuclear cells.
- Absence of osteoid and cartilaginous matrix.

Differential diagnosis and problems in diagnosis:
- Aneurysmal bone cyst
- Brown tumor of hyperparathyroidism
- Reparative giant cell granuloma
- Osteoblastoma
- Giant cell-rich osteosarcoma

Because of thinning of the cortical bone, GCT is usually easy to aspirate and the specimen is abundantly cellular. Although it has been emphasized that clusters of mononuclear cells bordered by giant cells at the periphery (see Fig. 16.26) is a characteristic cytologic feature, similar pattern may also be present in smears from brown tumors of hyperparathyroidism. Morphology of other benign giant cell lesions occurring in the skeleton may show overlapping features with GCT in FNA smears. A short summary of main cytologic diagnostic criteria in benign lesions exhibiting osteoclast-like giant cells is present in Table 16.3. From the clinical management point of view, the most important differential is giant cell-rich osteosarcoma. The marked pleomorphism of the tumor cells in giant cell-rich osteosarcoma helps to distinguish it from GCT. Recently, H3F3A (G34 W/V/L) mutations have been identified in most GCTs, and mutation-specific IHC is highly specific for GCT. Therefore, H3G34W IHC is very helpful to distinguish GCT from other giant cell-rich tumors in difficult cases [66].

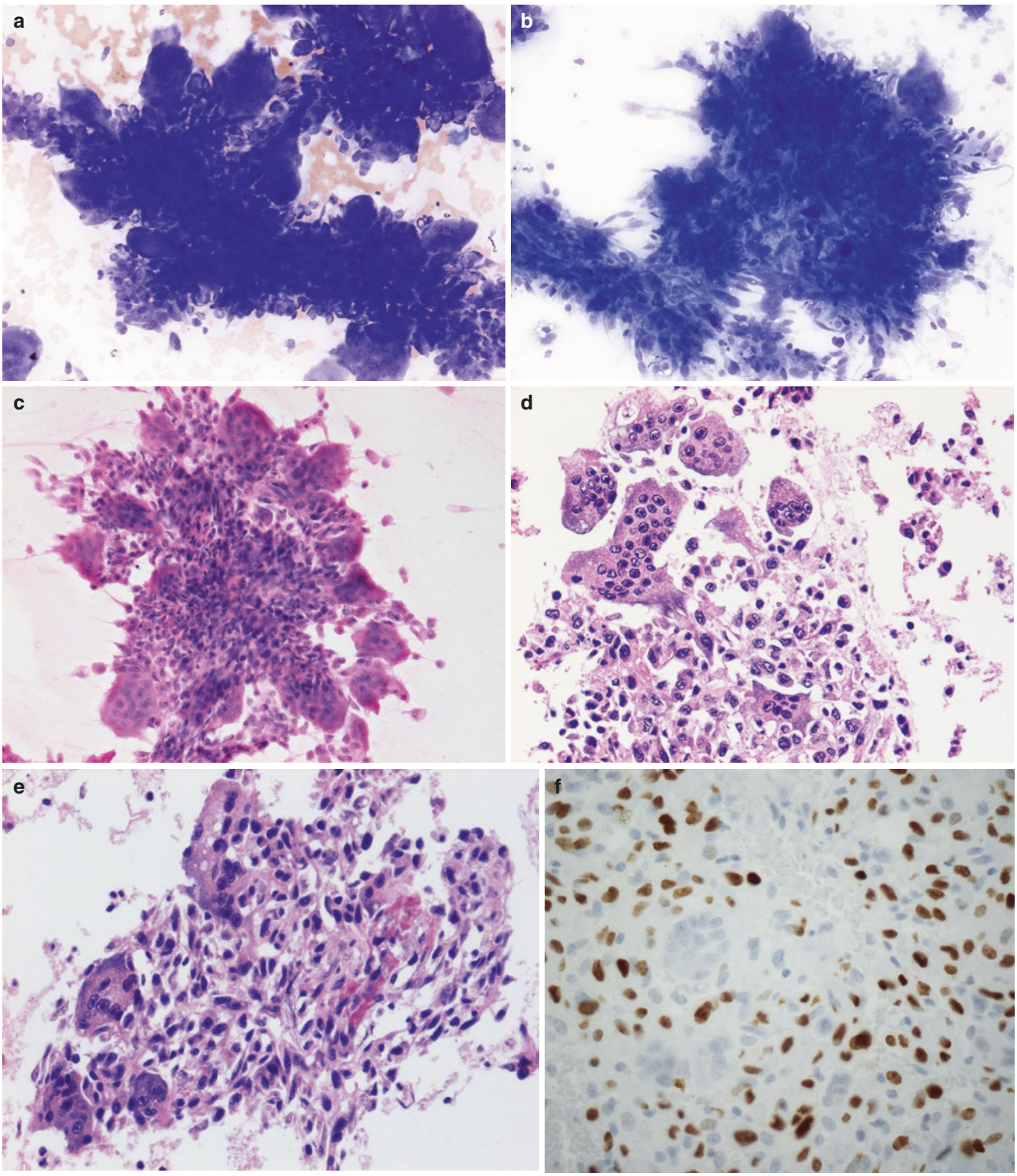

Fig. 16.26 Giant cell tumor (GCT). (**a**–**c**) Cohesive clusters of slightly pleomorphic rounded, ovoid, or spindle cells bordered by multiple multinucleated giant cells (MGG; H&E). (**d**, **e**) Cell block prepared from the aspirated material corresponds well with cytology (H&E). (**f**) H3G34W IHC is positive in mononuclear tumor cells and negative in multinucleated giant cells

Table 16.3 Summary of main cytologic diagnostic findings in benign tumors/lesions containing osteoclast-like giant cells

Tumor/lesion	Age, year	Predilection sites	Cytology
Osteoblastoma	10–30	Spine; sacrum	Osteoblasts
		Proximal and distal femur	Osteoclasts
			Clusters of uniform of spindle cells
Chondroblastoma	20–30	Long tubular bones	Fragments of chondroid matrix with chondroblasts
		Epiphysis	Often indented nuclei (“coffee-bean nuclei”)
			Occasionally giant cells
Giant cell tumor	20–40	Long tubular bones epiphysis	Clusters of uniform or slightly pleomorphic spindle, ovoid or occasionally epithelioid mononuclear cells
			Numerous giant cells, often attached to clusters periphery
			Rare mitotic figures
Aneurysmal bone cyst	10–25	Long tubular bones, metaphysis	Hemorrhagic smears
			Small clusters or dissociated bland spindle and ovoid cells
			Giant cells
			Histiocytes
Giant cell reparative granuloma	10–30	Craniofacial bones	Clusters of mononuclear spindle cells
		Small bones of hands and feet	Giant cells
			Histiocytes
			Rare osteoblasts
Osteitis fibrosa cystica (brown tumor of hyperparathyroidism)	40–70	Fascial and pelvic bones	Small dyscohesive clusters of mononuclear spindle and ovoid cells, numerous giant cells
		Femur, ribs dia- and metaphysis	

Giant Cell Reparative Granuloma

Giant cell reparative granuloma is a benign reactive lesion occurring in the craniofacial bones and the small tubular bones of hands and feet. The so-called solid variant of aneurysmal bone cyst and giant cell reparative granuloma likely represent the same process, and they share the same translocation involving the *USP6* gene with classic aneurysmal bone cyst. Giant cell reparative granuloma may occur in normal bone secondary to trauma or hemorrhage or may be associated with lesions such as brown tumor of hyperparathyroidism. Most patients are between 10 and 30 years of age. Giant cell reparative granuloma mimics other giant cell lesions in smears, and it is cytomorphologically indistinguishable from giant cell tumor and brown tumor (see Fig. 16.27).

Cytologic features:
- Sheets and clusters of spindle cells
- Multinucleated giant cells
- Osteoblasts
- Histiocytes

Differential diagnosis and problems in diagnosis:
- Conventional giant cell tumor
- Aneurysmal bone cyst
- Brown tumor

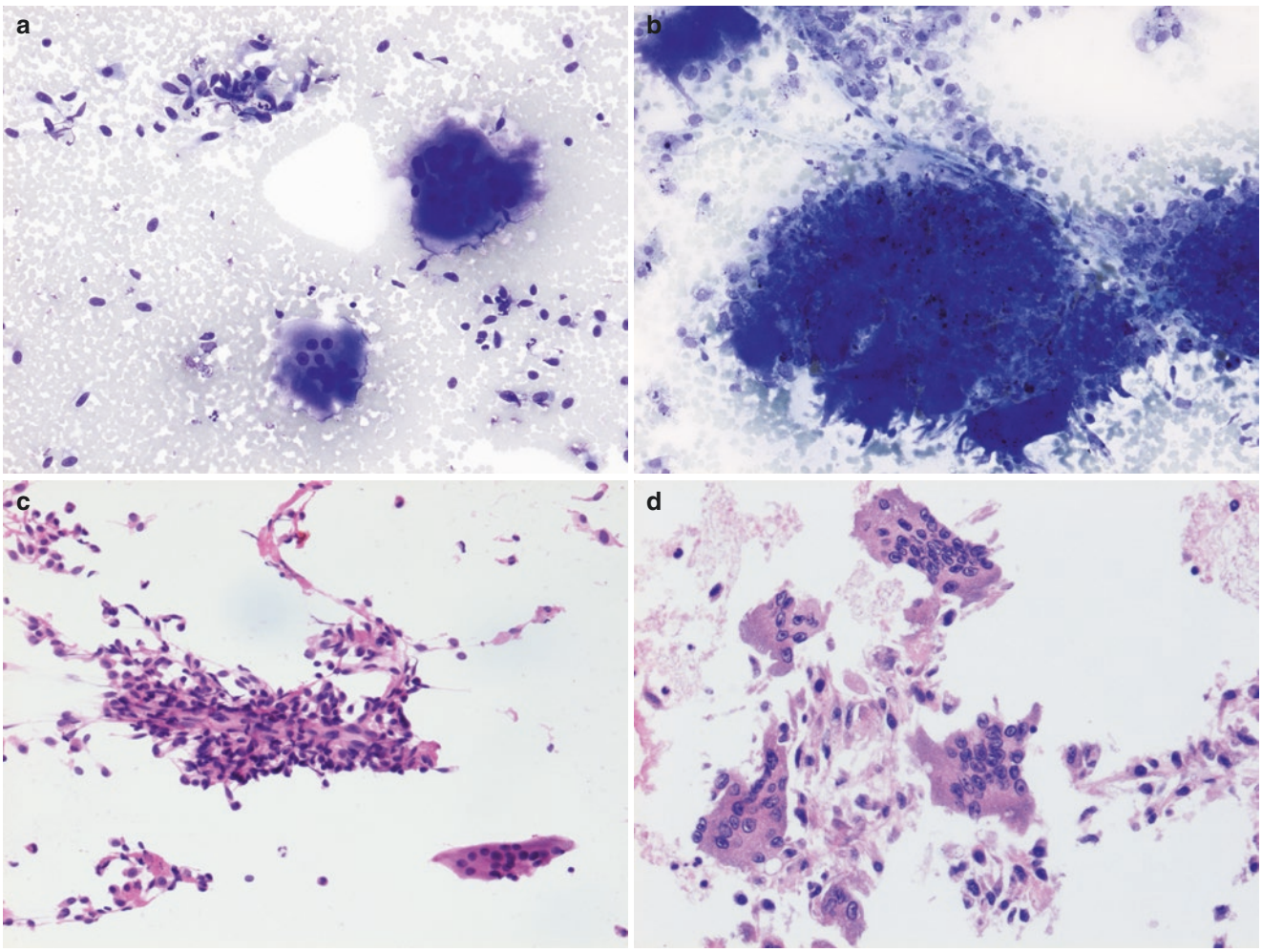

Fig. 16.27 Giant cell reparative granuloma. (**a**–**c**) Tight or loose clusters of oval and spindle cells with admixture of hemosiderin-laden histiocytes and some giant cells, both dissociated and attached to the periphery of the mononuclear cell clusters (MGG; H&E). (**d**) Cell block prepared from the aspirated material shows loosely cohesive sheets of mononuclear cells with an admixture of osteoclast-like giant cells (H&E)

Aneurysmal Bone Cyst

Aneurysmal bone cyst (ABC) is a multilocular, locally destructive lesion. Approximately 60% of ABC arises in the vertebral column, the craniofacial bones, and metaphysis of long tubular bones, but any bone can be affected. The majority (80%) of patients are younger than 20 years of age. Approximately 30% of ABC is associated with another tumor/lesion occurring in bone, commonly with GCT, spinal osteoblastoma, chondroblastoma, and chondromyxoid fibroma.

Cytologic features (*see* Fig. 16.28):
- Hemorrhagic aspirates
- Variable numbers of multinucleated giant cells
- Variable presence of clusters of spindled myofibroblastic cells
- Histiocytes and inflammatory cells
- Lack of significant cytologic atypia

Differential diagnosis and problems in diagnosis:
- Conventional giant cell tumor
- Solitary bone cyst
- Giant cell reparative granuloma
- Brown tumor of hyperparathyroidism
- Telangiectatic osteosarcoma

The cytologic features of aneurysmal bone cyst, often nonspecific, do not permit a precise diagnosis but can prompt the categorization of ABC to the group of giant cell-rich lesions. Radiologic and clinical data are necessary for making a specific diagnosis. Recently, *USP6* gene rearrangement has been identified in approximately 70% of primary ABC but not in secondary ABC and only in spindled myofibroblasts, not in other cell types, such as multinucleated osteoclast-like giant cells.

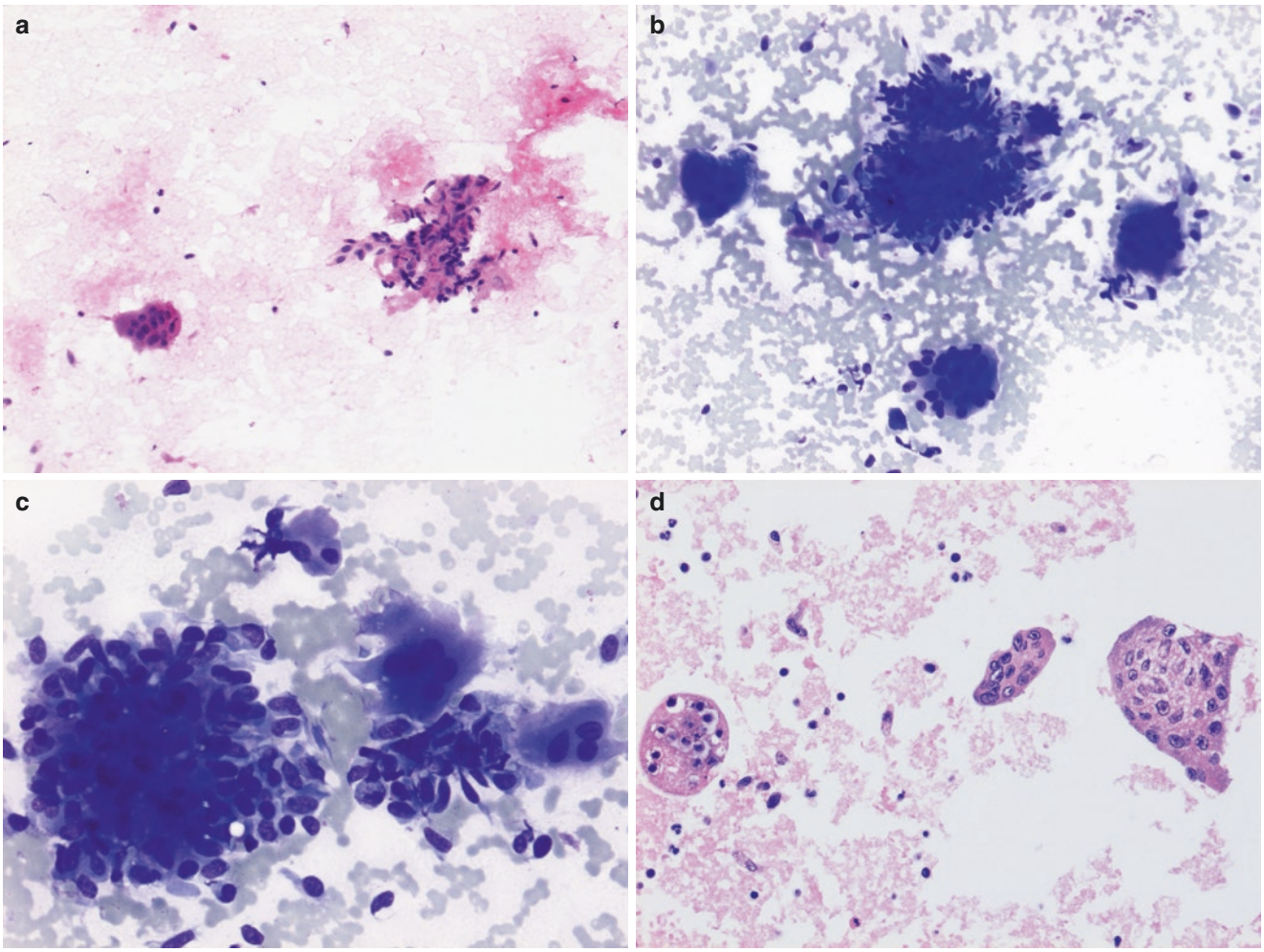

Fig. 16.28 Aneurysmal bone cyst. (**a**–**c**) Poorly cellular smears showing two cell populations, clustered spindle cells, and multinucleated giant cells. A specific diagnosis depends on the radiographic findings (H&E, MGG, Diff-Quik). (**d**) Cell block prepared from the aspirated material shows scattered osteoclast-like giant cells and single spindle cells and inflammatory cells (H&E)

Brown Tumor of Hyperparathyroidism

Rare tumor-like lesion occurring in the skeleton is brown tumor of hyperparathyroidism, formerly osteitis fibrosa cystica, caused by a high level of parathyroid hormone. Brown tumor is commonly seen in patients with secondary hyperparathyroidism due to chronic renal failure. The predilection sites for this lesion are the facial and pelvic bones, ribs, and femur. The site in the long bones is predominantly dia- or metaphyseal. In brown tumor, the bone trabeculae are replaced by fibrous tissue containing variable amount of osteoclastic giant cells. Hemosiderin-laden macrophages secondary to hemorrhage are always seen.

Cytologic features (*see* Fig. 16.29):
- Dispersed spindle cells or small- to medium-sized clusters of spindle cells
- Osteoclast-like giant cells
- Hemosiderin-laden macrophages

Differential diagnosis and problems in diagnosis:
- Conventional giant cell tumor
- Aneurysmal bone cyst
- Reparative giant cell granuloma

Brown tumors of hyperparathyroidism are rare targets for FNAC. Single case reports have been published, and the cytologic findings are very similar to those in a giant cell tumor. Without knowledge of patient age, clinical history, site of lesion, and radiographic features, it may be impossible to distinguish a brown tumor from GCT in FNA smears.

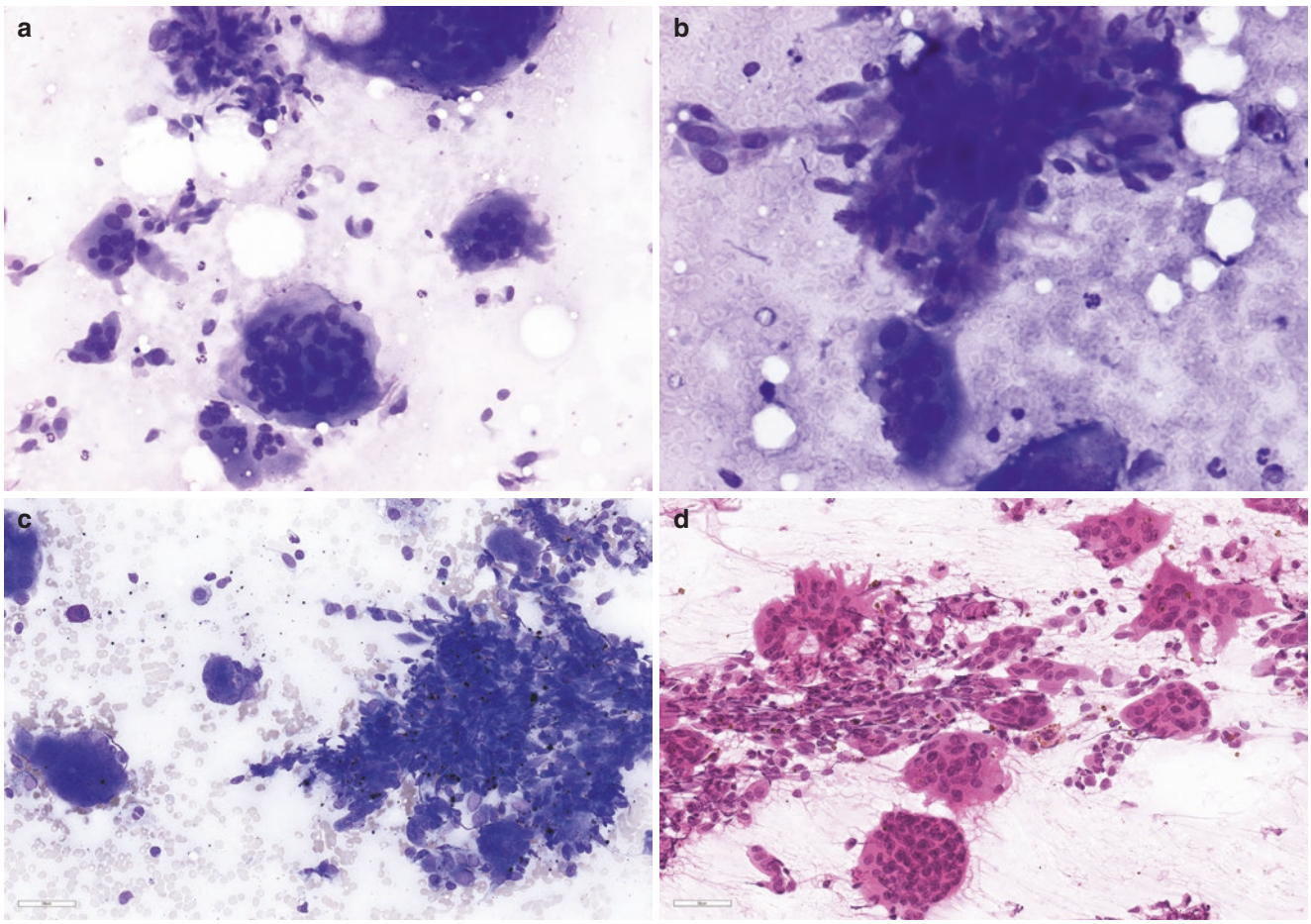

Fig. 16.29 Brown tumor of hyperparathyroidism. (**a**, **b**) Smears show small clusters and few dispersed spindle cells, inflammatory cells and osteoclast-like giant cells (MGG). (**c**, **d**) Middle-sized loos clusters of spindle cells, osteoclasts-like giant cells and hemosiderin-laden macrophages (MGG; H&E)

Ewing Sarcoma

Ewing sarcoma is a primitive small round cell neoplasm in the group of neuroectodermal neoplasms, whereas the term "peripheral neuroectodermal tumor (PNET)" was traditionally used when the tumor displays neuroectodermal differentiation. In the World Health Organization (WHO) Classification 2013, both neoplasms share the same name of Ewing sarcoma.

Ewing sarcoma is the third most frequent primary bone sarcoma after osteosarcoma and chondrosarcoma. These neoplasms are rare before age 5 and after age 30 and extremely rare in elderly patients. Approximately 80% of cases arise in patients younger than 20 years old. Most common sites are the shafts of the long bones, pelvic bones, ribs, and spine. They may, however, occur in almost any bone. Sites of extraskeletal Ewing sarcoma include various parts of the body (cutaneous, subcutaneous, soft tissue, paraspinal, retroperitoneum, kidney, and breast). More than 90% of Ewing sarcomas show cytoplasmic membrane positivity with CD99 and about 75% nuclear staining with the FLI-1-antibody. Differentiated subtype (previously PNET) expresses neuroectodermal markers: neuron-specific enolase (NSE), chromogranin A, and synaptophysin. Approximately 85% of Ewing sarcomas harbor the chromosomal translocation t(11;22)(q24;q12) involving the *EWSR1* gene on chromosome 22 and the *FLI-1* gene on chromosome 11, resulting in the production of EWS-FLI-1 fusion oncoprotein.

Cytologic features:
- Often hypercellular aspirates
- Dispersed cells admixed with clusters of loosely cohesive cells
- Fragile cells, "tigroid" cytoplasmic background often visible on air-dried smears
- Two cell types: large light cells and small dark cells
- Intracytoplasmic vacuoles in the intact large light cells
- Occasionally rosette-like structures

Differential diagnosis and problems in diagnosis:
- Neuroblastoma/esthesioneuroblastoma
- Alveolar rhabdomyosarcoma
- Non-Hodgkin lymphoma (precursor lymphoma)
- Desmoplastic small round cell tumor
- Poorly differentiated synovial sarcoma
- Small cell osteosarcoma
- Mesenchymal chondrosarcoma

The cytologic diagnostic criteria of Ewing sarcoma have been reported in several publications [67–71]. Correct diagnosis of Ewing sarcoma may be suggested from technically satisfactory smears and requires both air-dried and wet-fixed smears. Double-cell population, large light cells with abundant, "thin" cytoplasm with clear spaces or vacuoles and round nuclei with finely chromatin texture and small nucleoli and small dark cells with hyperchromatic nuclei and scanty cytoplasm, is better appreciated in the air-dried smears, so are the "tigroid" background and intracytoplasmic vacuoles (see Fig. 16.30). Nuclear characteristics are better appreciated in wet-fixed smears with H&E or Papanicolaou staining (see Fig. 16.30). When only wet-fixed material is available, Ewing sarcoma may be difficult to be separated from poorly differentiated synovial sarcoma and other small round cell malignancies. Despite the fact that diagnosis of Ewing sarcoma can be suggestive on routine-stained smears, ancillary methods remain necessary to confirm the diagnosis. CD99 and FLI-1 are considered highly sensitive (see Fig. 16.31), but only diffuse and strong membranous staining pattern for CD99 is considered specific for Ewing sarcoma [72]. CD99 and FLI-1 must be used together with a panel of other antibodies to exclude other small round cell tumors [73]. Demonstration of the characteristic chromosomal aberration is considered the gold standard for diagnosing Ewing sarcoma [27, 74]. Best results are achieved with reverse transcriptase–polymerase chain reaction (RT-PCR) and fluorescence in situ hybridization (FISH) analysis [75]. Ewing sarcoma often presents with a soft tissue extension, which can be misinterpreted as a true soft tissue neoplasm prior to radiologic investigation. The clinical setting of other small round cell tumors aids in the differential diagnoses (e.g., esthesioneuroblastoma occurs in nasopharyngeal space; desmoplastic small round cell tumor most often has extensive intra-abdominal involvement).

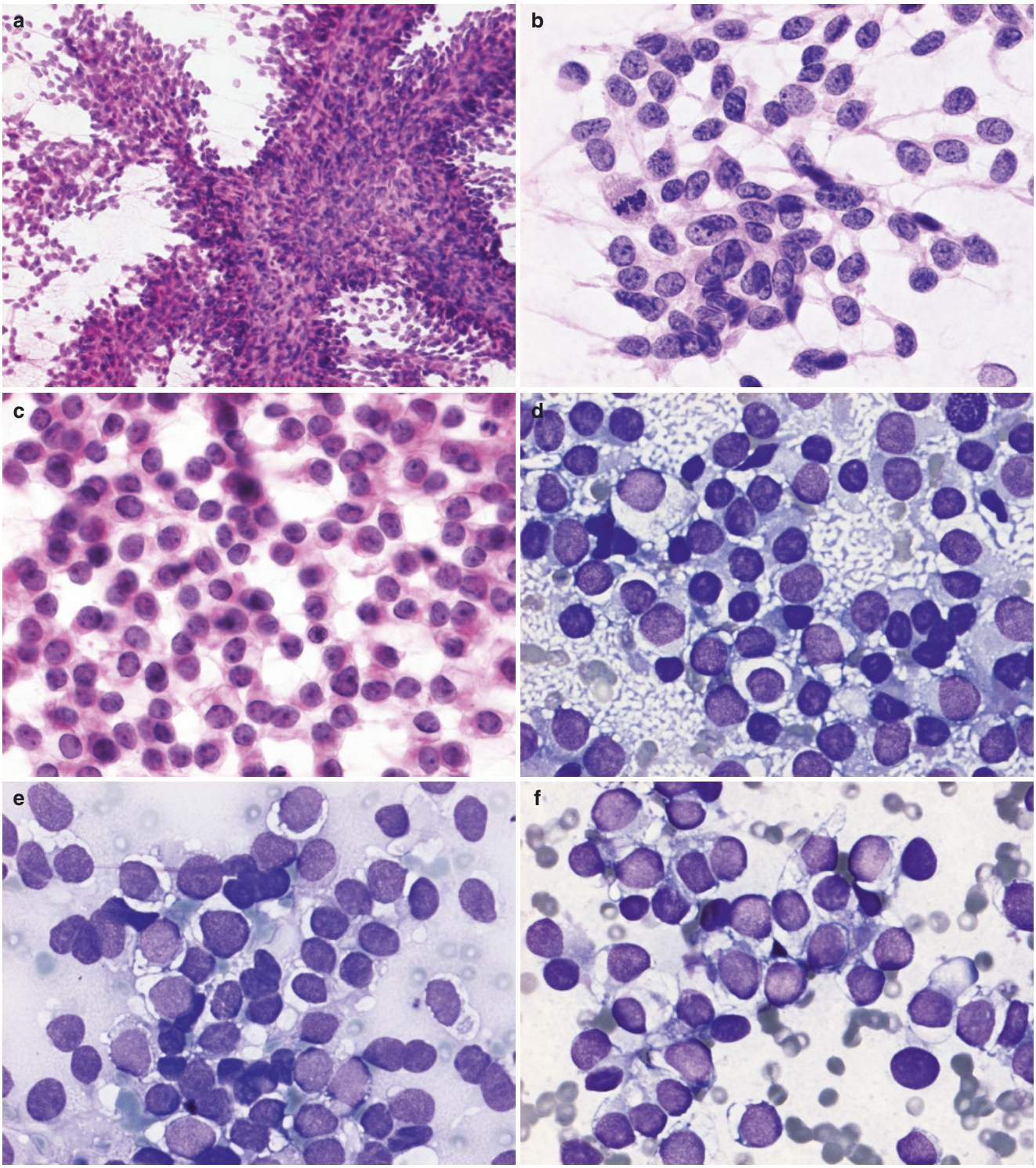

Fig. 16.30 Ewing sarcoma. (**a**) Clusters of cohesive, small, round tumor cells attached to the capillaries. (**b**, **c**) Tumor cells show small- to medium-sized irregular nuclei with tiny nucleoli and mitoses (H&E). (**d–f**) Tigroid background of the smears and two cell types: large light cells with vacuolated and clear cytoplasm mixed with small dark cells are evident in air-dried smears (MGG)

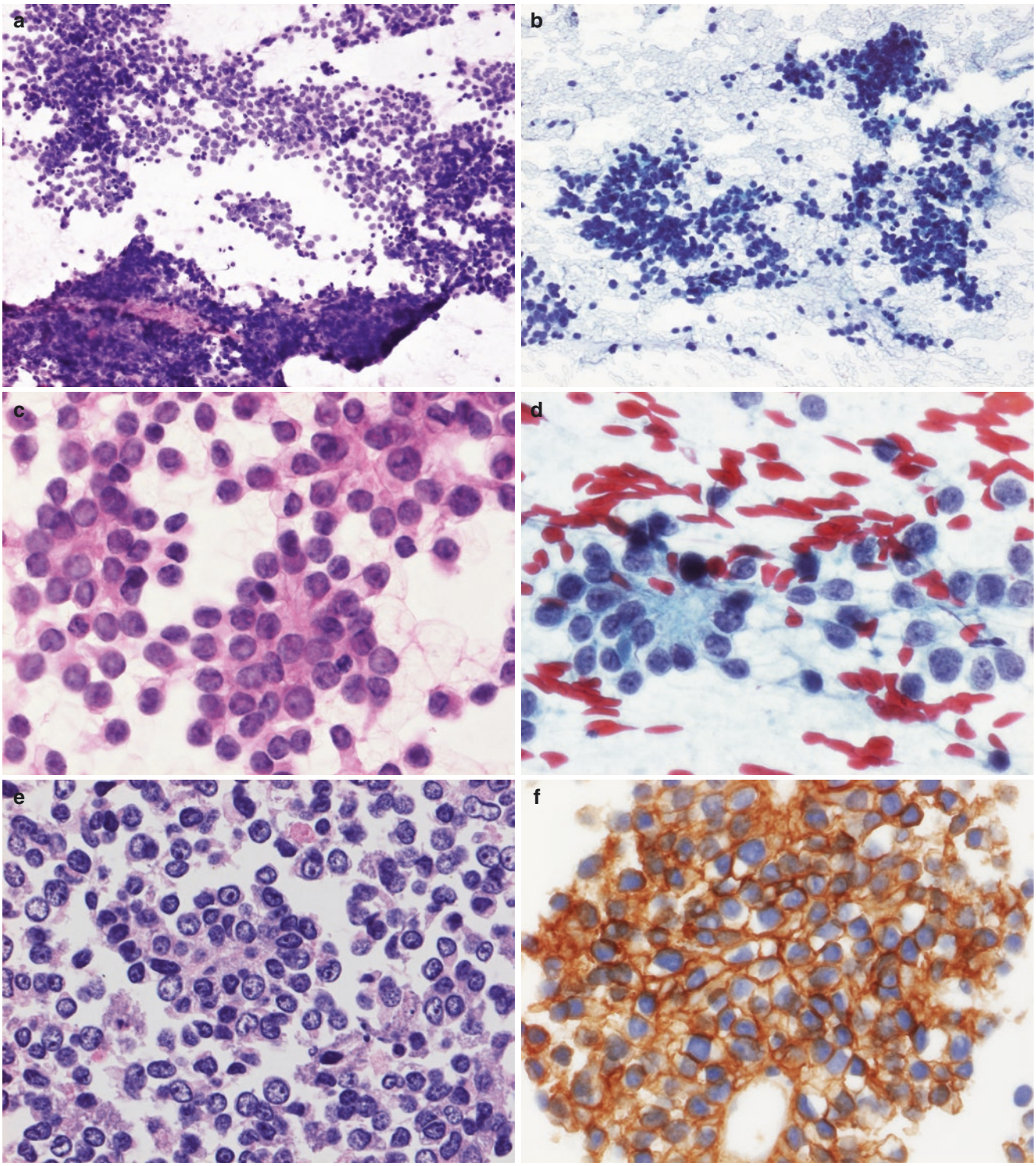

Fig. 16.31 Ewing sarcoma. (**a**, **b**) Dispersed cells admixed with clusters of loosely cohesive small cells with round and spindle to oval, irregular nuclei with coarse chromatin texture (H&E; Pap stain). (**c**, **d**) Smears with rosettes (H&E; Pap stain). (**e**) Cell block showing well-preserved morphology with presence of rosettes and (**f**) distinct membranous CD99 positivity

Notochordal Tumors

Chordoma

Chordoma, a malignant tumor arising from remnants of the notochord, accounts for up to 4% of the primary bone sarcomas. Chordoma most commonly occurs in the sixth to seventh decades and is very rare under age 30. Chordomas are all most exclusively located in the axial spine. The sacrum is the most common site, followed by the spheno-occipital area, cervical spine, and thoracolumbar spine. Sacral chordoma is a slowly growing, locally destructive neoplasm, which tends to expand into soft tissue, whereas intracranial chordoma invades sella turcica, petrous, and sphenoid bones.

Cytologic features [76–79]
- Abundant myxochondroid matrix.
- Large epithelioid cells with abundant (multi)vacuolated cytoplasm (physaliferous cells).
- Smaller round to oval and polygonal cells with granular cytoplasm, slight to moderate anisokaryosis, bland chromatin, and small nucleoli.
- Strands and clusters of medium-sized epithelial-like, at times binucleated cells.
- Myxoid and fibrillar matrix encircles single cells and small clusters of cells.
- Rare pleomorphic cells with prominent nucleoli and multinucleated tumor giant cells.

Differential diagnosis and problems in diagnosis:
- Chondrosarcoma
- Clear cell- or mucin-producing adenocarcinoma
- Myxopapillary ependymoma
- Chordoid meningioma

The characteristic features in smears are the abundant, myxoid, often fibrillar background substance, which encircles groups of cells and/or single tumor cells and the presence of the physaliferous cells with their abundant, “bubbly” cytoplasm and round nuclei with inconspicuous nucleoli (see Fig. 16.32). Tumor cells may be vacuolated with eccentric, at times scalloped, nuclei, resembling lipoblasts or signet-ring cells in adenocarcinoma. The myxoid matrix stains red blue or violet in MGG and Diff-Quik, pale pink in H&E, and pale green gray in Papanicolaou. Physaliferous cells are pathognomonic in smears from chordoma, which helps to distinguish them from chondrosarcoma (see Fig. 16.33).

Immunocytochemistry helps to establish the correct diagnosis in difficult cases. Chordomas express S-100 protein together with EMA and/or low molecular weight keratin (see Fig. 16.33). Recently, Brachyury staining with nuclear positivity has been shown to be highly sensitive and specific for chordomas (see Fig. 16.33) [80].

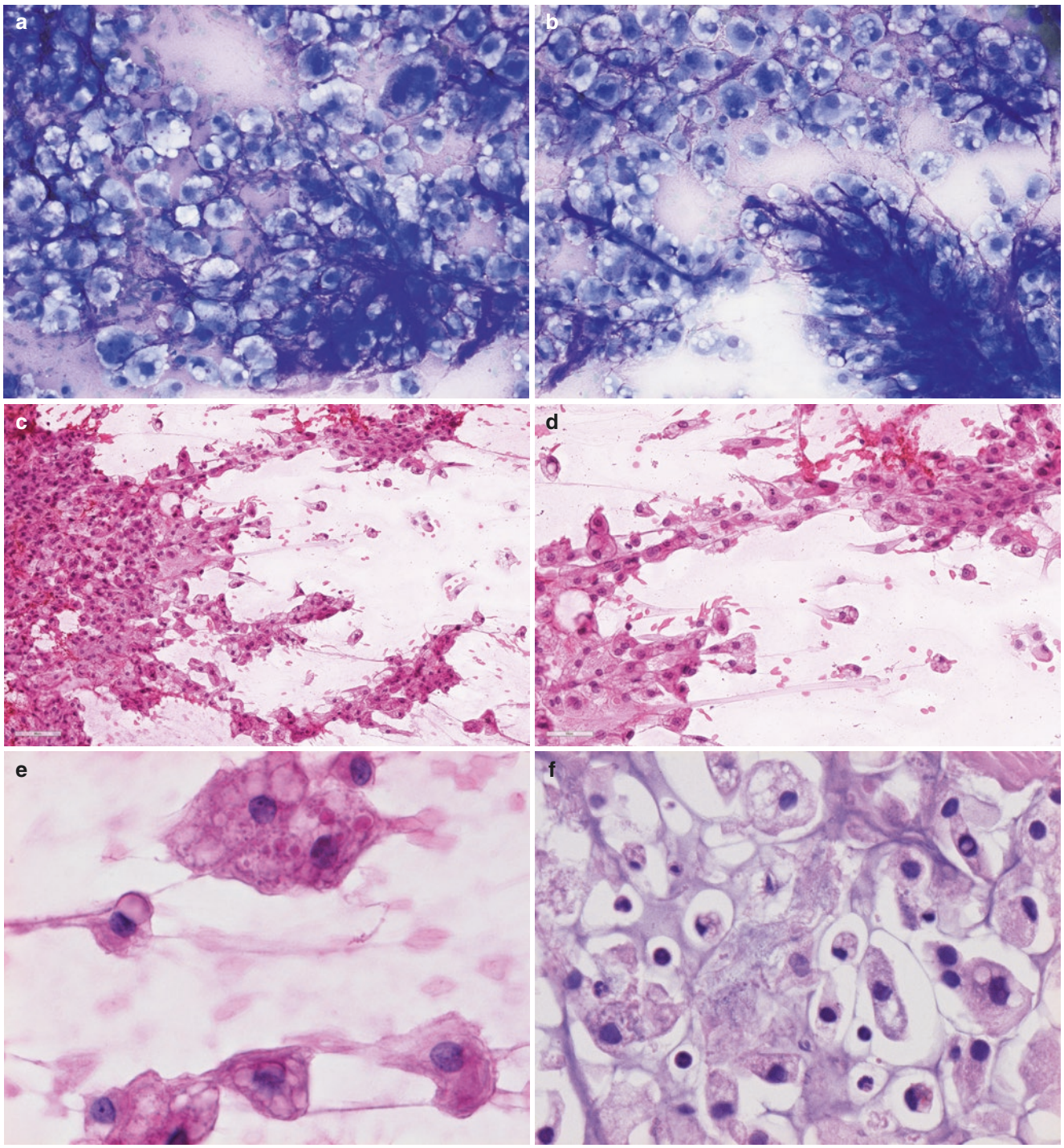

Fig. 16.32 Chordoma. (**a**, **b**) Loosely clusters of tumor cells embedded in a fibrillary blue-violet myxoid matrix that encircles many single tumor cells (MGG). (**c**, **d**) The fibrillary/myxoid background matrix is usually less obvious in wet-fixed smears than in air-dried smears (H&E). (**e**) Large cells corresponding to physaliferous cells, with abundant, multivacuolated cytoplasm, and uniform, round nuclei with small nucleoli (H&E). (**f**) Cell block section showing cells with abundant vacuolated or granular cytoplasm and uniform nuclei (H&E)

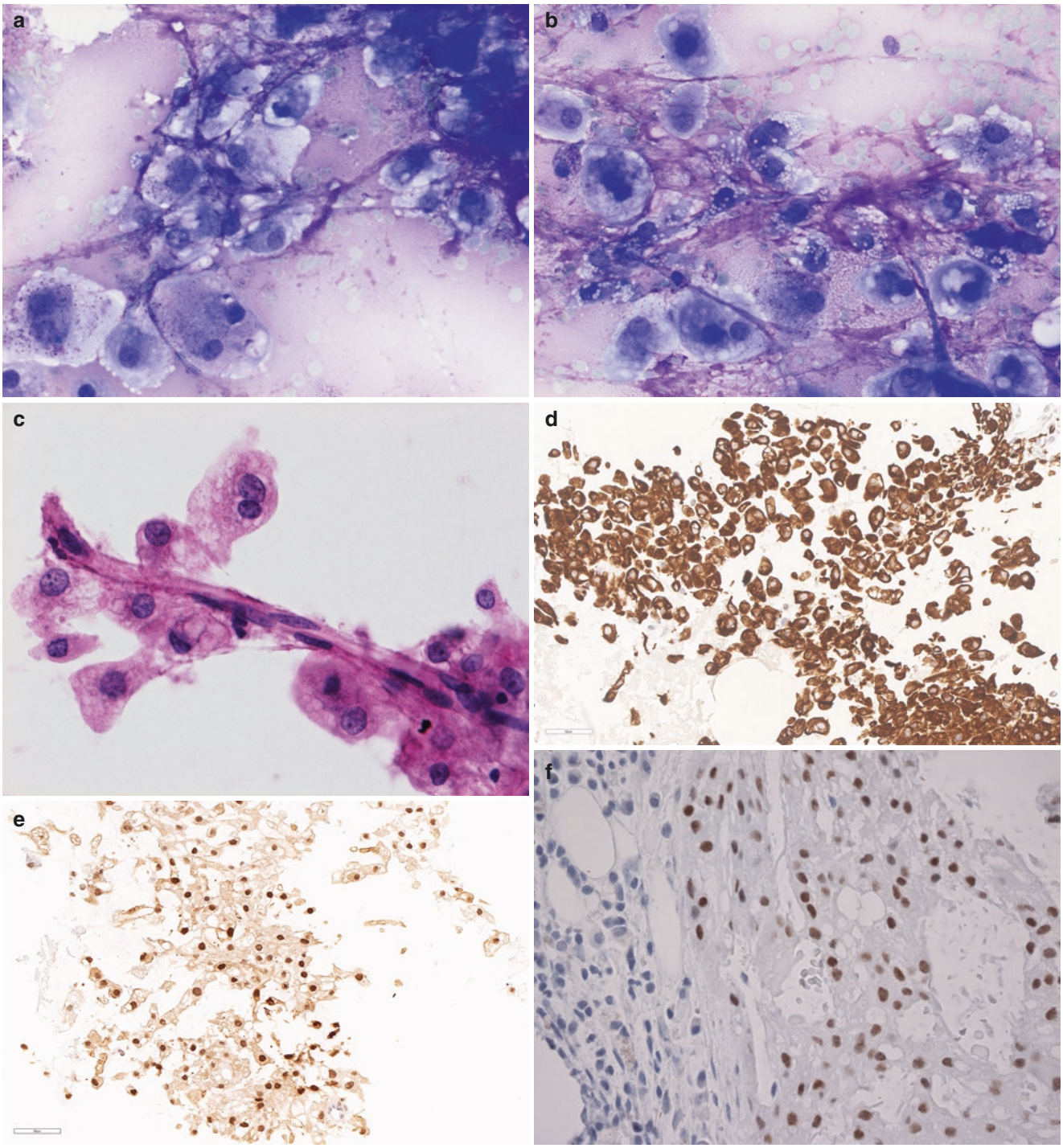

Fig. 16.33 Chordoma. (**a**, **b**) Large epithelioid cells with abundant multivacuolated cytoplasm in the myxoid background matrix (MGG). (**c**) Tumor cells attached to the capillaries (H&E; ThinPrep; Hologic; Bedford, MA, USA). (**d**, **e**) Tumor cells are positive for keratin and S100 protein (Keratin and S-100; cell block). (**f**) Brachyury staining with nuclear positivity has been shown to be highly sensitive and specific for chordomas (Brachyury; histologic section)

Lymphohematopoietic and Histiocytic Tumors

Plasma Cell Neoplasm: Solitary Plasmacytoma and Plasma Cell Myeloma

Plasma cell neoplasm of the bone constitutes a spectrum of clonal proliferations of plasma cells including solitary bone lesion composed of neoplastic plasma cells identical to plasma cells in myeloma, with osteolytic defects of the skeleton and monoclonal gammopathy. Plasma cell neoplasm of the bone occurs predominantly in elderly patients and is rare before age 40. The lesion is most common in bones with active hematopoiesis such as the vertebrae, ribs, pelvic bones, skull, and femur. Due to cortical bone destruction, plasma cell neoplasms are most often easy to needle, and the yield is rich [6, 81, 82]. It may be difficult to distinguish reactive plasmacytosis from plasmacytoma/multiple myeloma in bloody, hypocellular smears containing only normal-appearing plasma cells (see Fig. 16.34). Cytologic diagnosis may be even more difficult when the sample is admixed with a prominent component of normal bone marrow cells. Flow cytometric analysis and/or immunocytochemical studies are necessary for a definitive diagnosis.

Cytologic features:

- Predominantly dispersed neoplastic plasma cells, occasionally in small loosely cohesive clusters
- Variable differentiation from all most normal-appearing plasma cells to highly pleomorphic (bi- or multinucleated) cells
- Occasionally, cells with plasmablastic morphology (immunoblast-like cells with prominent central nucleoli)

Differential diagnosis and problems in diagnosis:

- Large B-cell lymphoma of immunoblastic type
- Reactive benign plasmacytosis
- Metastatic carcinoma

The neoplastic plasma cells express monotypic immunoglobulin light chains and heavy chains and, in most cases, express CD138 and CD79A and, in approximately 40% of cases, EMA (see Fig. 16.34).

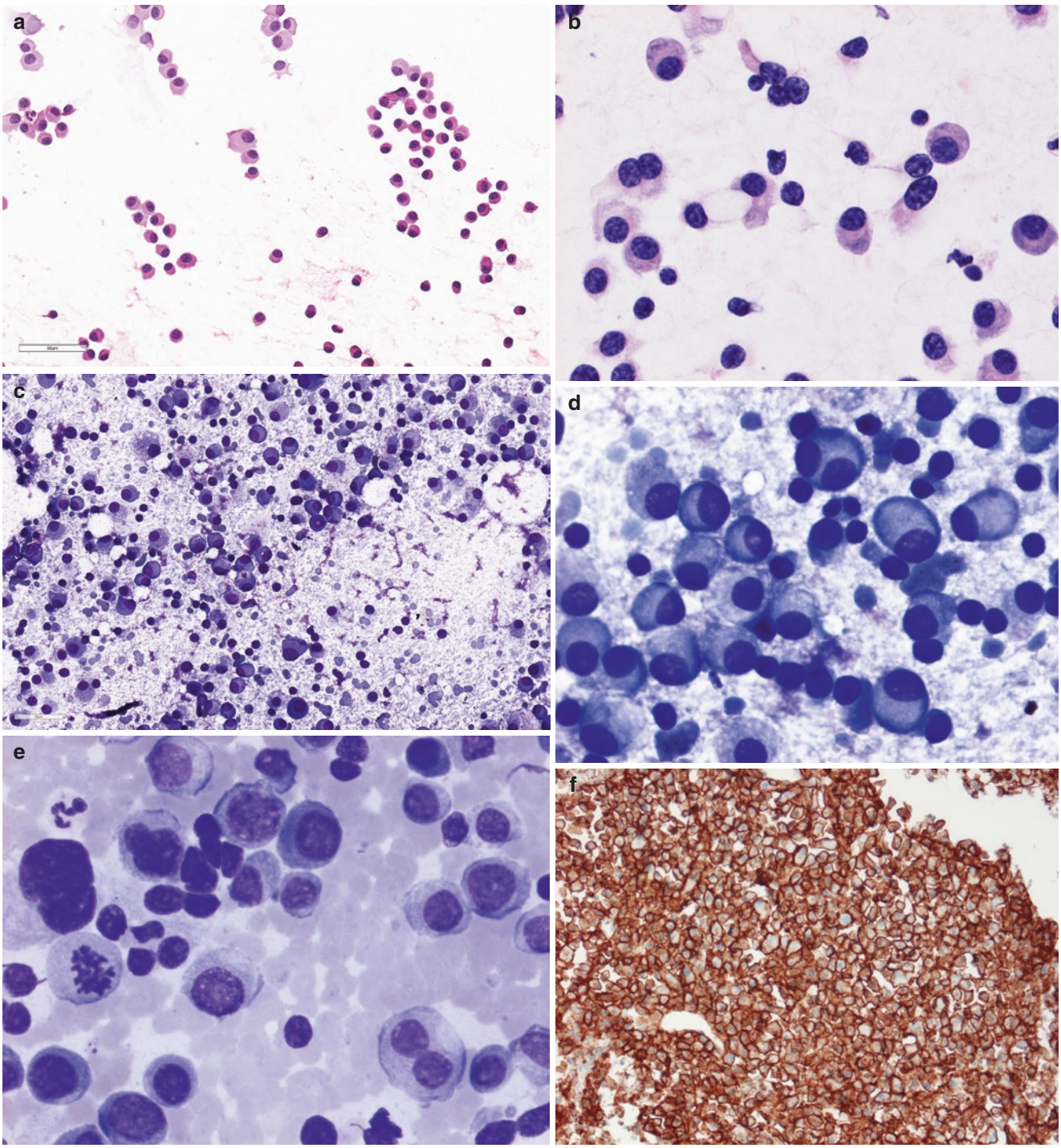

Fig. 16.34 Plasma cell neoplasm. (**a**–**d**) Smears containing predominantly dispersed, slightly atypical, neoplastic plasma cells (H&E; MGG). (**e**) Variable differentiation from almost normal-appearing plasma cells to highly pleomorphic (bi- or multinucleated) cells (MGG). (**f**) Tumor cells are positive for CD138 (CD138; cell block)

Primary Lymphoma of the Bone

Primary bone lymphomas are rare lesions and comprise approximately 3–7% of all malignant bone tumors. The majority of lymphomas occur in the long bones followed by the pelvic bones and the spine. Any age group may be affected, but most patients are older than 45 years of age. The vast majority of lymphomas are aggressive B-cell lymphomas (diffuse large B-cell lymphoma). Certain subtypes such as precursor (lymphoblastic) lymphoma and anaplastic large cell lymphoma may arise in children and young adults. Cytologic diagnostic criteria are the same as for nonosseous lymphoma (see Chap. 9).

Differential diagnosis and problems in diagnosis:
- Ewing sarcoma
- Immunoblastic or plasmablastic variants of plasmacytoma [83]
- Granulocytic sarcoma
- Metastatic small cell undifferentiated carcinoma

Langerhans Cell Histiocytosis (Eosinophilic Granuloma)

Langerhans cell histiocytosis (LCH) is a localized or systemic clonal proliferation of Langerhans cells. Most frequent sites of LCH are the bones and skin. LCH may appear at any age, but most cases occur in children between 5 and 10 years of age. The bone lesions might be solitary (most common) or multiple. Although any bone can be involved, the skull, femur, and humerus are commonly affected in children and the skull, pelvic bones, and ribs in adults. Cytologic features of Langerhans cell histiocytosis have been infrequently reported [6, 84–88].

Cytologic features (*see* Fig. 16.35):
- Langerhans cells in loosely cohesive clusters or sheets or single cells
- Ovoid, reniform, or lobulated nuclei
- Nuclear grooves ("coffee-bean" nuclei)
- Binucleated and multinucleated histiocytes often present
- Bland chromatin and small nucleoli
- Abundant pale cytoplasm
- Variable numbers of eosinophils, neutrophils, and lymphocytes
- Occasional osteoclast-like giant cells

Differential diagnosis:
- Nonspecific osteomyelitis

The Langerhans cells stain for S-100 protein (nuclear and cytoplasmic) and CD1a and Langerin/CD207 (membranous). Another diagnostic feature is the presence of Birbeck granules in EM. Recently, somatic BRAF mutation has been shown in more than half of LCH cases, which can be detected by BRAF V600E IHC.

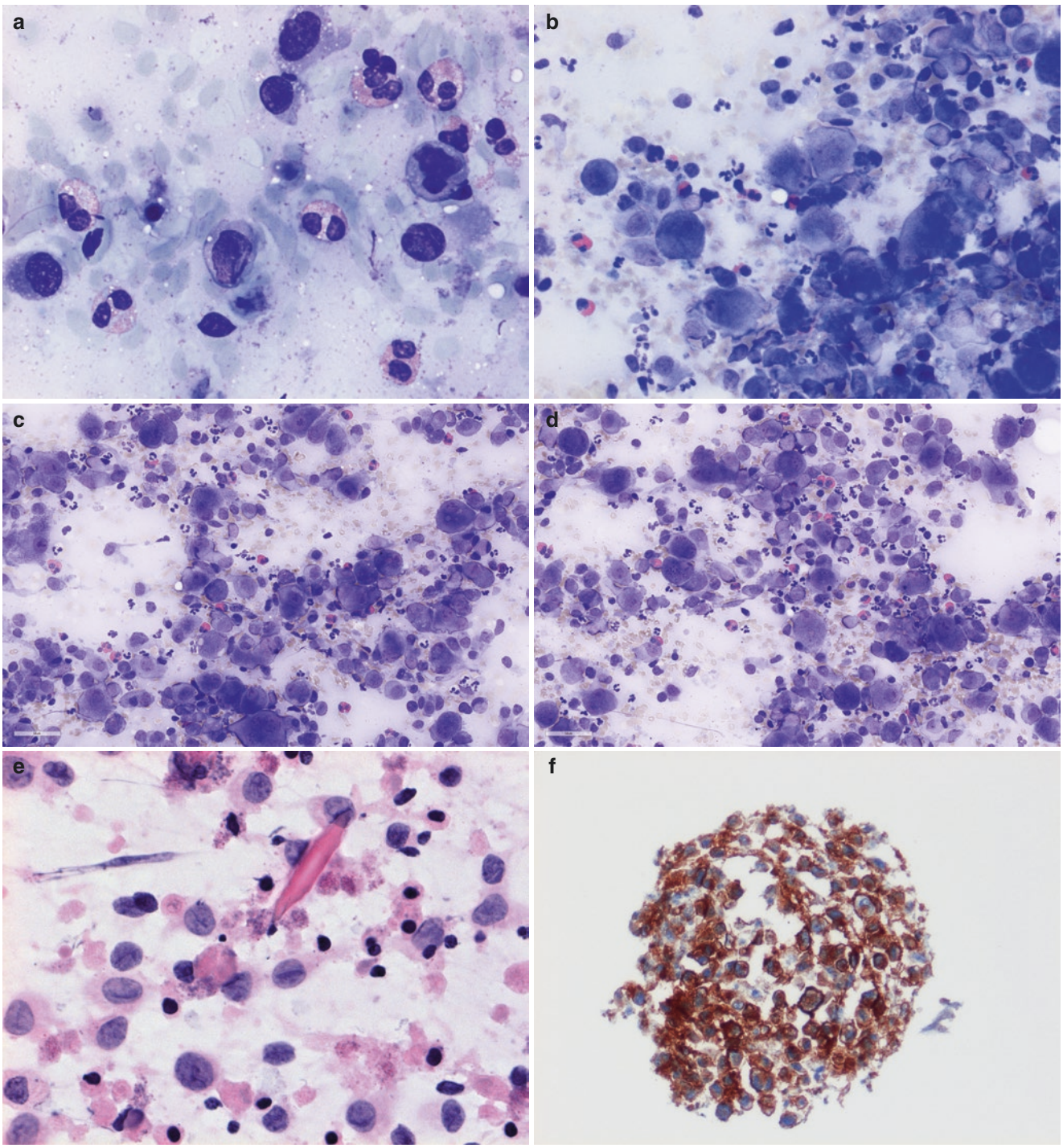

Fig. 16.35 Langerhans cells histiocytosis. (**a**–**d**) Loosely cohesive clusters or single Langerhans cells with moderate to abundant cytoplasm and rounded or ovoid, reniform or lobulated nuclei with nuclear grooves and admixture of eosinophilic granulocytes (MGG). (**e**) Admixture of eosinophilic and neutrophilic granulocytes and occasional Charcot–Leyden crystals (H&E). (**f**) Langerhans histiocytes are positive for CD1a (cell block)

Bone Metastases

The skeleton is the third most common site to be involved by metastases following the lungs and liver. Metastatic carcinomas are the most frequent malignant neoplasm of the skeleton. Metastatic deposits occur usually in bones with active bone marrow such as the vertebrae, pelvic bones, sternum, ribs, and proximal femur. Any bone can be affected, however. Any malignant tumors can metastasize to the skeleton, but approximately 80% of metastases are from carcinomas of the breast, prostate, kidney, lung, and gastrointestinal tract.

According to Shih et al. [89] the kidney, lung, liver, prostate, and thyroid gland were the most common sources of solitary bone metastasis, and in another study the most common primary sites were the lung, prostate, breast, and liver [90]. Malignant melanoma is a not uncommon metastatic tumor in adults.

In the pediatric age, most common neoplasms metastasizing to the bone are rhabdomyosarcoma, neuroblastoma, and clear cell sarcoma of the kidney. When a solitary destructive bone lesion is the first sign of malignancy, FNA is very useful to rapidly identify or suggest the primary site. Many metastatic tumors attempt to recapitulate the original neoplasm [22, 91, 92]. Access to ancillary techniques, especially immunocytochemical examinations, is necessary to establish origin of metastasis in majority of cases (see Fig. 16.36). Examples of useful antibodies are suggested in Table 16.4.

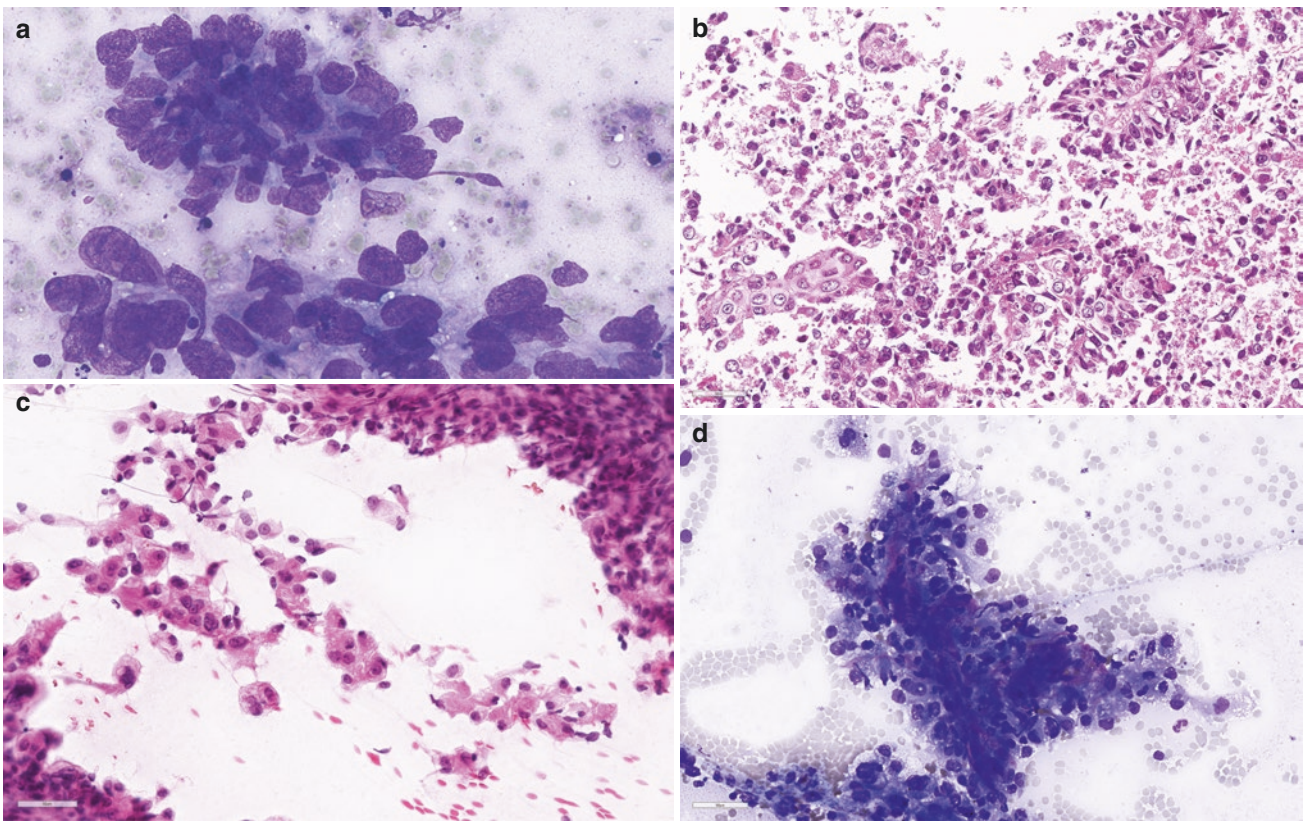

Fig. 16.36 Bone metastases. Skeletal metastasis of uterine mixed Müllerian tumor: (**a**) smears and (**b**) cell block show poorly cohesive clusters of pleomorphic tumor cells with epithelial and mesenchymal differentiation (MGG; H&E). (**c**) Skeletal metastasis of renal cell carcinoma: clusters of round, oval, and polygonal cells with abundant granular, foamy, and vacuolated cytoplasm and (**d**) tumor cells attached to capillary vessels (H&E; MGG). (**e**) Skeletal carcinoma metastasis in patient with history of mammary carcinoma (MGG). (**f**) Tumor cells are positive for estrogen, which indicates a diagnosis of metastasis from breast carcinoma (ThinPrep; Hologic, Bedford, MA)

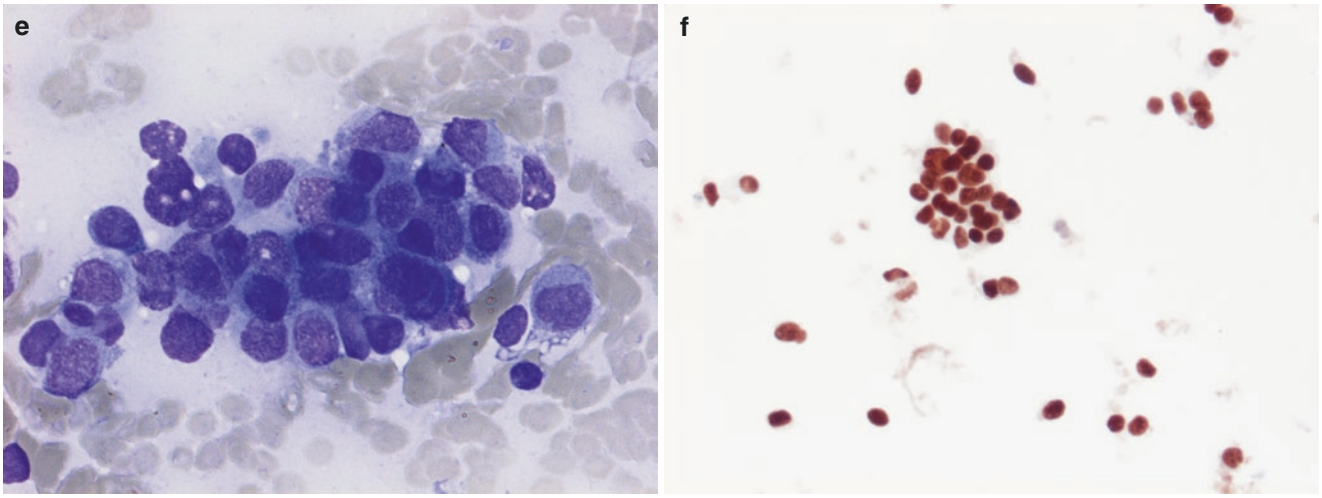

Fig. 16.36 (continued)

Table 16.4 Useful antibodies in the diagnosis of metastases to the bone

Primary site/tumor	Antibody	Comments
Kidney		
Renal cell carcinoma	CK8/18; CK7/20; CD10, PAX8 and PAX2, RCC	CK8/18+; CD10+; CK7/20-, PAX-8+(nuclear)
Urothelial carcinoma	CK7/20, p63, GATA3	CK7/20+; p63+, GATA3+
Lung		
Squamous carcinoma	CK5/6, CK7	CK5/6+; CK7+ or –
Adenocarcinoma	CK7/20, TTF-1, napsin A	CK20-/CK7+; TTF-1/napsin A+
Small cell carcinoma	CK7/20; TTF-1, chromogranin/synaptophysin	CK7/20-; TTF-1+; chromogranin/synaptophysin+
Breast	CK7/20, ER, PR, GATA3	CK7+/GATA3+; CK20−
Thyroid		
Follicular cell neoplasm	Thyroglobulin, TTF-1, PAX-8	
Medullary carcinoma	Calcitonin, CEA, TTF-1	
Colon	CK7/20; CDX-2, SATB2	CK20/CDX-2+SATB2+; CK7−
Prostate	CK8/18, CK7/20, PSA, NKX3.1	CK8/18+; PSA+, NKX3.1, CK7/20−
Melanoma	S-100, HMB45, MelanA, SOX10	
Rhabdomyosarcoma	Desmin, Myo-D1 (or myogenin)	
Neuroblastoma	NSE, chromogranin	

Bone Lesions Rarely Examined by FNA

Fibrous Cortical Defect (Nonossifying Fibroma)

Fibrous cortical defect is usually an incidental finding involving the metaphyseal region of long bones or the pelvis; occasionally, fracture may be the first sign of presentation. When the tumors extend from the cortex to the medullary cavity, the term "nonossifying fibroma" is used. Predilection sites are the femur and the tibia. The tumors occur in the second decade of life and are virtually never seen after age 30. The lesions have a characteristic radiographic appearance, and FNA examination is most often unnecessary.

Fibrous Dysplasia

Fibrous dysplasia is a solitary or multifocal intramedullary benign lesion. The solitary (monostotic) type is more common accounting for approximately 70–90% of lesions. Most cases are diagnosed before age 40, and the highest incidence is in the second decade of life. Commonly affected bones are the craniofacial bones, ribs, femur, and tibia, although any bone may be involved. Common symptoms are bone deformity and soft tissue swelling, sometimes pathological fracture.

While histologic sections of fibrous dysplasia display characteristic diagnostic features of cellular fibrous matrix containing a variable amount of irregular arranged bony trabeculae similar to Chinese characters and with admixture of osteoclasts, cytologic features are less characteristic, a mixture of uniform spindle cells or cohesive clusters of spindle cells with some osteoclasts and occasionally osteoblastic cells (see Fig. 16.37). Cytologic findings in single case reports of fibrous dysplasia have been reported. The smears contained osteoclast-like giant cells and tissue fragments probably representing woven bone [93, 94]. Presumably, the only indication for FNAC is when the presenting symptom is a pathological fracture.

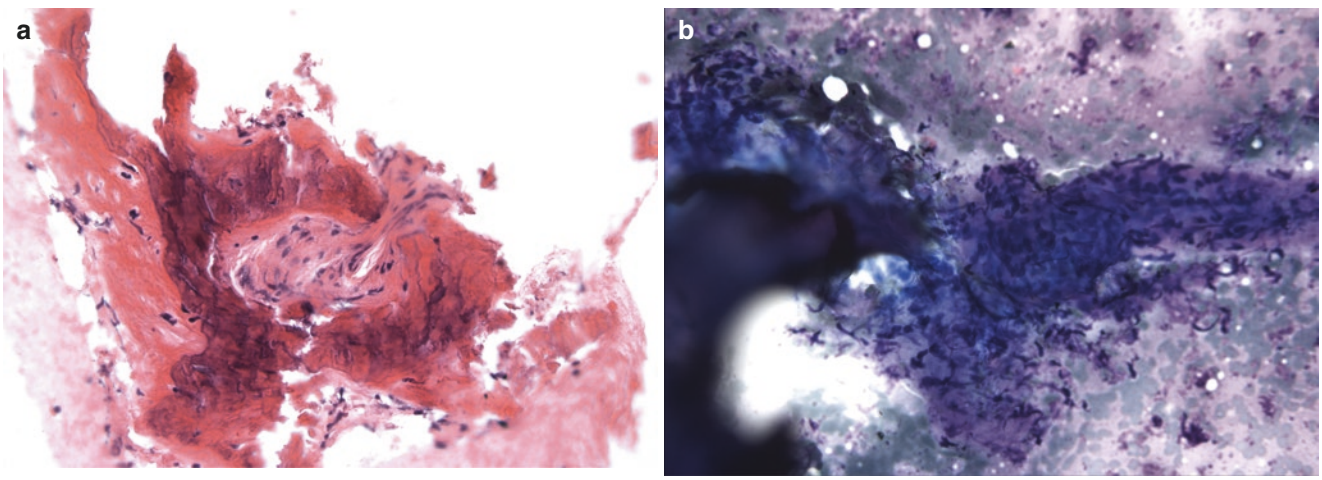

Fig. 16.37 Fibrous dysplasia. (**a**, **b**) Juxtaposed fragments of irregular ossifying bone and bland spindle cells often with crush artifact (H&E and Diff-Quik)

Adamantinoma

Adamantinoma is a rare biphasic (mesenchymal and epithelial) malignant tumor arising in the tibia, occasionally in the fibula. Two subtypes of adamantinoma, classical (mainly in children and young adults) and osteofibrous dysplasia-like (mainly in adults), have been reported. The classic type may show cortical destruction and involve soft tissue, while the osteofibrous dysplasia-like adamantinoma is an intracortical tumor.

Cytologic features (*see* Fig. 16.38):

- Predominantly bland-appearing spindle cells
- Cohesive clusters of epithelial cells (often basaloid or squamoid)

Only single case reports of FNAC of adamantinoma have been published [95]. The clue to the diagnosis is the presence of double-cell population of spindle-shaped mesenchymal cells and epithelial cells.

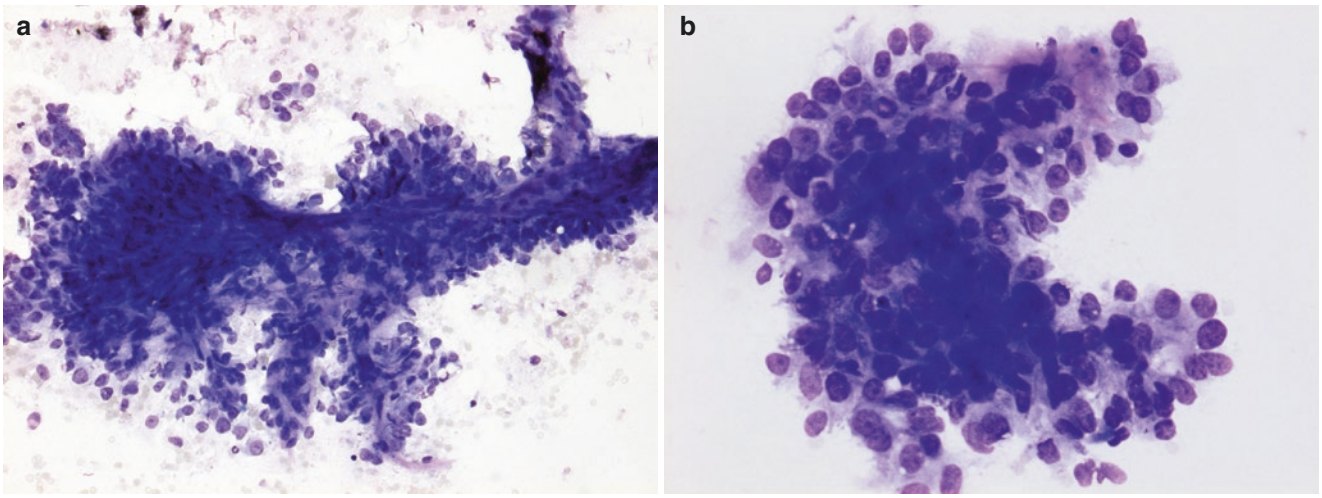

Fig. 16.38 Adamantinoma. (**a**, **b**) Cohesive clusters of epithelioid cells with moderate cytoplasm and round, somewhat irregular nuclei with small nucleoli (MGG)

Vascular Neoplasm

While solitary or multiple hemangiomas, usually involving vertebral bodies of the spine, are common neoplasms in the bone, epithelioid hemangioendothelioma and angiosarcoma arising primarily in the bone are uncommon. Few reports describing FNA features of primary vascular neoplasm of the bone exist [96–98]; morphology of smears is comparable with morphology in other settings (see Fig. 16.39).

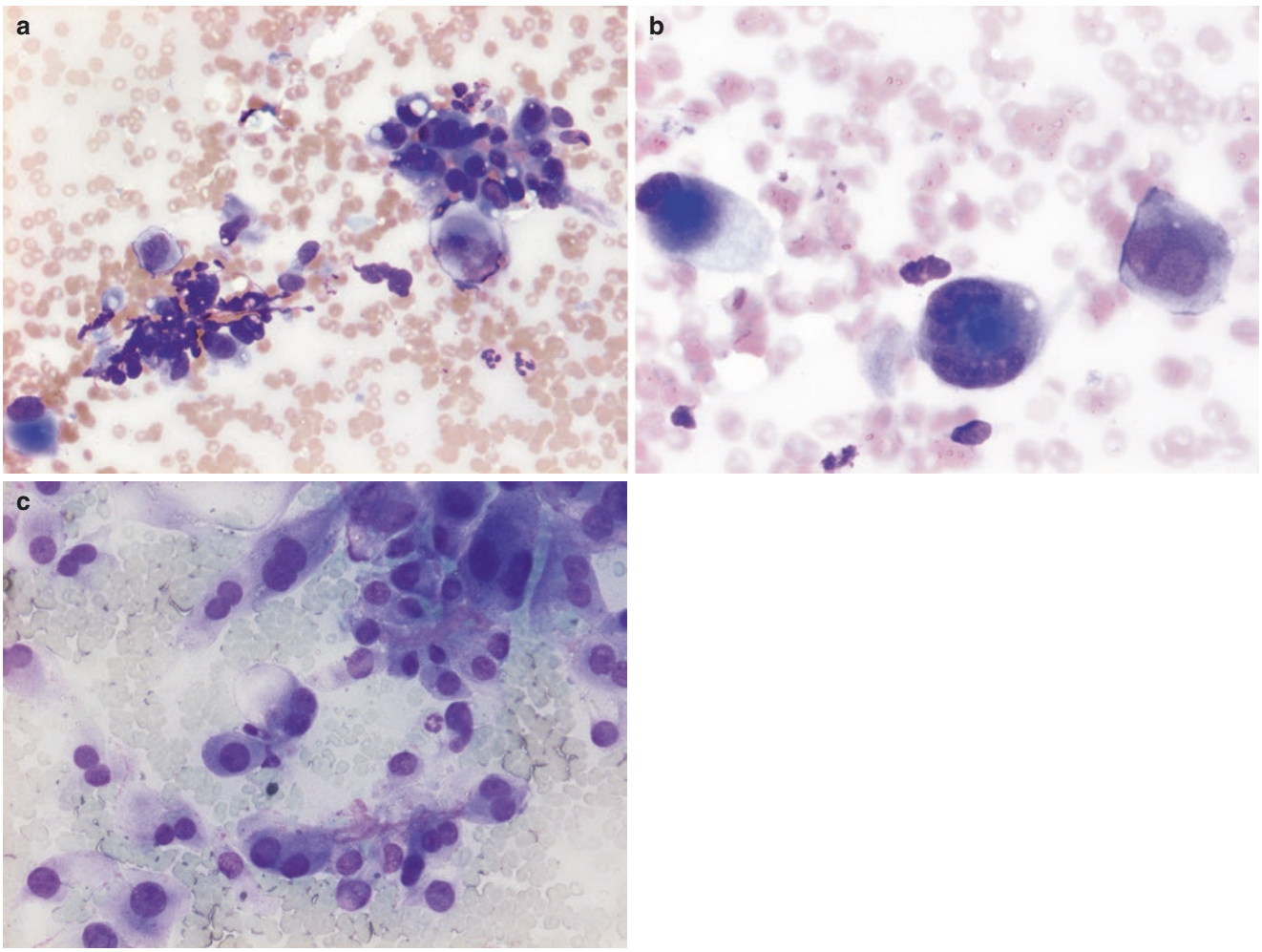

Fig. 16.39 Epithelioid hemangioendothelioma. (**a**–**c**) Small dyscohesive clusters and dispersed single cells with variable-sized, round to oval nuclei and moderate to abundant cytoplasm with occasional cytoplasmic densities (MGG)

References

1. Martin HE, Ellis EB. Biopsy by needle puncture and aspiration. Ann Surg. 1930;92:169–81.
2. Khalbuss WE, Teot LA, Monaco SE. Diagnostic accuracy and limitations of fine-needle aspiration cytology of bone and soft tissue lesions: a review of 1114 cases with cytological-histological correlation. Cancer Cytopathol. 2010;118:24–32.
3. Layfield LJ. Cytologic diagnosis of osseous lesions: a review with emphasis on the diagnosis of primary neoplasms of bone. Diagn Cytopathol. 2009;37:299–310.
4. Handa U, Bal A, Mohan H, Bhardwaj S. Fine needle aspiration cytology in the diagnosis of bone lesions. Cytopathology. 2005;16:59–64.
5. Layfield LJ, Dodd LG, Hirschowitz S, Crabtree SN. Fine-needle aspiration of primary osseous lesions: a cost effectiveness study. Diagn Cytopathol. 2010;38:239–43.
6. Willen H. Fine needle aspiration in the diagnosis of bone tumors. Acta Orthop Scand Suppl. 1997;273:47–53.
7. Bommer KK, Ramzy I, Mody D. Fine-needle aspiration biopsy in the diagnosis and management of bone lesions: a study of 450 cases. Cancer. 1997;81:148–56.
8. Jayaram G, Gupta M. Fine needle aspiration cytology in the diagnosis of bone tumours. Malays J Pathol. 1994;16:137–44.
9. Kreicbergs A, Bauer HC, Brosjö O, Lindholm J, Skoog L, Söderlund V. Cytological diagnosis of bone tumours. J Bone Joint Surg Br. 1996;78:258–63.
10. Akerman M, Berg NO, Persson BM. Fine needle aspiration biopsy in the evaluation of tumor-like lesions of bone. Acta Orthop Scand. 1976;47:129–36.
11. Akerman M, Killander D, Rydholm A, Rööser B. Aspiration of musculoskeletal tumors for cytodiagnosis and DNA analysis. Acta Orthop Scand. 1987;58:523–8.
12. Shergill U, Vitkovski T, Stoffels G, Klein M, Gimenez C, Laser A, et al. Fine-needle aspiration biopsy of lytic bone lesions: an institution's experience. Diagn Cytopathol. 2017;45(11):989–97.
13. Patel K, Kinnear D, Quintanilla NM, Hicks J, Castro E, Curry C, et al. Optimal diagnostic yield achieved with on-site pathology evaluation of fine-needle aspiration-assisted core biopsies for pediatric osseous lesions: a single-center experience. Arch Pathol Lab Med. 2017;141(5):678–83.
14. Domanski HA, Akerman M, Carlen B, Engellau J, Gustafson P, Jonsson K, et al. Core-needle biopsy performed by the cytopathologist: a technique to complement fine-needle aspiration of soft tissue and bone lesions. Cancer. 2005;105(4):229–39.
15. Koscick RL, Petersilge CA, Makley JT, Abdul-Karim FW. CT-guided fine needle aspiration and needle core biopsy of skeletal lesions. complementary diagnostic techniques. Acta Cytol. 1998;42:697–702.
16. Söderlund V, Tani E, Domanski H, Kreicbergs A. Representativeness of radiologically guided fine-needle aspiration biopsy of bone lesions. Sarcoma. 2002;6:61–8.
17. Soderlund V, Skoog L, Kreicbergs A. Combined radiology and cytology in the diagnosis of bone lesions: a retrospective study of 370 cases. Acta Orthop Scand. 2004;75:492–9.
18. Akerman M, Domanski HA, Jonsson K. Morphological diagnosis of bone tumours. Monogr Clin Cytol. 2010;19:7–12.
19. Akerman M, Domanski HA. Fine needle aspiration (FNA) of bone tumours. With special emphasis on definitive treatment of primary malignant bone tumours based on FNA. Curr Diagn Pathol. 1998;5:82–92.
20. Jorda M, Rey L, Hanly A, Ganjei-Azar P. Fine-needle aspiration cytology of bone: accuracy and pitfalls of cytodiagnosis. Cancer. 2000;90:47–54.
21. Agarwal S, Agarwal T, Agarwal R, Agarwal PK, Jain UK. Fine needle aspiration of bone tumors. Cancer Detect Prev. 2000;24:602–9.
22. Wedin R, Bauer HC, Skoog L, Söderlund V, Tani E. Cytological diagnosis of skeletal lesions. Fine-needle aspiration biopsy in 110 tumours. J Bone Joint Surg Br. 2000;82:673–8.
23. Kilpatrick SE, Cappellari JO, Bos GD, Gold SH, Ward WG. Is fine-needle aspiration biopsy a practical alternative to open biopsy for the primary diagnosis of sarcoma? Experience with 140 patients. Am J Clin Pathol. 2001;115(1):59–68.
24. Kabukçuoğlu F, Kabukçuoğlu Y, Kuzgun U, Evren I. Fine needle aspiration of malignant bone lesions. Acta Cytol. 1998;42:875–82.
25. Aström KG, Sundström JC, Lindgren PG, Ahlström KH. Automatic biopsy instruments used through a coaxial bone biopsy system with an eccentric drill tip. Acta Radiol. 1995;36:237–42.
26. Walther C, Domanski HA, von Steyern FV, Mandahl N, Mertens F. Chromosome banding analysis of cells from fine-needle aspiration biopsy samples from soft tissue and bone tumors: is it clinically meaningful? Cancer Gene Ther. 2011;204:203–6.
27. Gautam U, Srinivasan R, Rajwanshi A, Bansal D, Marwaha RK, Vasishtha RK. Reverse transcriptase-polymerase chain reaction as an ancillary molecular technique in the diagnosis of small blue round cell tumors by fine-needle aspiration cytology. Am J Clin Pathol. 2010;133:633–45.
28. Gautam U, Srinivasan R, Rajwanshi A, Bansal D, Marwaha RK. Comparative evaluation of flow-cytometric immunophenotyping and immunocytochemistry in the categorization of malignant small round cell tumors in fine-needle aspiration cytologic specimens. Cancer. 2008;114:494–503.
29. Sanati S, Lu DW, Schmidt E, Perry A, Dehner LP, Pfeifer JD. Cytologic diagnosis of Ewing sarcoma/peripheral neuroectodermal tumor with paired prospective molecular genetic analysis. Cancer. 2007;111:192–9.
30. Walaas L, Kindblom LG. Light and electron microscopic examination of fine-needle aspirates in the preoperative diagnosis of osteogenic tumors: a study of 21 osteosarcomas and two osteoblastomas. Diagn Cytopathol. 1990;6:27–38.
31. Domanski HA, Akerman M. Fine-needle aspiration of primary osteosarcoma: a cytological-histological study. Diagn Cytopathol. 2005;32:269–75.
32. McLaughlin RE, Miller WR, Miller CW, et al. J Bone Joint Surg Am. 1976;58:1167–8.
33. Rhode MG, Lucas DR, Krueger CH, Pu RT. Fine-needle aspiration of spinal osteoblastoma in a patient with lymphangiomatosis. Diagn Cytopathol. 2006;34:295–7.
34. Mondal A, Misra DK. CT-guided needle aspiration cytology (FNAC) of 112 vertebral lesions. Indian J Pathol Microbiol. 1994;37:255–61.
35. Venugopal SB, Prasad S. Cytological diagnosis of osteoblastoma of cervical spine: a case report with review of literature. Diagn Cytopathol. 2015;43(3):218–21.
36. Sathiyamoorthy S, Ali SZ. Osteoblastic osteosarcoma: cytomorphologic characteristics and differential diagnosis on fine-needle aspiration. Acta Cytol. 2012;56:481–6.
37. Dodd LG, Scully SP, Cothran RL, Harrelson JM. Utility of fine-needle aspiration in the diagnosis of primary osteosarcoma. Diagn Cytopathol. 2002;27:350–3.
38. Dodd LG, Chai C, McAdams HP, Layfield LJ. Fine needle aspiration of osteogenic sarcoma metastatic to the lung. A report of four cases. Acta Cytol. 1998;42:754–8.
39. Gupta N, Rajwanshi A, Gupta P, Vaiphei K, Gupta AK. Chondroblastic osteosarcoma of the temporal region: a diagnostic dilemma. Diagn Cytopathol. 2011;39:377–9.
40. Klijanienko J, Caillaud JM, Orbach D, Brisse H, Lagacé R, Sastre-Gareau X. Cyto-histological correlations in primary, recurrent, and metastatic bone and soft tissue osteosarcoma. Institut Curie's experience. Diagn Cytopathol. 2007;35:270–5.
41. Söderlund V, Skoog L, Unni KK, Bertoni F, Brosjö O, Kreicbergs A. Diagnosis of high-grade osteosarcoma by radiology and cytology: a retrospective study of 52 cases. Sarcoma. 2004;8:31–6.

42. Kilpatrick SE, Ward WG, Bos GD, Chauvenet AR, Gold SH. The role of fine needle aspiration biopsy in the diagnosis and management of osteosarcoma. Pediatr Pathol Mol Med. 2001;20:175–87.
43. Nicol KK, Ward WG, Savage PD, Kilpatrick SE. Fine-needle aspiration biopsy of skeletal versus extraskeletal osteosarcoma. Cancer. 1998;84:176–85.
44. Bhatia A, Ashokraj G. Cytological diversity of osteosarcoma. Indian J Cancer. 1992;29:56–60.
45. VandenBussche CJ, Sathiyamoorthy S, Wakely PE Jr, Ali SZ. Chondroblastic osteosarcoma: cytomorphologic characteristics and differential diagnosis on FNA. Cancer Cytopathol. 2016;124(7):493–500.
46. Mehdi G, Siddiqui F, Maheshwari V, Khan AQ. Imprint smear cytology of chondroblastic osteosarcoma: a case report. Diagn Cytopathol. 2009;37:446–9.
47. Ali RH, Lee CH, Hayes MM. Metastatic small cell osteosarcoma to the liver: a diagnostic pitfall for fine-needle aspiration cytology. Diagn Cytopathol. 2012;36:42–6. [Epub ahead of print].
48. White VA, Fanning CV, Ayala AG, Raymond AK, Carrasco CH, Murray JA. Osteosarcoma and the role of fine-needle aspiration. A study of 51 cases. Cancer. 1988;62:1238–46.
49. Cabrera RA, Almeida M, Mendonça ME, Frable WJ. Diagnostic pitfalls in fine-needle aspiration cytology of temporomandibular chondroblastoma: report of two cases. Diagn Cytopathol. 2006;34:424–9.
50. Cozzolino I, Zeppa P, Zabatta A, Merolla F, Vetrani A, Sadile F. Benign chondroblastoma on fine-needle aspiration smears: a seven-case experience and review of the literature. Diagn Cytopathol. 2015;43(9):734–8.
51. Krishnappa A, Shobha SN, Shankar SV, Aradhya S. Fine needle aspiration cytology of chondroblastoma: a report of two cases with brief review of pitfalls. J Cytol Indian Acad Cytologists. 2016;33(1):40–2.
52. Abdul-Karim FW, Wasman JK, Pitlik D. Needle aspiration cytology of chondrosarcomas. Acta Cytol. 1993;37:655–60.
53. Dodd LG. Fine-needle aspiration of chondrosarcoma. Diagn Cytopathol. 2006;34:413–8.
54. Lerma E, Tani E, Brosjö O, Bauer H, Söderlund V, Skoog L. Diagnosis and grading of chondrosarcomas on FNA biopsy material. Diagn Cytopathol. 2003;28:13–7.
55. Skoog L, Pereira ST, Tani E. Fine-needle aspiration cytology and immunocytochemistry of soft-tissue tumors and osteo/chondrosarcomas of the head and neck. Diagn Cytopathol. 1999;20:131–6.
56. Jiang XS, Pantanowitz L, Bui MM, Esther R, Budwit D, Dodd LG. Clear cell chondrosarcoma: cytologic findings in six cases. Diagn Cytopathol. 2014;42(9):784–91.
57. McHugh KE, Emory CL, Parks GE, Kilpatrick SE. Fine needle aspiration biopsy diagnosis of primary clear cell chondrosarcoma: a case report. Diagn Cytopathol. 2018;46(2):165–9.
58. Cheim AP Jr, Queiroz TL, Alencar WM, Rezende RM, Vencio EF. Mesenchymal chondrosarcoma in the mandible: report of a case with cytological findings. J Oral Sci. 2011;53:245–7.
59. Handa U, Singhal N, Punia RS, Garg S, Mohan H. Cytologic features and differential diagnosis in a case of extraskeletal mesenchymal chondrosarcoma: a case report. Acta Cytol. 2009;53:704–6.
60. Trembath DG, Dash R, Major NM, Dodd LG. Cytopathology of mesenchymal chondrosarcomas: a report and comparison of four patients. Cancer. 2003;99:211–6.
61. Witt BL, Garcia CA, Cohen MB. Giant cell tumor of bone presenting in the lumbar spine of a 35-year-old female: cytodiagnosis and other diagnostic considerations. Diagn Cytopathol. 2014;42:624–7.
62. Sneige N, Ayala AG, Carrasco CH, Murray J, Raymond AK. Giant cell tumor of bone. A cytologic study of 24 cases. Diagn Cytopathol. 1985;1:111–7.
63. Vetrani A, Fulciniti F, Boschi R, Marino G, Zeppa P, Troncone G, et al. Fine needle aspiration biopsy diagnosis of giant-cell tumor of bone. An experience with nine cases. Acta Cytol. 1990;34:863–7.
64. Gupta A, Singh U, Singh P, Kundu ZS, Gupta S, Gupta S. Fine needle aspiration of a huge pelvic mass involving the iliac bone. Cytopathol Off J Br Soc Clin Cytol. 2009;20:63–5.
65. Khare P, Kishore B, Gupta RJ, Vanita, Dhal A. GCT of proximal phalanx of ring finger: a case report. Diagn Cytopathol. 2012;40(Suppl 2):E165–8.
66. Schaefer IM, Fletcher JA, Nielsen GP, Shih AR, Ferrone ML, Hornick JL, et al. Immunohistochemistry for histone H3G34W and H3K36M is highly specific for giant cell tumor of bone and chondroblastoma, respectively, in FNA and core needle biopsy. Cancer Cytopathol. 2018; https://doi.org/10.1002/cncy.22000. [Epub ahead of print].
67. Dahl I, Akerman M, Angervall L. Ewing's sarcoma of bone. A correlative cytological and histological study of 14 cases. Acta Pathol Microbiol Immunol Scand A. 1986;94:363–9.
68. Klijanienko J, Couturier J, Bourdeaut F, Fréneaux P, Ballet S, Brisse H, et al. Fine-needle aspiration as a diagnostic technique in 50 cases of primary Ewing sarcoma/peripheral neuroectodermal tumor. Institut Curie's experience. Diagn Cytopathol. 2012;40:19–25.
69. Pohar-Marinsek Z. Difficulties in diagnosing small round cell tumours of childhood from fine needle aspiration cytology samples. Cytopathology. 2008;19:67–79.
70. Fröstad B, Tani E, Brosjö O, Skoog L, Kogner P. Fine needle aspiration cytology in the diagnosis and management of children and adolescents with Ewing sarcoma and peripheral primitive neuroectodermal tumor. Med Pediatr Oncol. 2002;38:33–40.
71. Sahu K, Pai RR, Khadilkar UN. Fine needle aspiration cytology of the Ewing's sarcoma family of tumors. Acta Cytol. 2000;44:332–6.
72. Folpe AL, Hill CE, Parham DM, O'Shea PA, Weiss SW. Immunohistochemical detection of FLI-1 protein expression: a study of 132 round cell tumors with emphasis on CD99-positive mimics of Ewing's sarcoma/primitive neuroectodermal tumor. Am J Surg Pathol. 2000;24:1657–62.
73. Folpe AL, Goldblum JR, Rubin BP, Shehata BM, Liu W, Dei Tos AP, et al. Morphologic and immunophenotypic diversity in Ewing family tumors: a study of 66 genetically confirmed cases. Am J Surg Pathol. 2005;29:1025–33.
74. Udayakumar AM, Sundareshan TS, Goud TM, Devi MG, Biswas S, Appaji L, et al. Cytogenetic characterization of Ewing tumors using fine needle aspiration samples. A 10-year experience and review of the literature. Cancer Genet Cytogenet. 2001;127:42–8.
75. Dal Cin P, Qian X, Cibas ES. The marriage of cytology and cytogenetics. Cancer Cytopathol. 2013;44:1165–70.
76. Layfield LJ. Cytologic differential diagnosis of myxoid and mucinous neoplasms of the sacrum and parasacral soft tissues. Diagn Cytopathol. 2003;28:264–71.
77. Moriki T, Takahashi T, Wada M, Ueda S, Ichien M, Miyazaki E. Chondroid chordoma: fine-needle aspiration cytology with histopathological, immunohistochemical, and ultrastructural study of two cases. Diagn Cytopathol. 1999;21:335–9.
78. Das DK, Francis IM, AbuZeidan FM. Fine-needle aspiration (FNA) cytology diagnosis of a sacrococcygeal chordoma and its recurrence. Diagn Cytopathol. 1994;10:194–5.
79. Syed R, Bishop JA, Ali SZ. Sacral and presacral lesions: cytopathologic analysis and clinical correlates. Diagn Cytopathol. 2012;40(1):7–13.
80. Jo VY, Hornick JL, Qian X. Utility of brachyury in distinction of chordoma from cytomorphologic mimics in fine-needle aspiration and core needle biopsy. Diagn Cytopathol. 2014;42(8):647–52.
81. Söderlund V, Tani E, Skoog L, Bauer HC, Kreicbergs A. Diagnosis of skeletal lymphoma and myeloma by radiology and fine needle aspiration cytology. Cytopathology. 2001;12:157–67.
82. Tani E, Santos GC, Svedmyr E, Skoog L. Fine-needle aspiration cytology and immunocytochemistry of soft-tissue extramedullary plasma-cell neoplasms. Diagn Cytopathol. 1999;20:120–4.
83. Mondal SK, Bera H, Biswas PK, Mallick MG. High-grade plasmablastic neoplasm of humerus in an HIV-negative patient, which was

indeterminate between plasmablastic lymphoma and plasmablastic myeloma. J Cancer Res Ther. 2011;7:214–6.
84. Hang JF, Siddiqui MT, Ali SZ. Fine needle aspiration of Langerhans cell histiocytosis: a cytopathologic study of 37 cases. Acta Cytol. 2017;61(2):96–102.
85. Kumar N, Sayed S, Vinayak S. Diagnosis of Langerhans cell histiocytosis on fine needle aspiration cytology: a case report and review of the cytology literature. Pathol Res Int. 2011;2011:439518.
86. Ramadas PT, Kattoor J, Mathews A, Abraham EK. Fine needle aspiration cytology of Langerhans cell thyroid histiocytosis and its draining lymph nodes. Acta Cytol. 2008;52:396–8.
87. Jayaram N, Ramprasad AV, Sujay RP. Langerhans cell histiocytosis—a clinicopathological spectrum. Indian J Pathol Microbiol. 1998;41:331–5.
88. Elsheikh T, Silverman JF, Wakely PE Jr, Holbrook CT, Joshi VV. Fine-needle aspiration cytology of Langerhans' cell histiocytosis (eosinophilic granuloma) of bone in children. Diagn Cytopathol. 1991;7:261–6.
89. Shih LY, Chen TH, Lo WH. Skeletal metastasis from occult carcinoma. J Surg Oncol. 1992;51:109–13.
90. Katagiri H, Takahashi M, Inagaki J, Sugiura H, Ito S, Iwata H. Determining the site of the primary cancer in patients with skeletal metastasis of unknown origin: a retrospective study. Cancer. 1999;86:533–7.
91. Treaba D, Assad L, Govil H, Sariya D, Reddy VB, Kluskens L. Diagnostic role of fine-needle aspiration of bone lesions in patients with a previous history of malignancy. Diagn Cytopathol. 2002;26:380–3.
92. Suterwala S, Volk EE, Danforth RD. Aspiration biopsy of osseous metastasis of occult hepatocellular carcinoma: case report, literature review, and differential diagnosis. Diagn Cytopathol. 2001;25:63–7.
93. Huening MA, Reddy S, Dodd LG. Fine-needle aspiration of fibrous dysplasia of bone: a worthwhile endeavor or not? Diagn Cytopathol. 2008;36:325–30.
94. Logrono R, Kurtycz DF, Wojtowycz M, Inhorn SL. Fine needle aspiration cytology of fibrous dysplasia: a case report. Acta Cytol. 1998;42:1172–6.
95. Bishop JA, Ali SZ. Primary tibial adamantinoma diagnosed by fine needle aspiration. Diagn Cytopathol. 2010;38:198–201.
96. Schindler S, Cajulis RS, Gokaslan ST, Frias-Hidvegi D, Yu GH. Fine needle aspiration of primary angiosarcoma of bone. Acta Cytol. 1997;41:1225–8.
97. Jayaram G, Kapoor R, Saha MM. Hemangioendothelioma. Cytologic appearances in two cases presenting with multiple soft tissue and bone lesions. Acta Cytol. 1987;31:497–501.
98. Mohan H, Palta A, Nada R, Punia RS, Jogai S, Gupta R. Epithelioid haemangioendothelioma of the rib—a case report. Indian J Pathol Microbiol. 2001;44:375–7.